Image-Based Simulation for Industry 2021 (IBSim-4i)

18-21 October 2021, Institue of Physics, London, UK

Image-based modelling of C/C and CMC: from µCT to FE models

Guillaume COUÉGNAT

couegnat@lcts.u-bordeaux.fr

Laboratoire des Composites Thermostructuraux (LCTS)

- Joint lab between CNRS, U. Bordeaux, Safran and CEA (~ 80 people)
- High-temperature composites for aeronautics, aerospace, defence & energy applications
- Elaboration, characterisation, testing & modelling

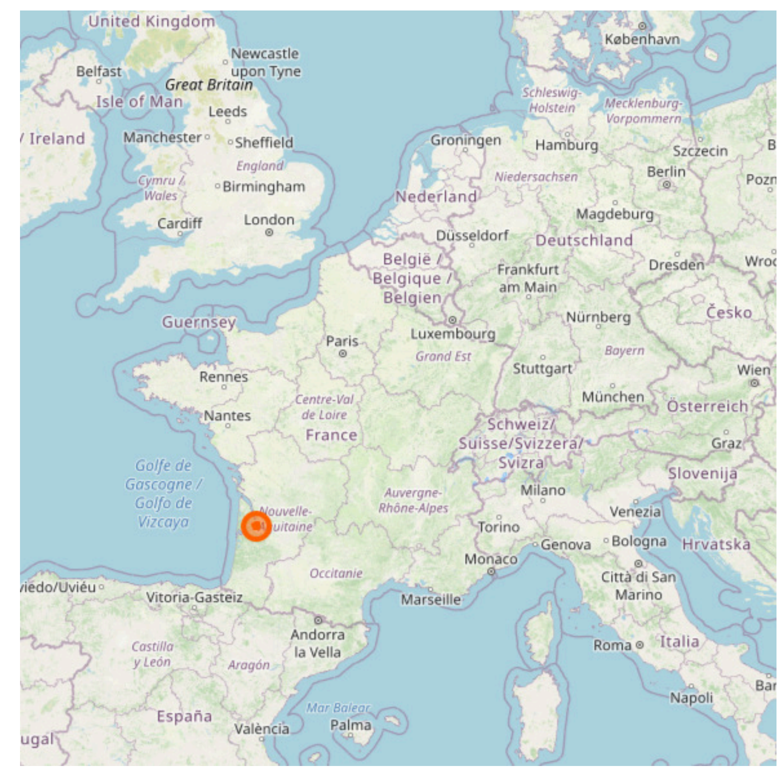

Carbon/Carbon composites (C/C)

- Aerospace applications (T up to 2000°C)
- Carbon fibres and pyrocarbon matrix
- Multilayer architecture + needle punching

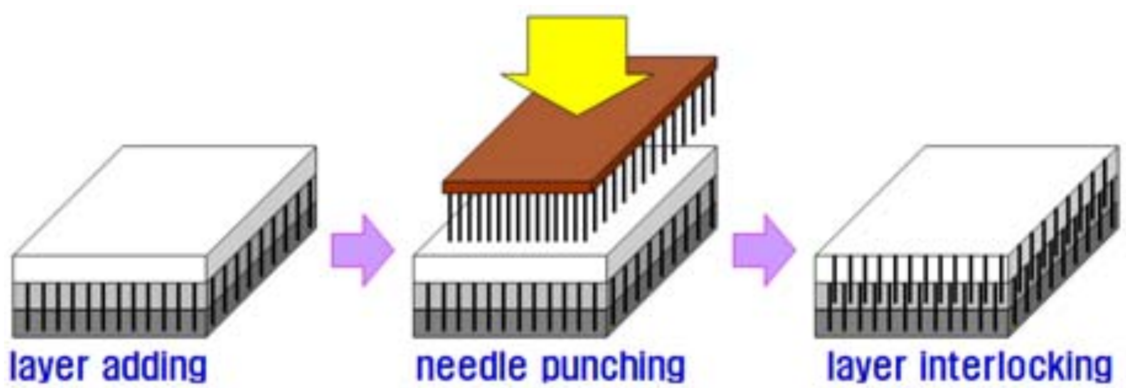

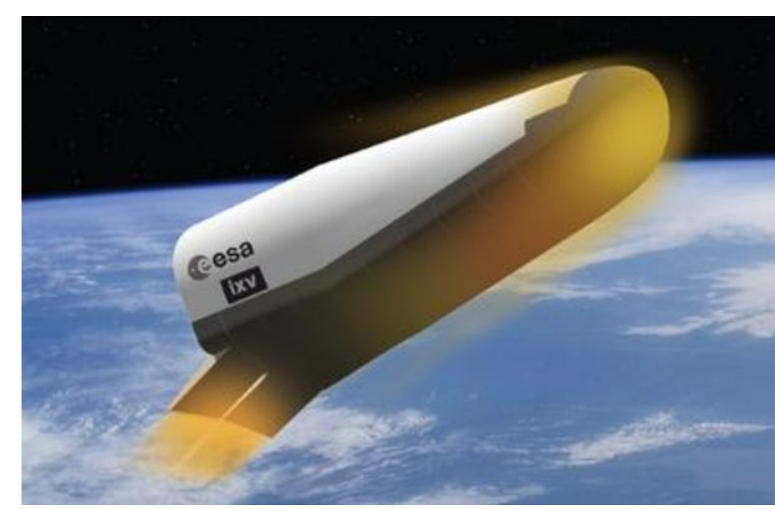

Ceramic Matrix Composites (CMC)

- Aeronautics applications
- C or SiC fibres and SiC matrix
- Woven preform

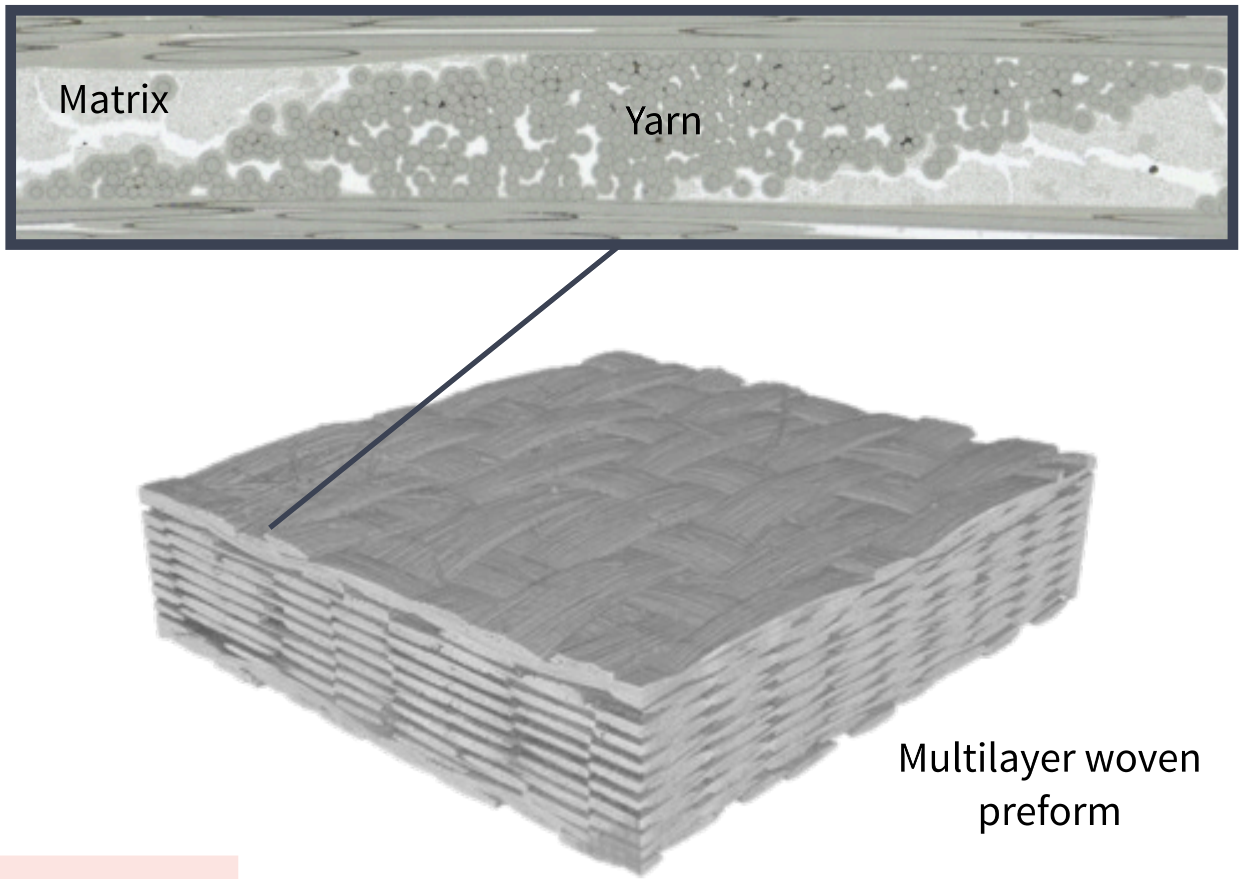

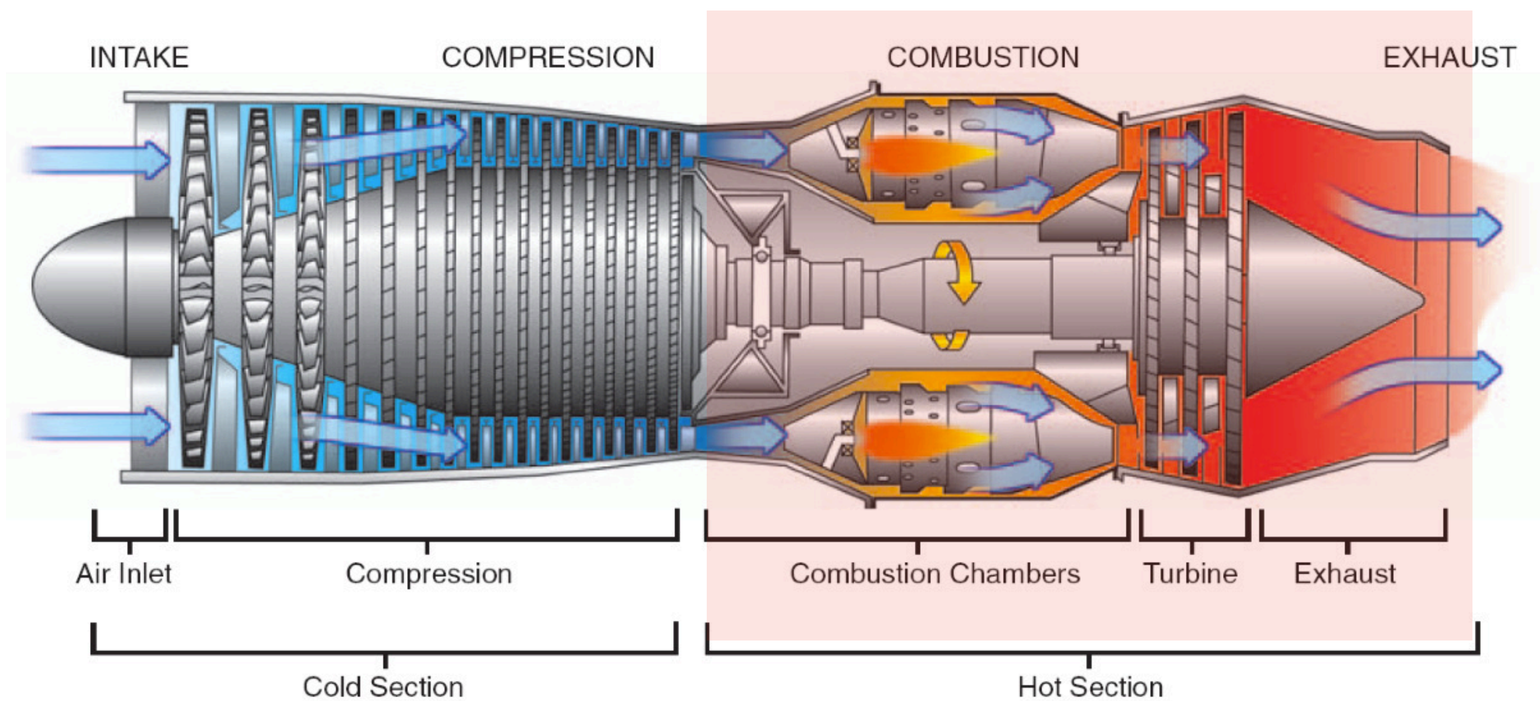

Image-based modelling of C/C and CMC

1

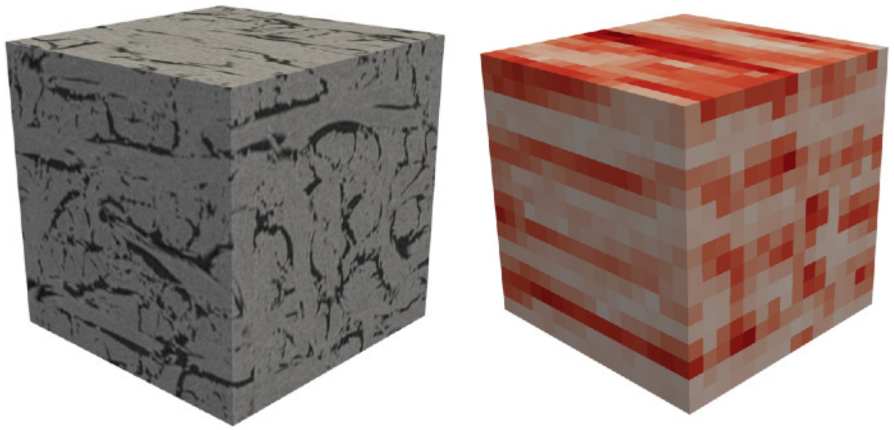

Prediction of the thermo-elastic properties of a 2.5D C/C

2

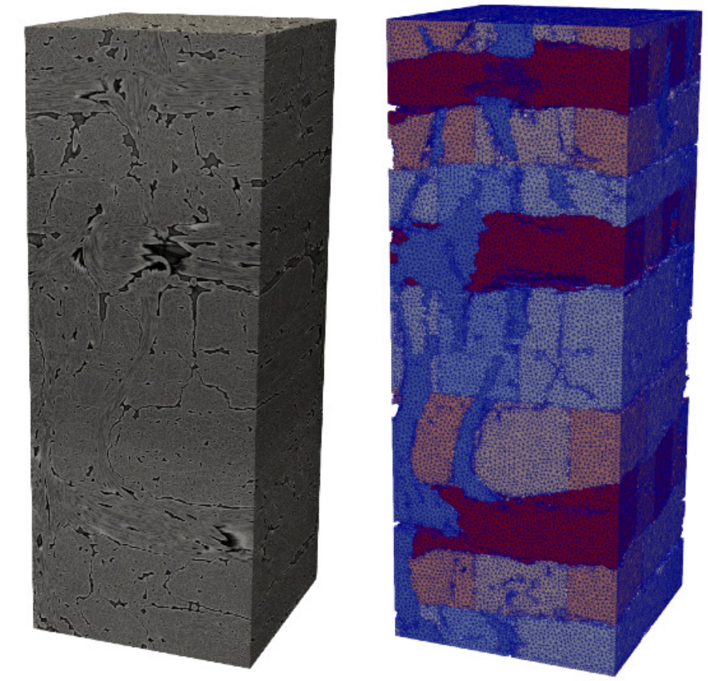

Modelling of a C/C with a non-linear interface model

3

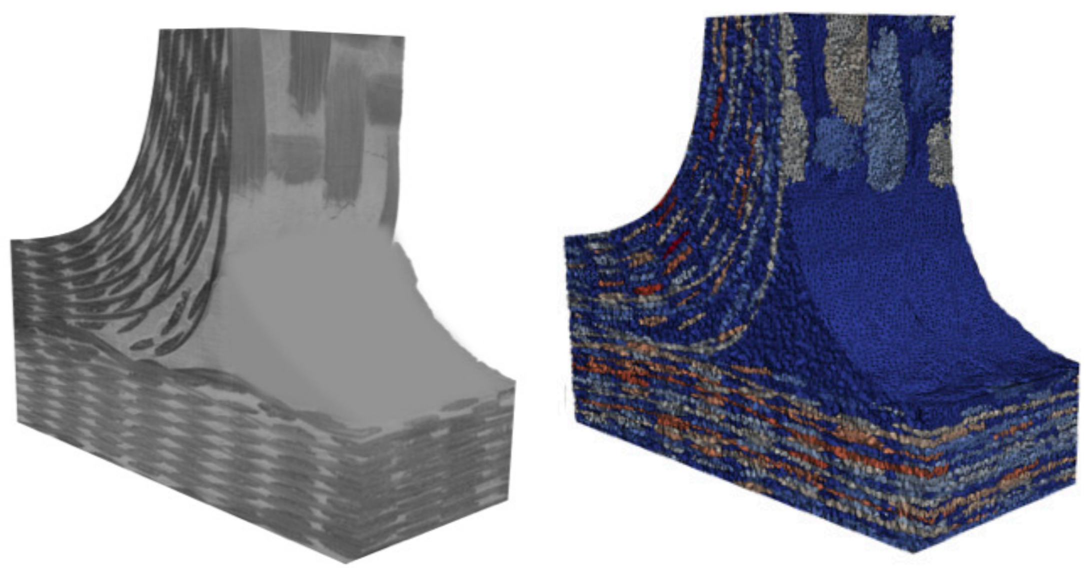

High-fidelity FE mesoscale models of woven CMC

Prediction of the thermo-elastic properties of a 2.5D C/C

Ph.D. of Morgan CHARRON (2017)

2.5D C/C

- Needle-punched 2D woven plies
- Ex-PAN C fibre and CVI pyC matrix; both anisotropic

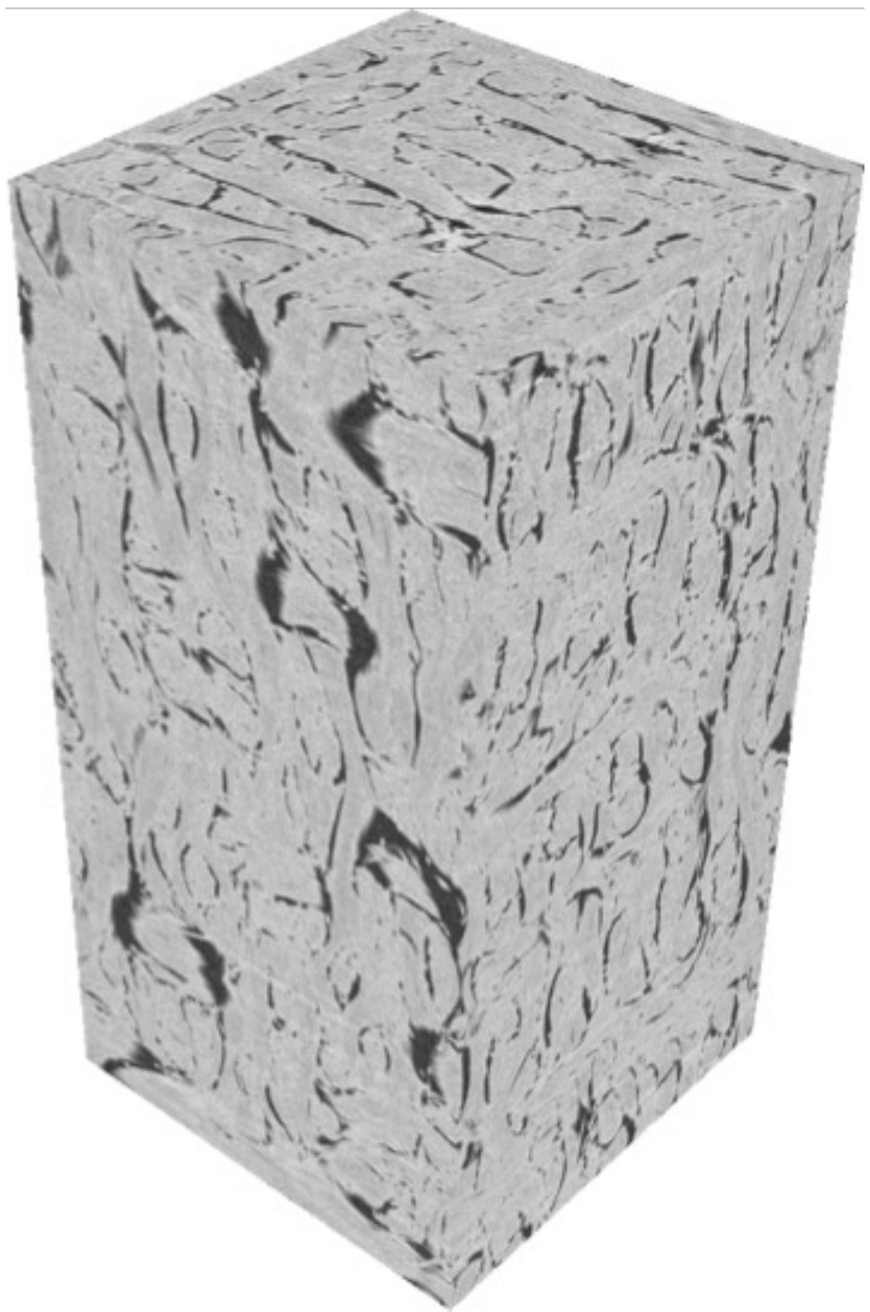

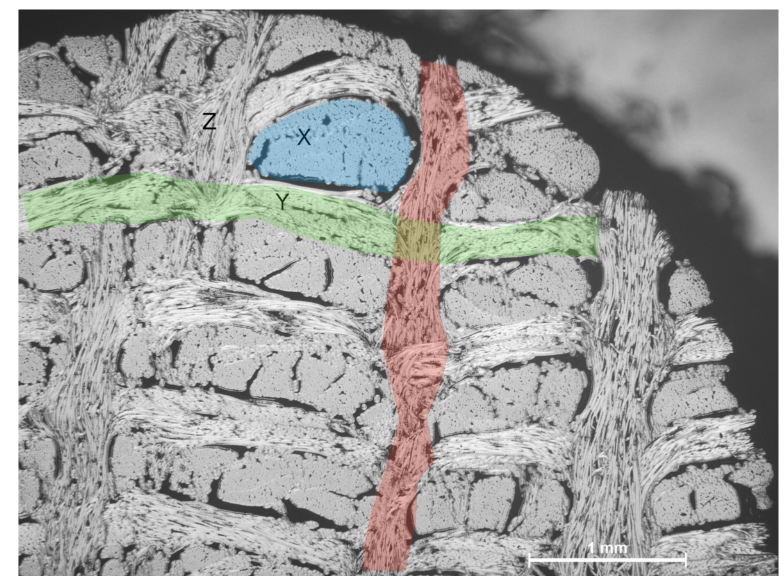

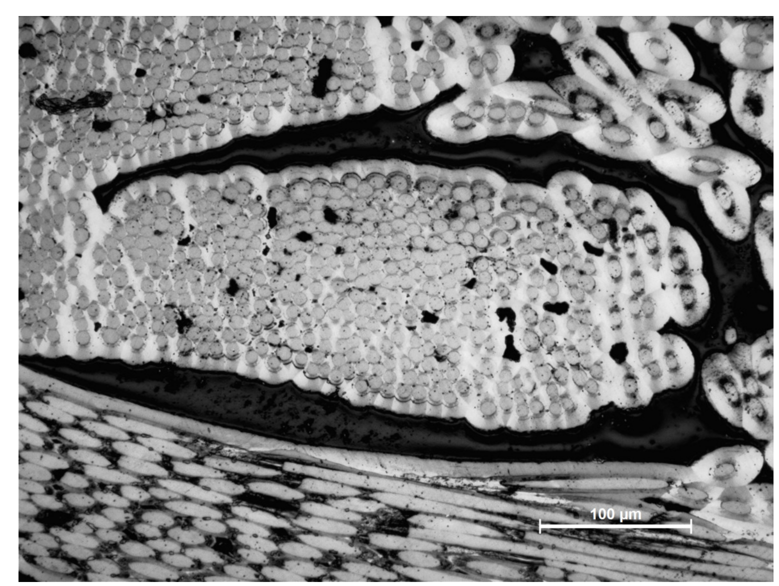

Data to be derived from µCT

- bulk/porosity segmentation + local fibre orientation

Bulk/porosity segmentation

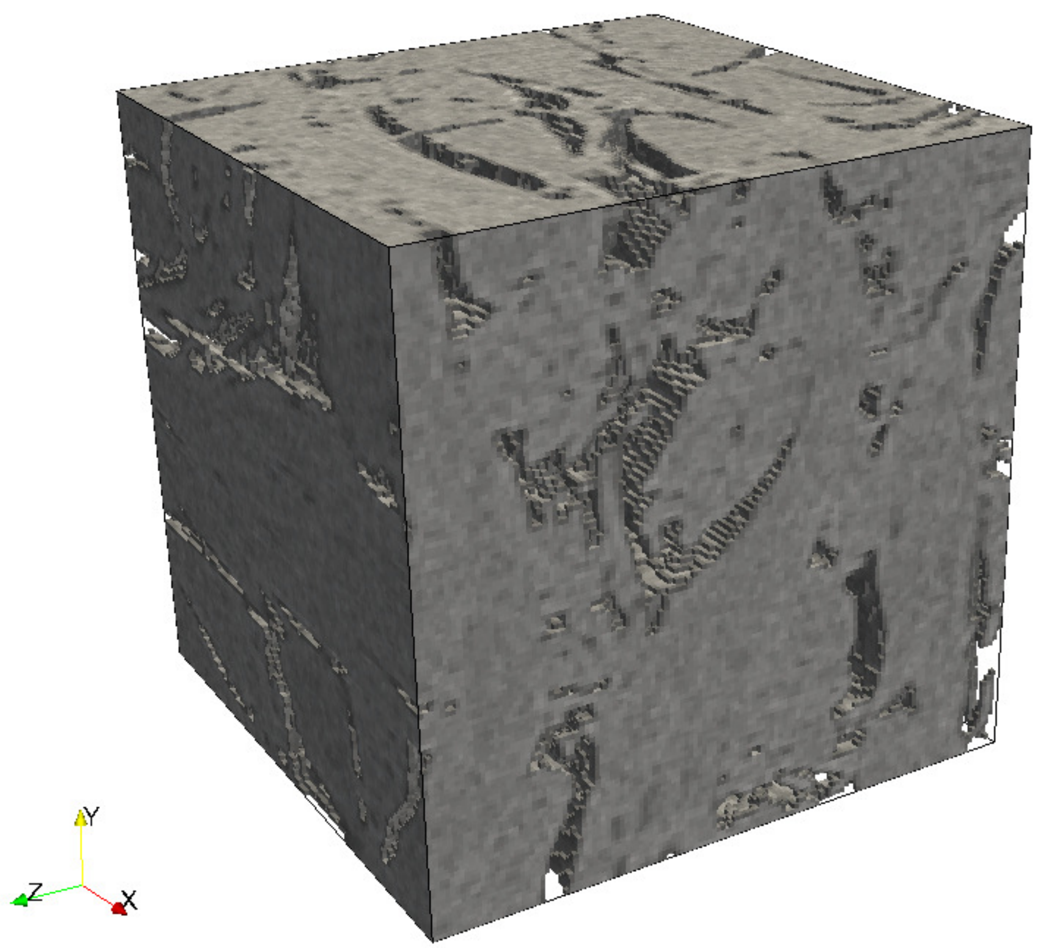

Local orientation

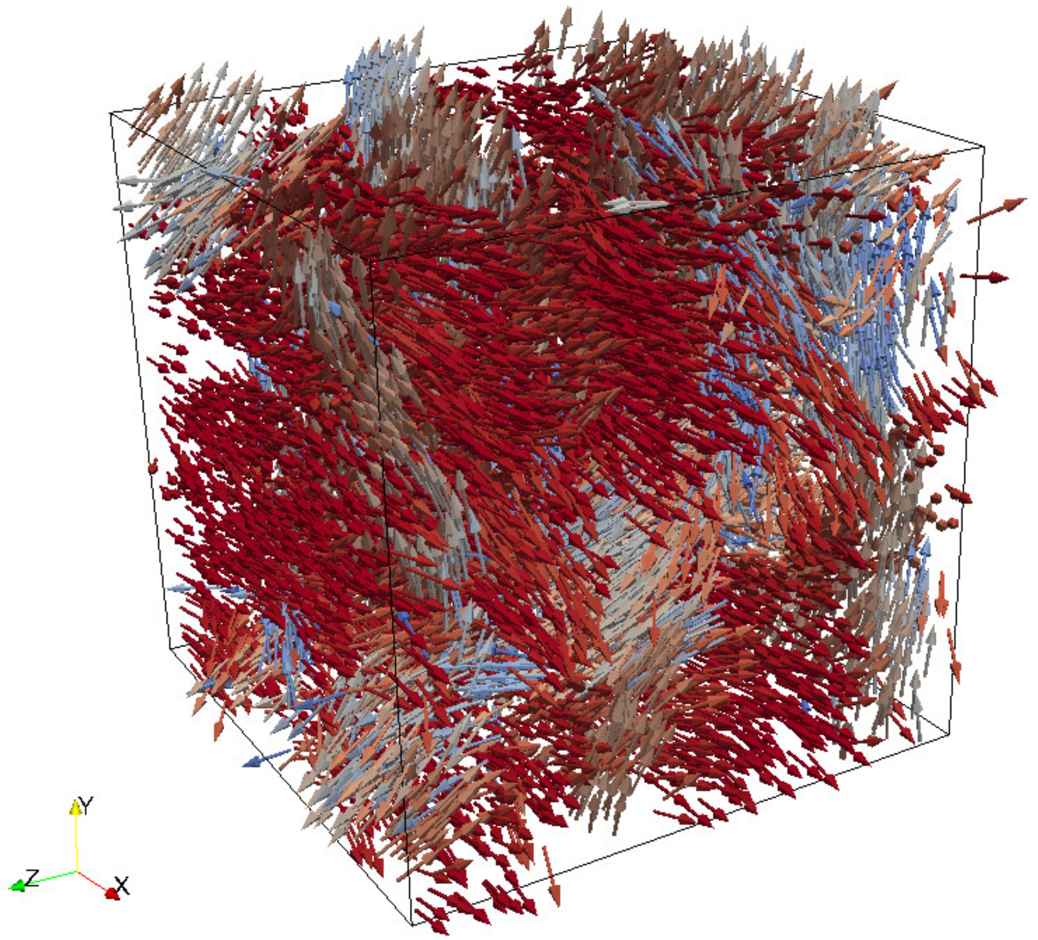

Segmentation of the porosity

Size distribution of open porosity (Hg pycnometry)

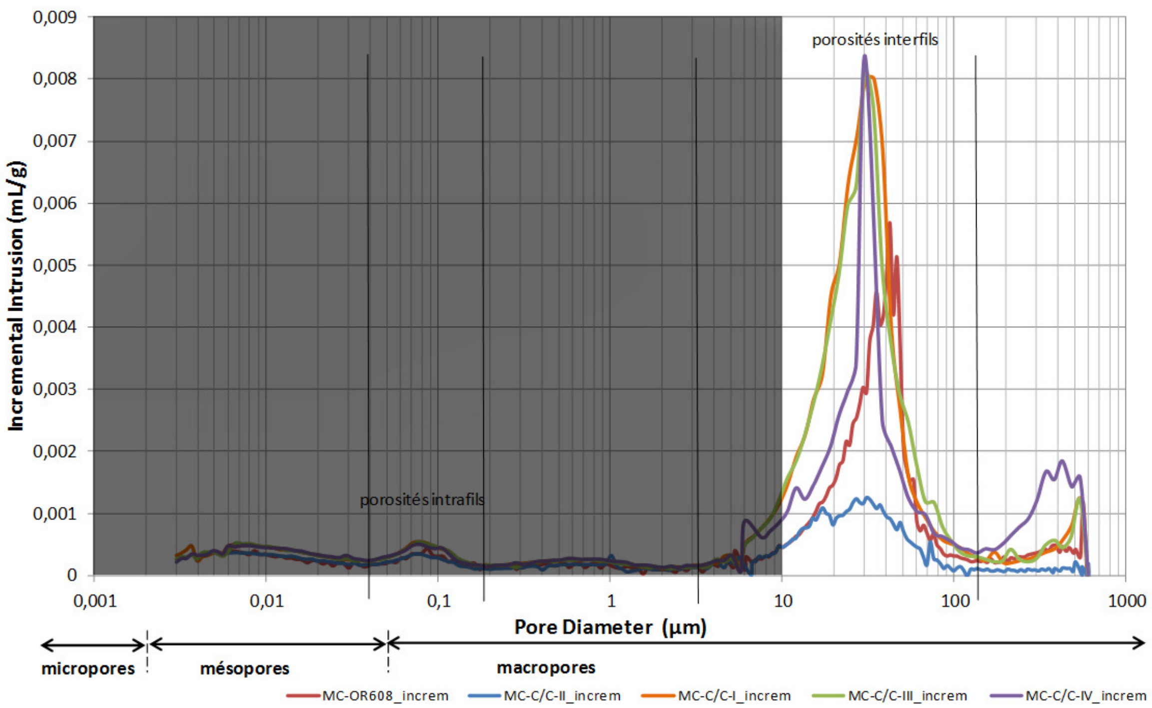

Total and open porosity from µCT

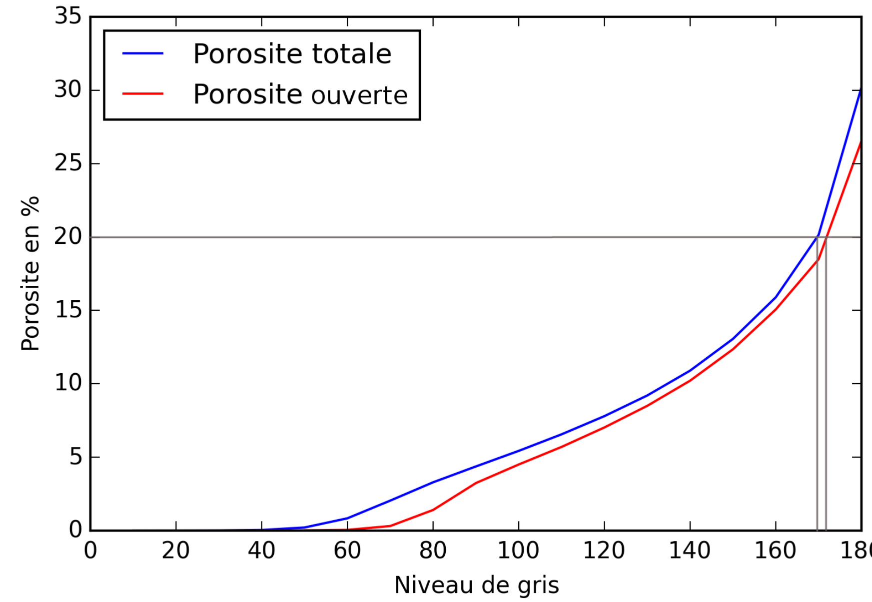

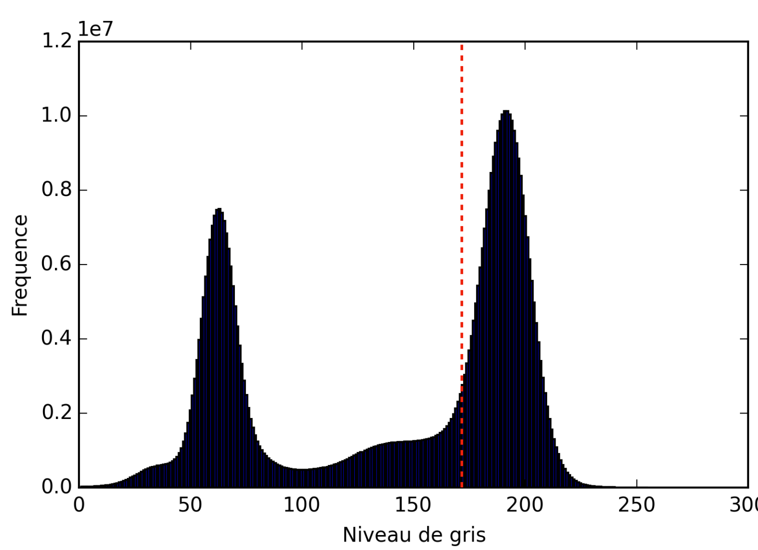

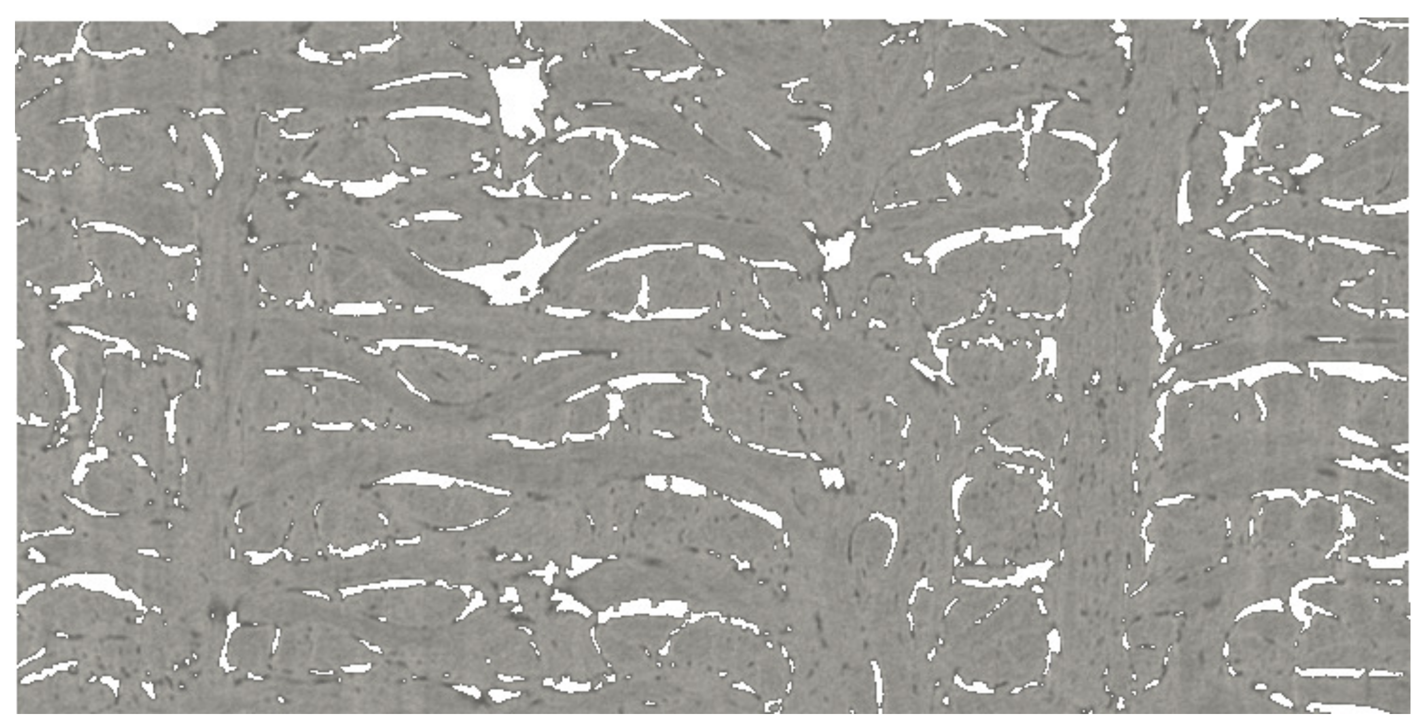

Estimation of local fibre direction

- G3D10: gradient filter for fibrous material

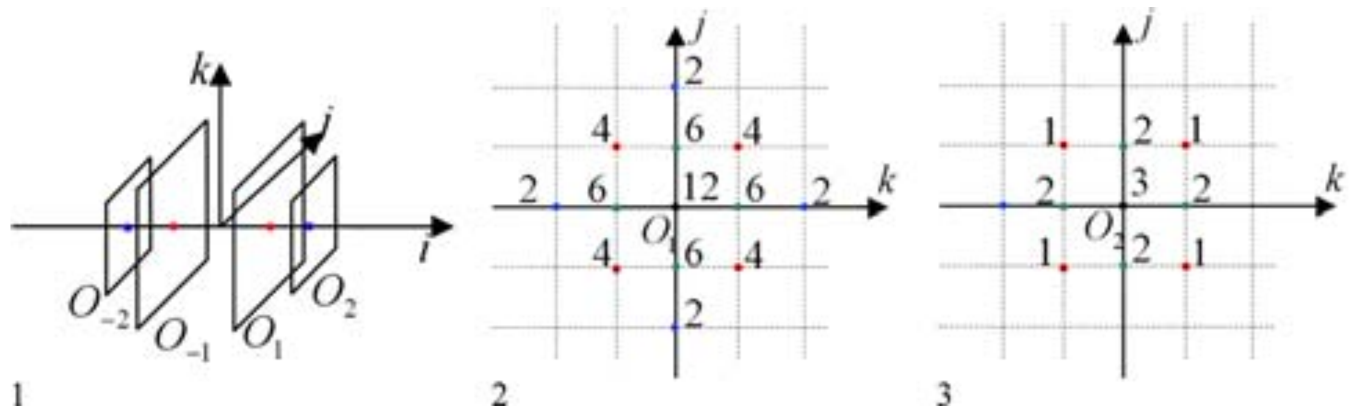

C. Mulat, M. Donias, P. Baylou, G. Vignoles, C. Germain, Optimal orientation estimators for detection of cylindrical objects, Signal, Image and Video Processing 2 (1) (2007) 51–58. doi:10.1007/s11760-007-0035-2.

- Use of the structure tensor

$$G = \nabla I \otimes \nabla I$$

$$G_{\Omega}(x) = \int_{\Omega(W_r)} K(y)G(x-y)\ \mathrm{d}y$$

$$G\mathbf{u} = \lambda\mathbf{u} \qquad \lambda_{\min} \to u_{\min}$$

Estimation of local fibre direction

XZ-plane

XY-plane

Estimation of local fibre direction

- Influence of the smoothing kernel size W_r

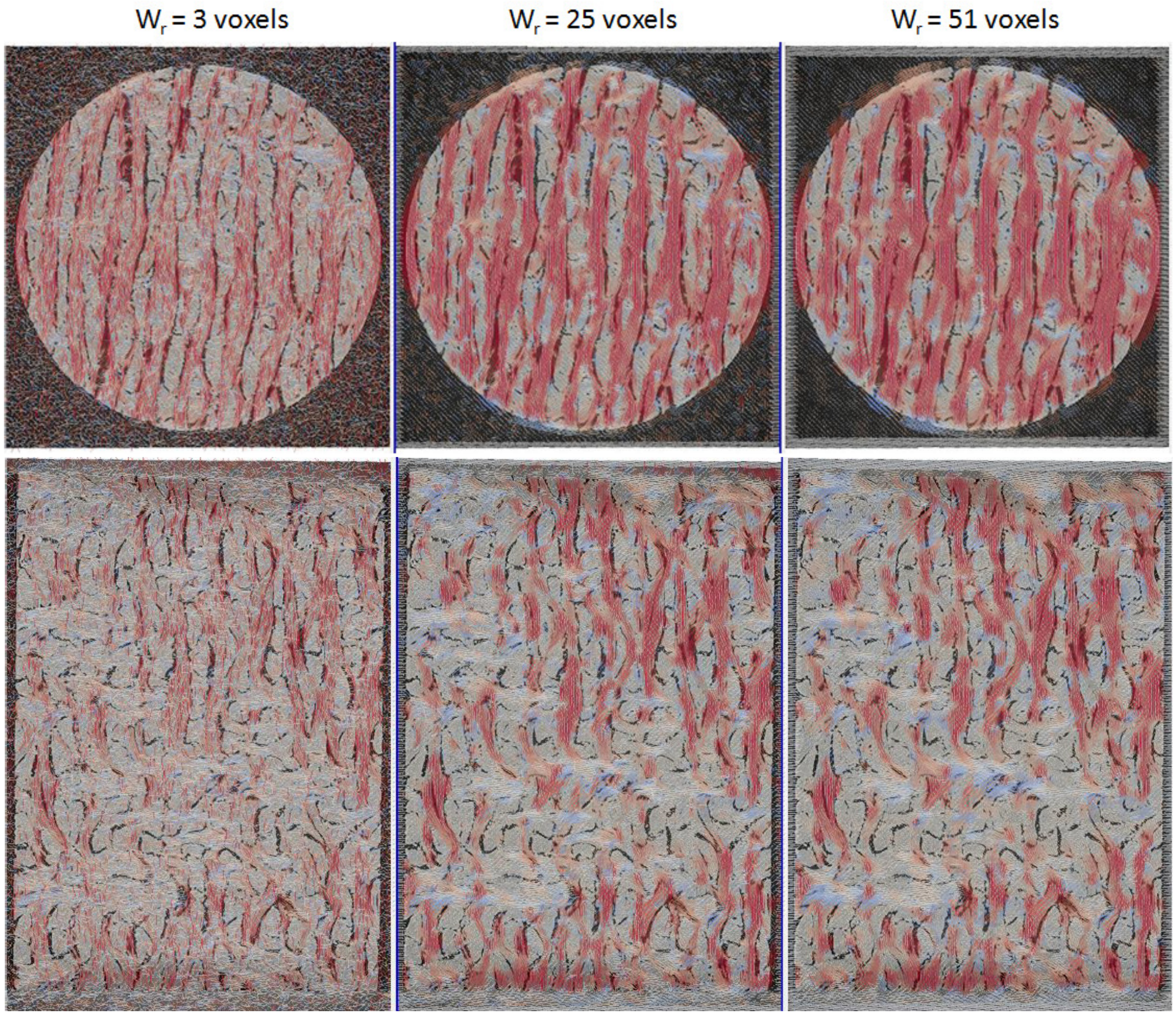

Estimation of local fibre direction

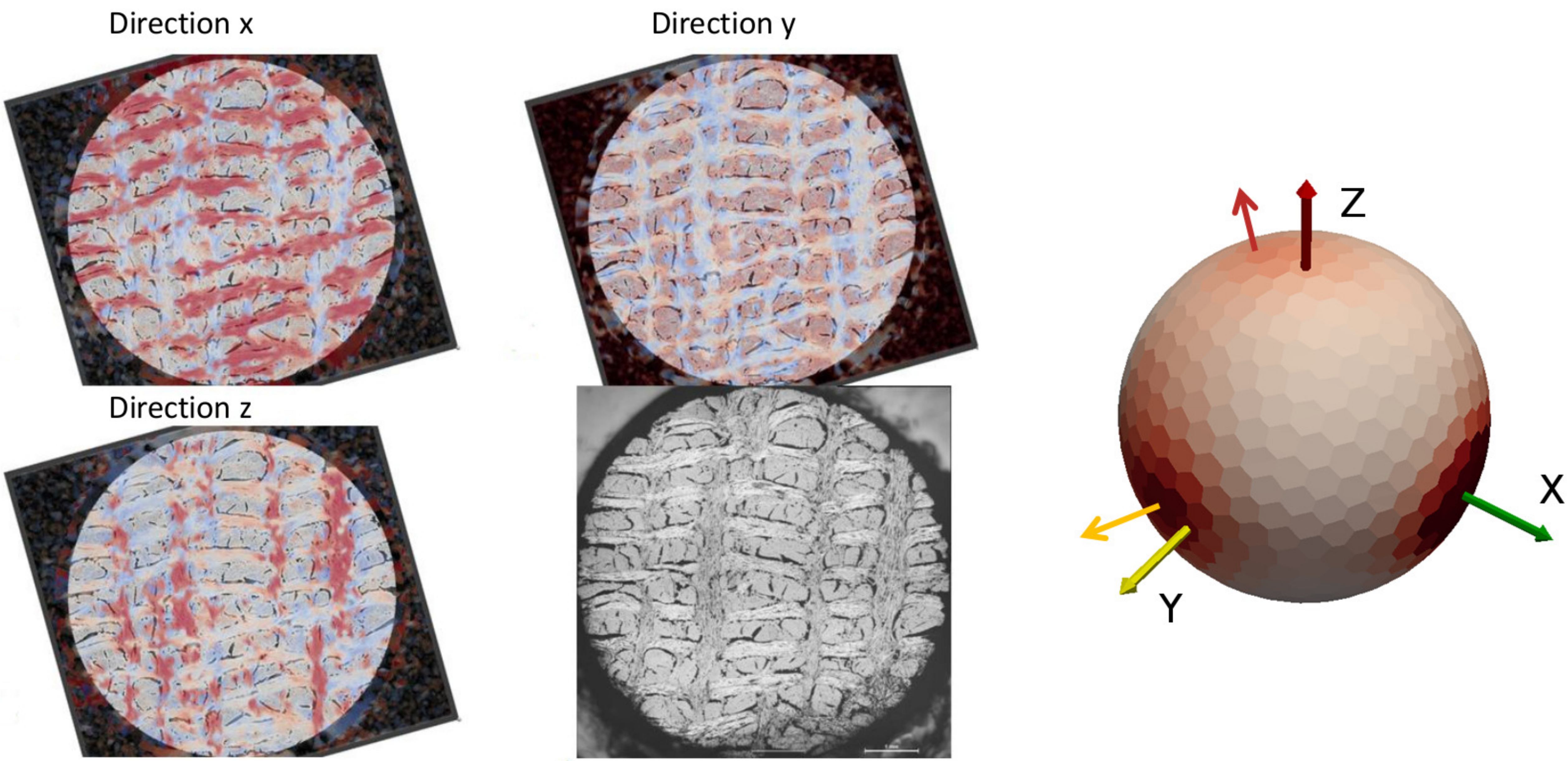

Apparent bundle properties

- Limited variation of fibre/matrix content between bundles
- Apparent properties from microscale image-based models

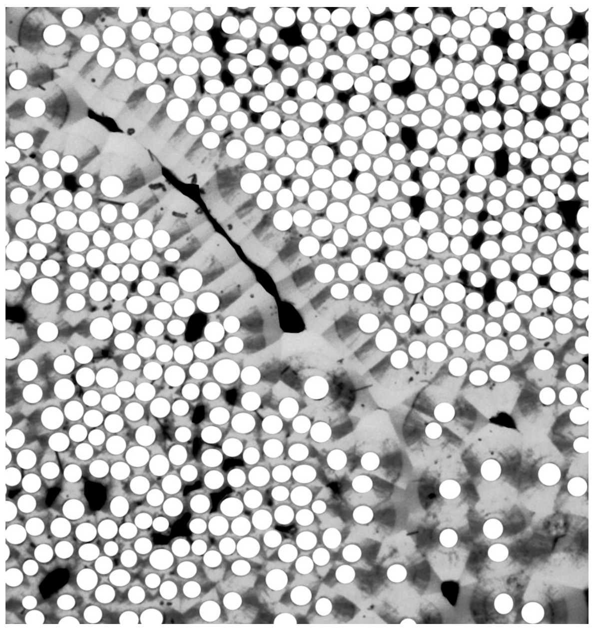

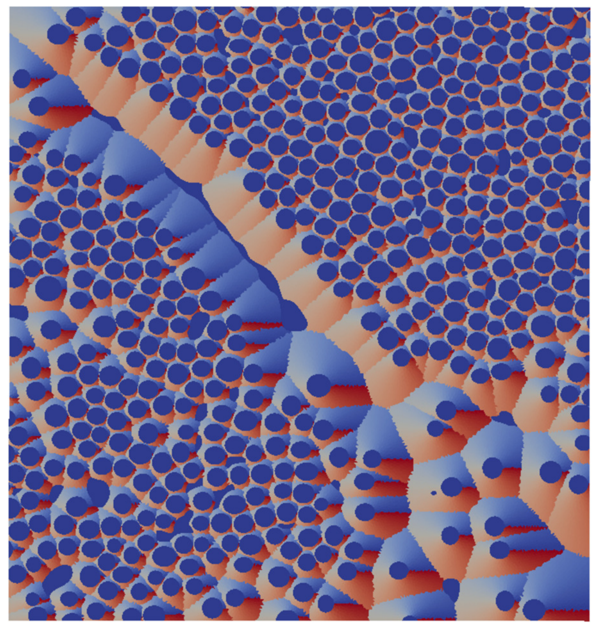

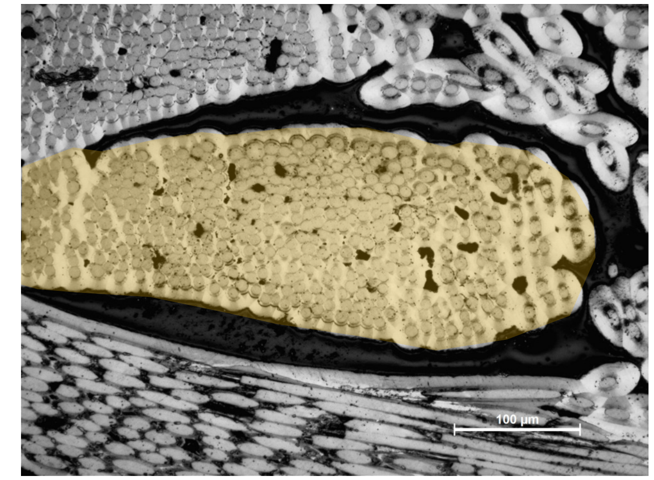

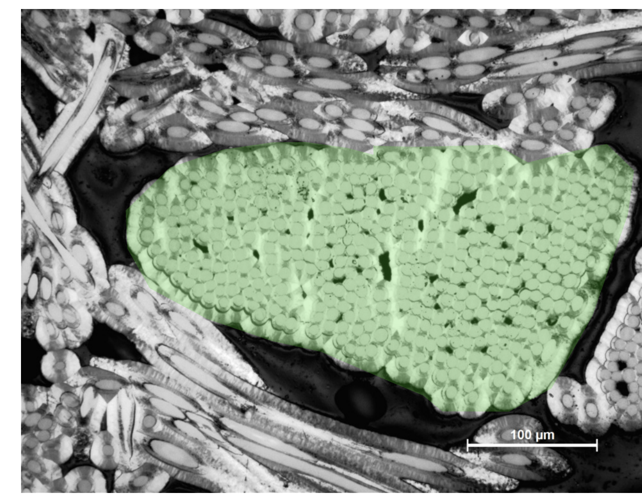

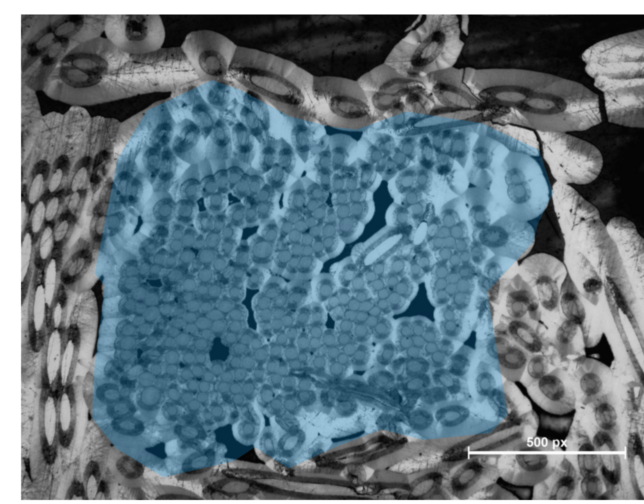

- Average properties (transverse isotropic)

  E_l = 150 GPa, E_t = 15 GPa

  a_l = 1.3 x 10^{-6} °C^{-1}, a_t = 4.5x10^{-6} °C^{-1}

Data derived from µCT

- For each voxel : bundle or porosity + local orientation

Bundle/porosity segmentation

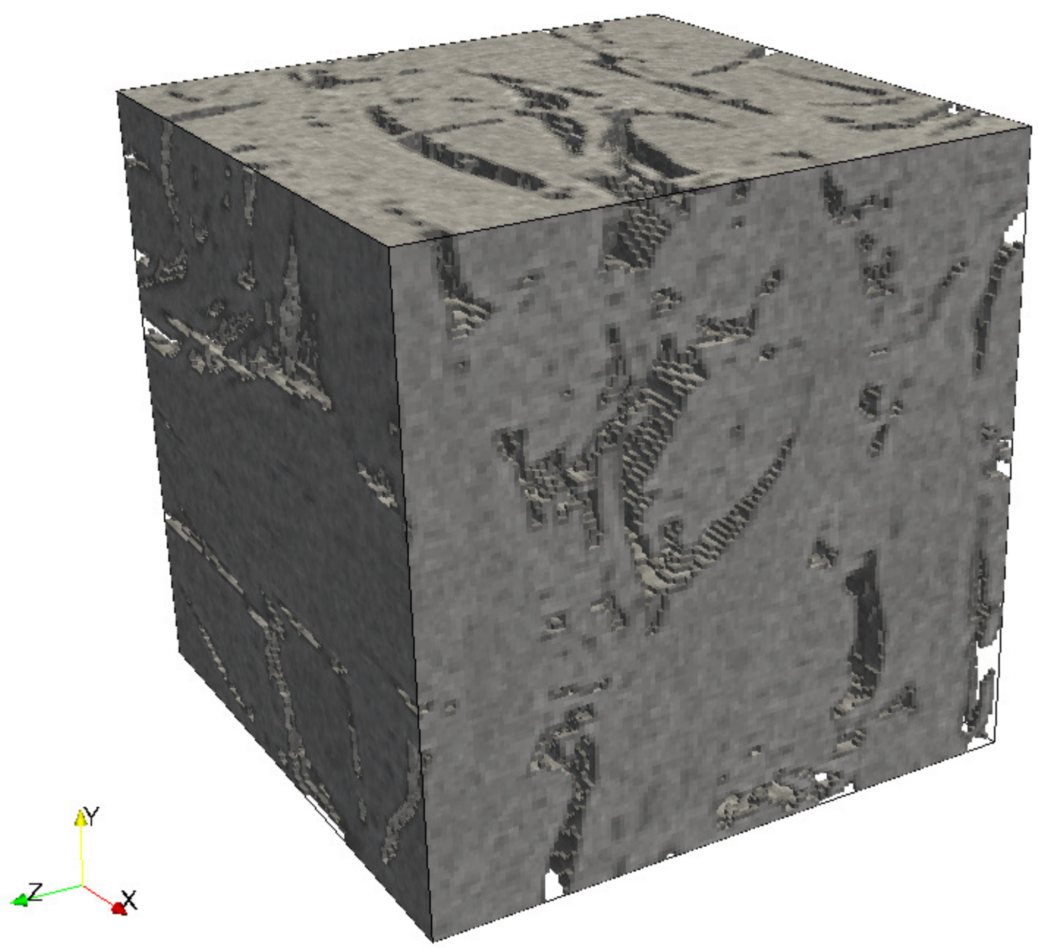

Local orientation

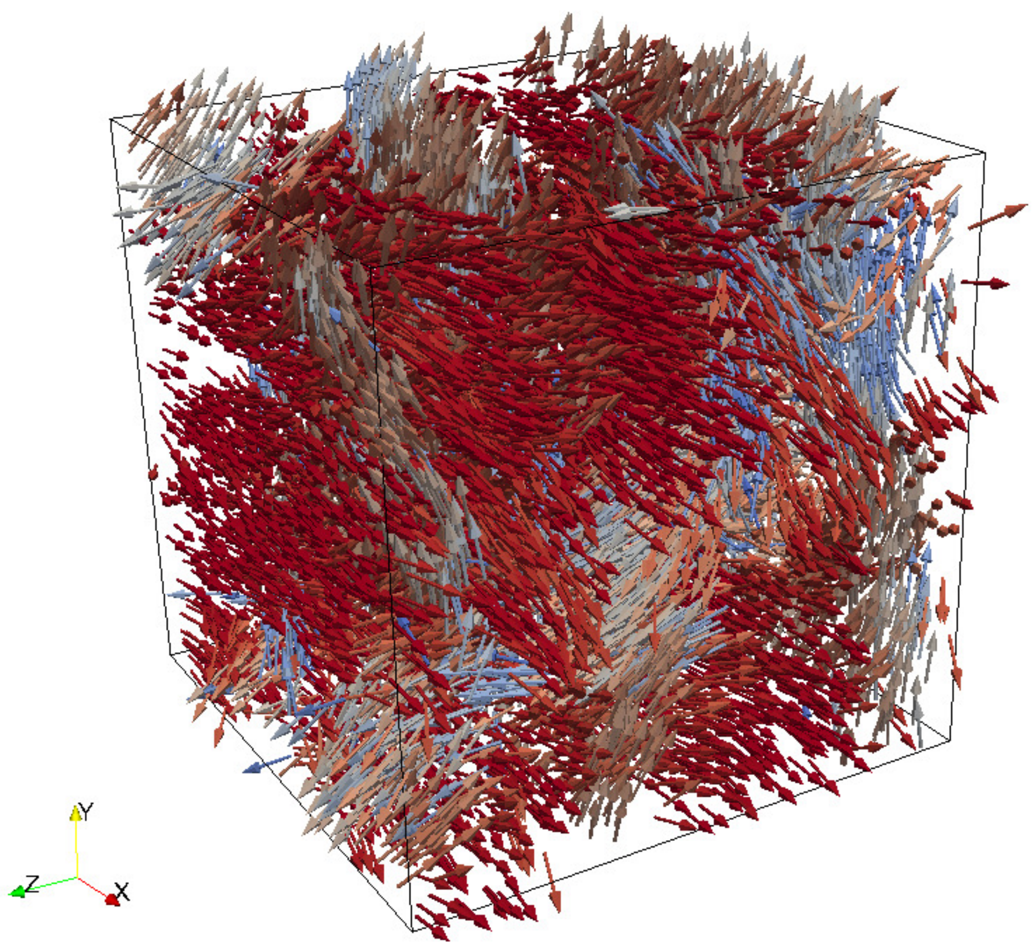

Full-field simulations for moderate-size model

- Lippman-Schwinger equation for thermo-elasticity
- Iterative solver using FFT

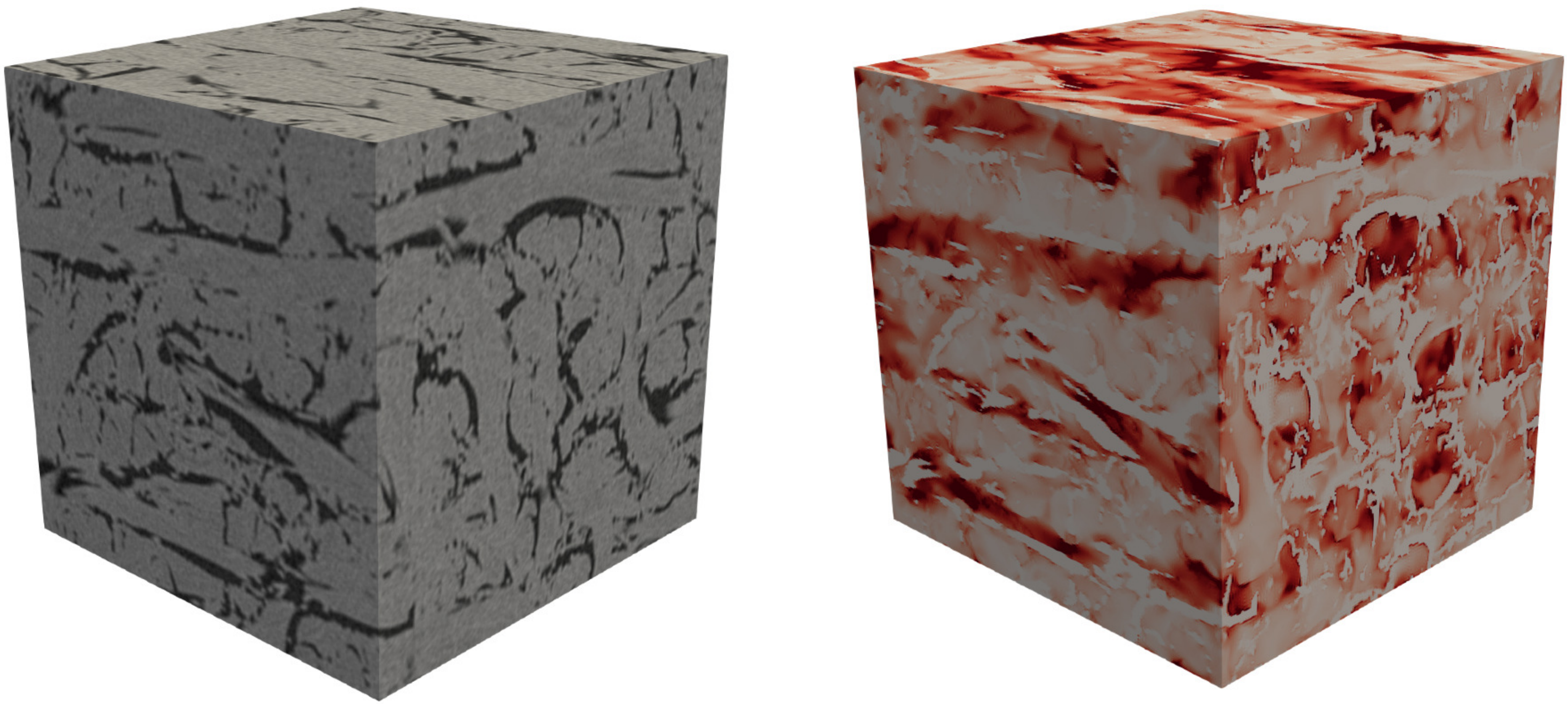

Domain decomposition for larger models

- Decomposition of µCT into sub-volumes
- Computation of apparent properties of each sub-volume (in parallel)
- Effective properties using the coarse mesh

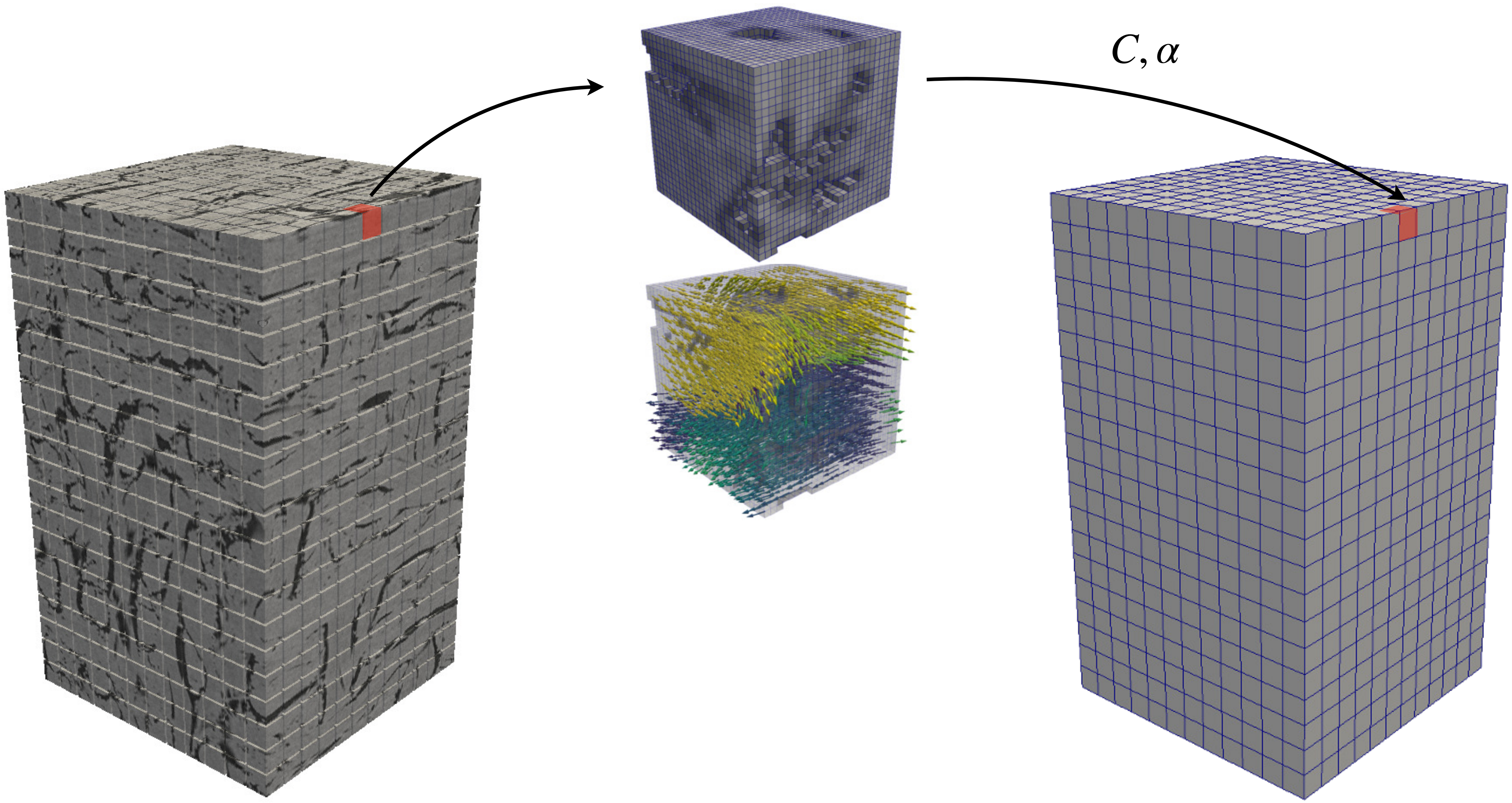

Full-field vs. domain decomposition

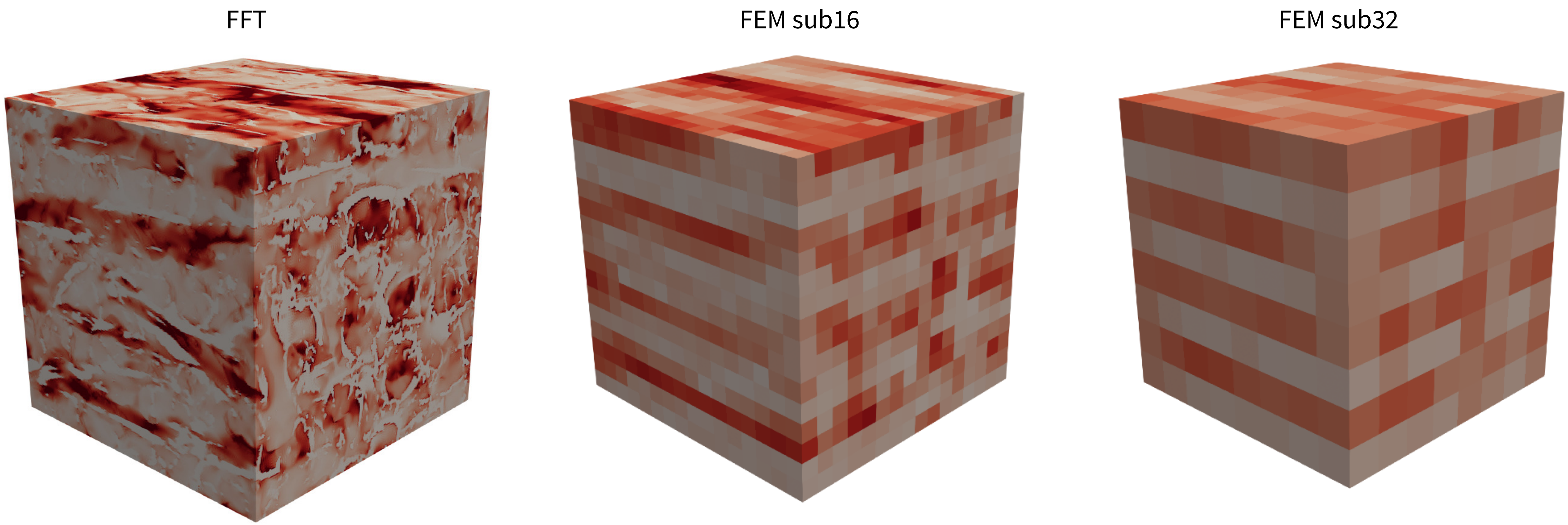

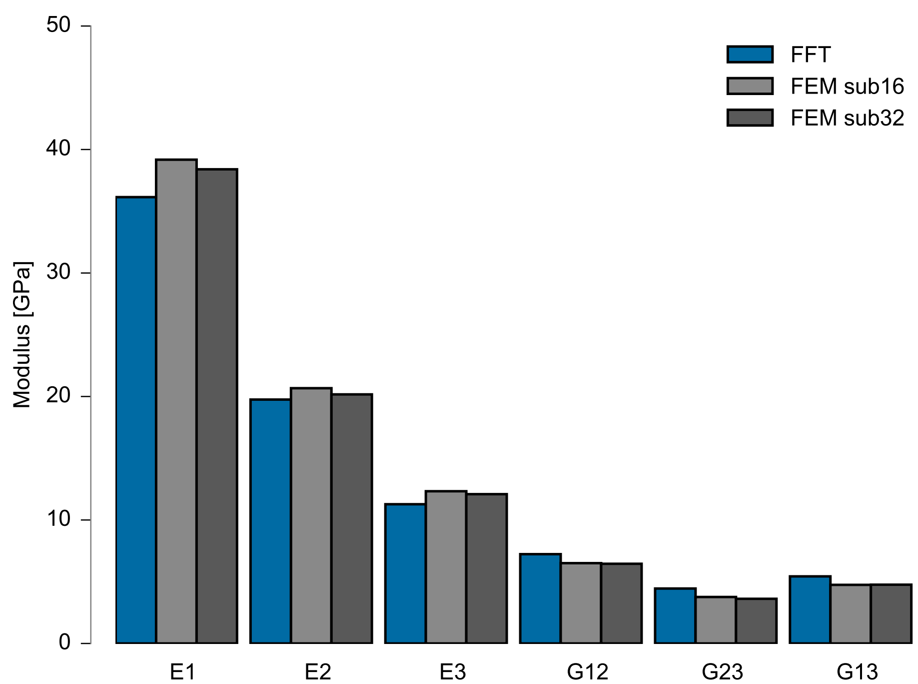

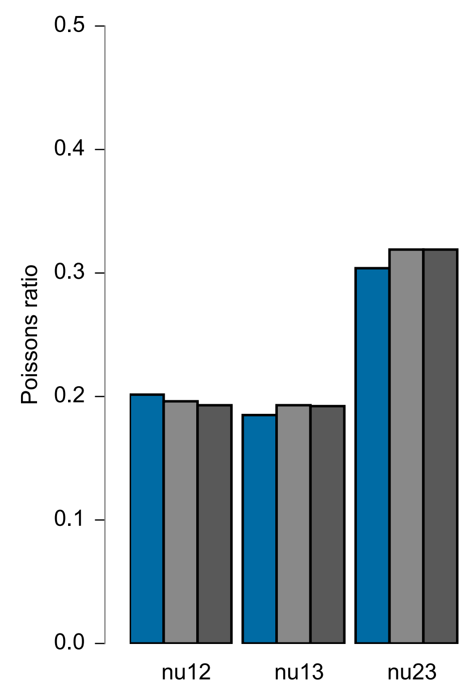

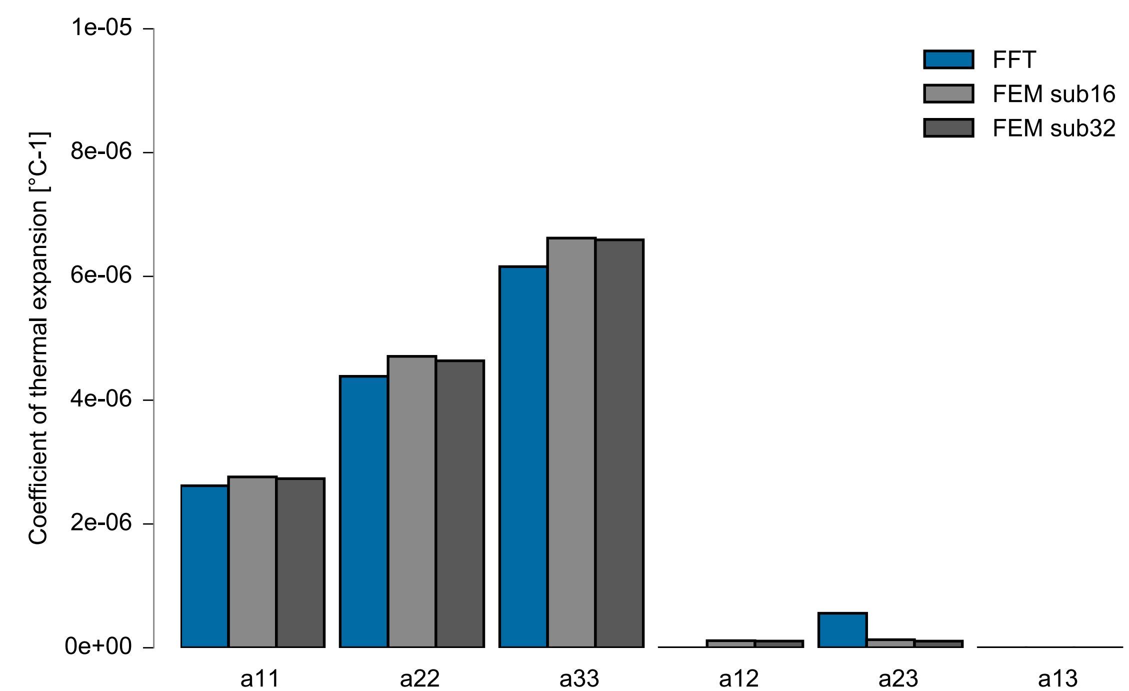

Comparison with experimental results

Elastic moduli @ 25 °C

(GPa)	E_x	E_y	E_z	G_{xy}	G_{yz}	G_{xz}
Exp.	**33**	**22**	-	**6**	-	-
Num.	**32**	**21**	14	**7**	4	5

Thermal expansion @ 1000 °C

(%)	e_x	e_y	e_z
Exp.	0.28	0.16	0.09
Num.	0.37	0.28	0.21

Modelling of a C/C with a non-linear interface model

Ph.D. of Amandine RAUDE (2018)

Needle-punched C/C composite

- Ex-PAN C fiber and CVI pyC matrix
- Needle-punched UD plies (0°/±60°)

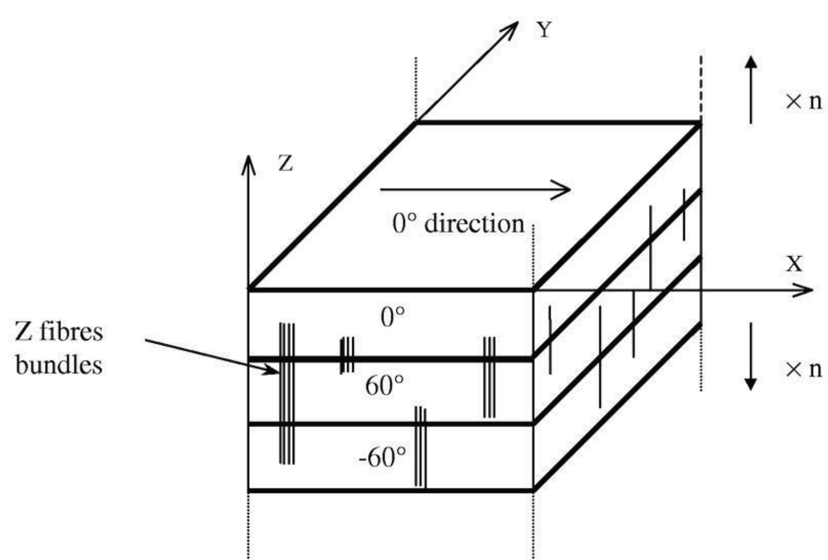

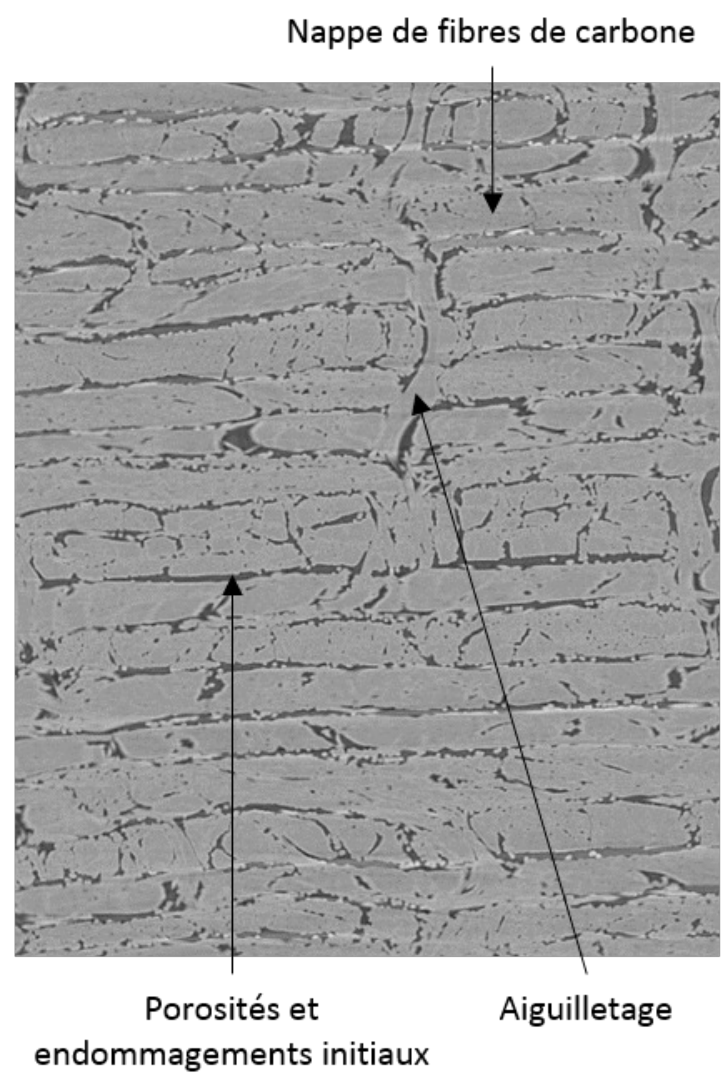

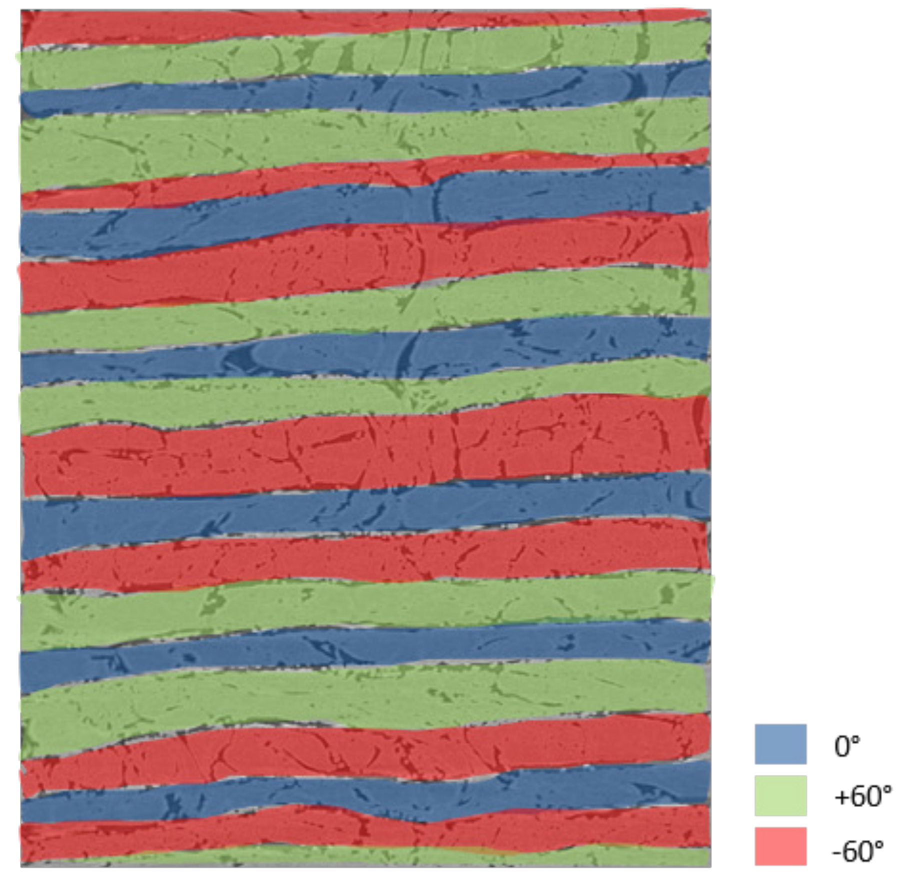

Needle-punched C/C composite

- Lower fibre volume fraction within Z-bundles
- Need to distinguish Z-bundle (needling) from XY-bundle (UD plies)

XY-bundle

Z-bundle

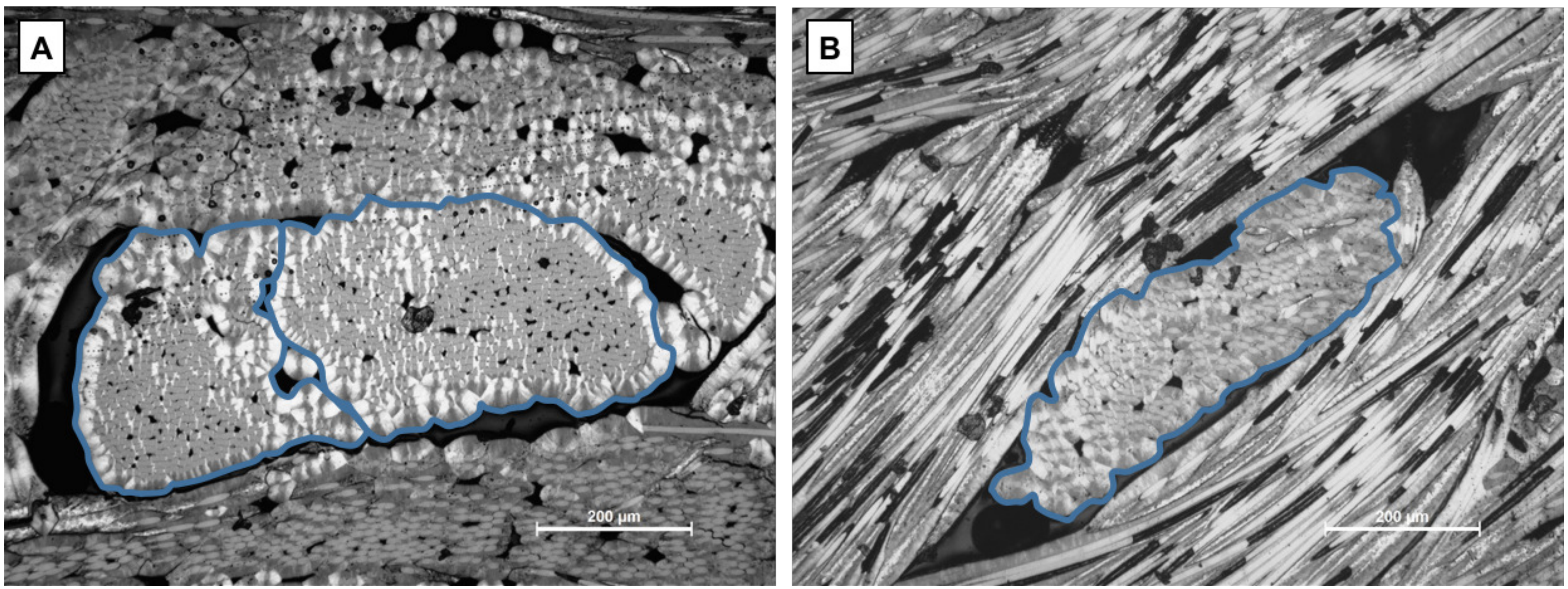

$V_f \approx 40\,\%$

$V_f \approx 20\,\%$

Introduction of non-linear interface models

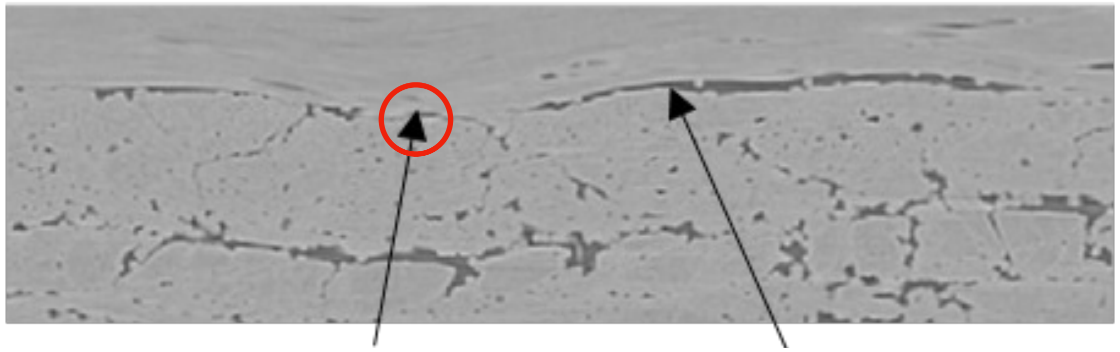

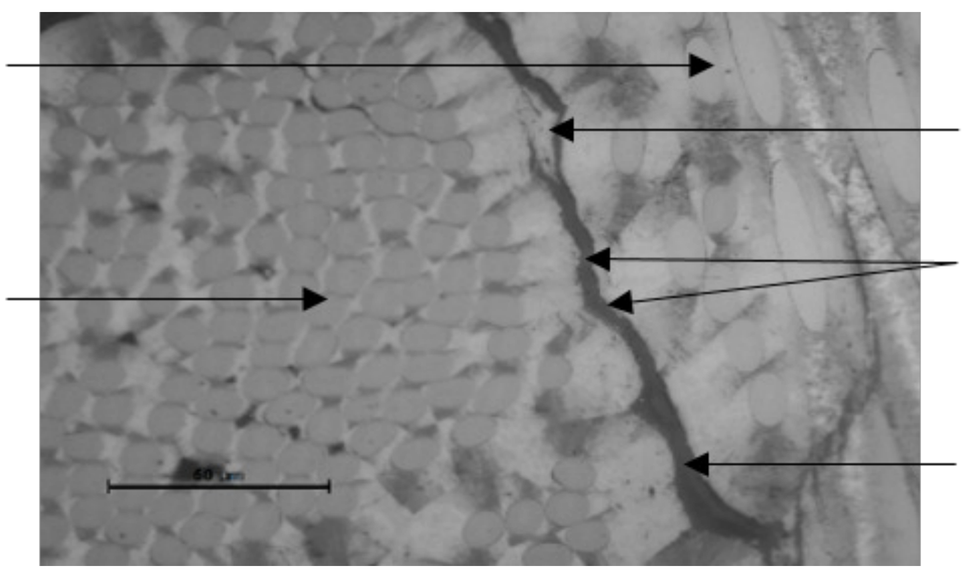

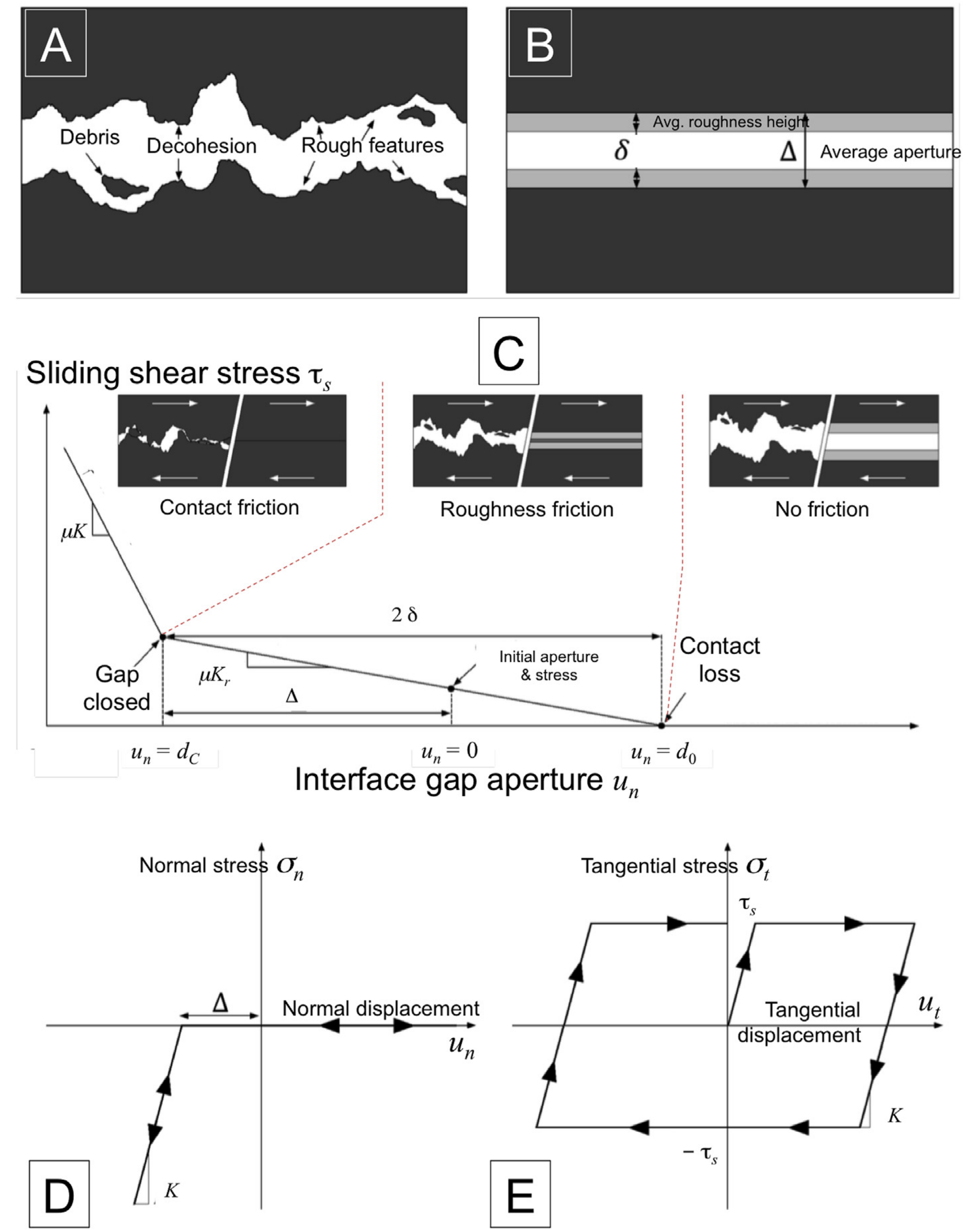

- Need to explicitly define interfaces between plies and with Z-bundles

A. P. Gillard, G. Couégnat, S. Chupin, G. L. Vignoles, Modeling of the non-linear mechanical and thermo-mechanical behavior of 3D carbon/carbon composites based on internal interfaces, Carbon 154 (2019) 178–191. doi:10.1016/j.carbon.2019.07.101.

Preliminary model

- Manual labelling on a small volume (4 plies)

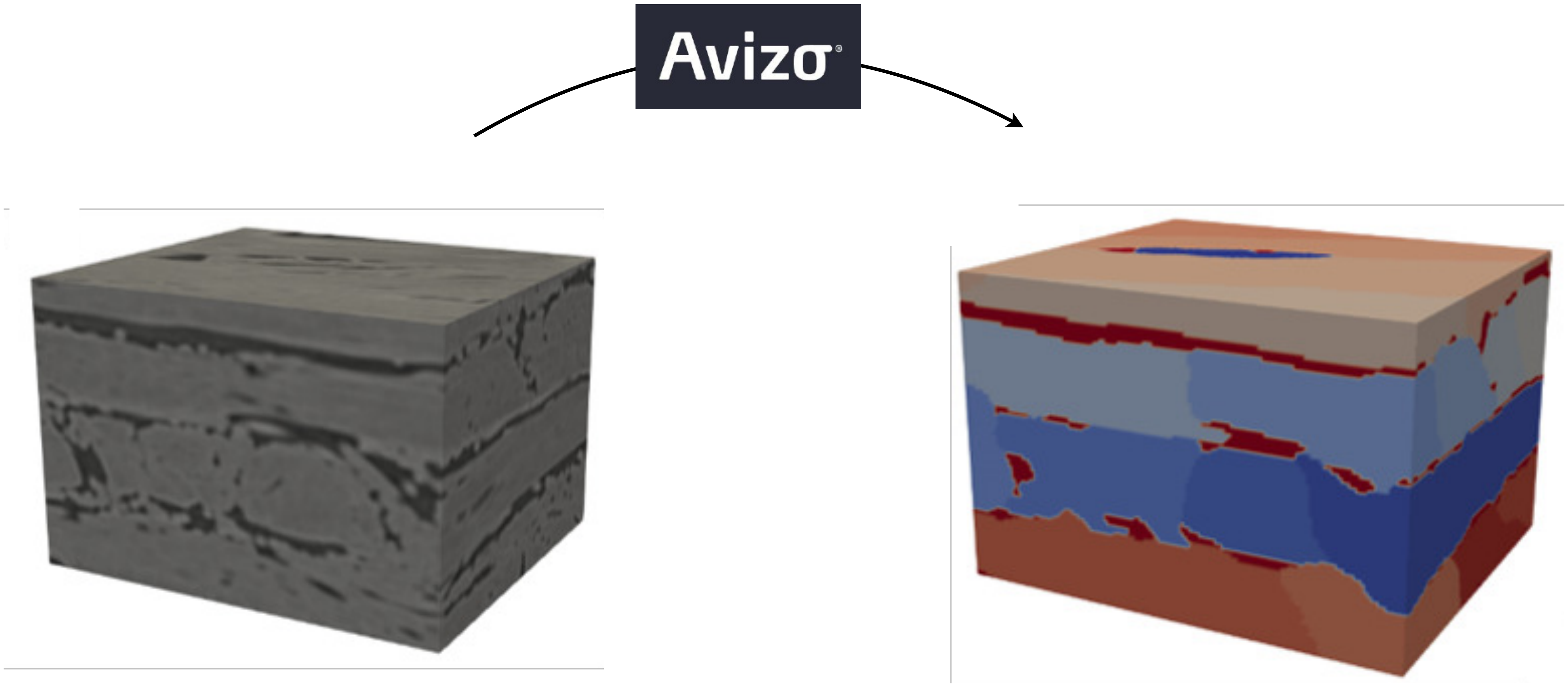

Preliminary model

- Conforming tetrahedral mesh from labelled volume
- Initial coarse volume mesh of the bounding box
- Iterative Delaunay refinement with criterion on Hausdorff distance

CGAL

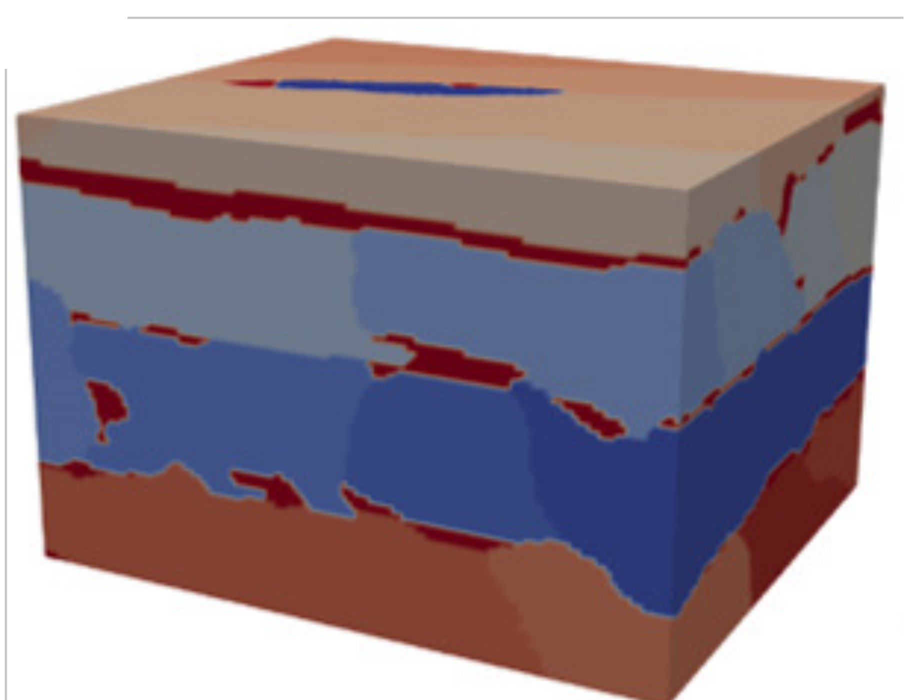

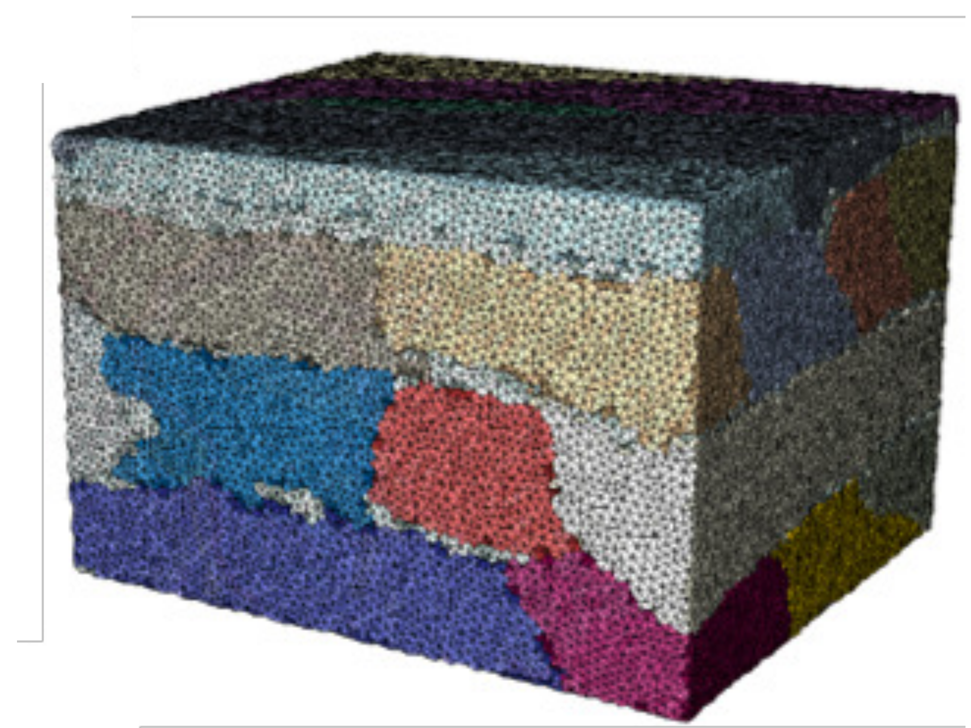

A side note on CGAL

- CGAL: Computational Geometry Algorithms Library
- C++ library, many packages including multi-domain 3D meshing, tetrahedral remeshing, etc.

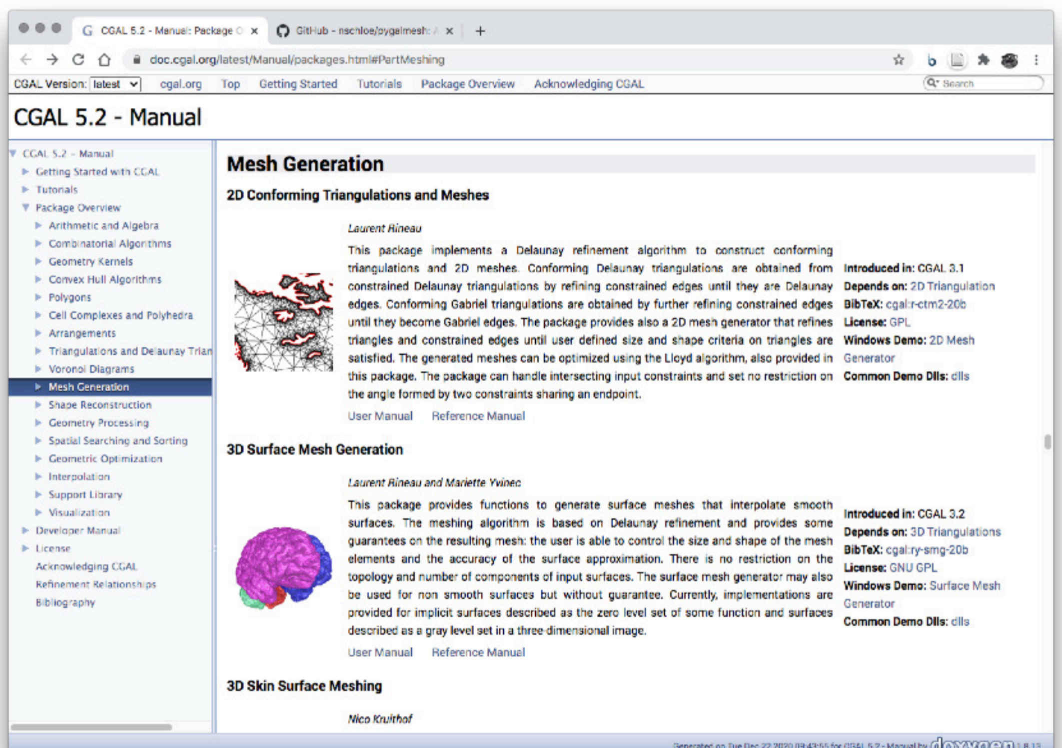

`https://www.cgal.org/`

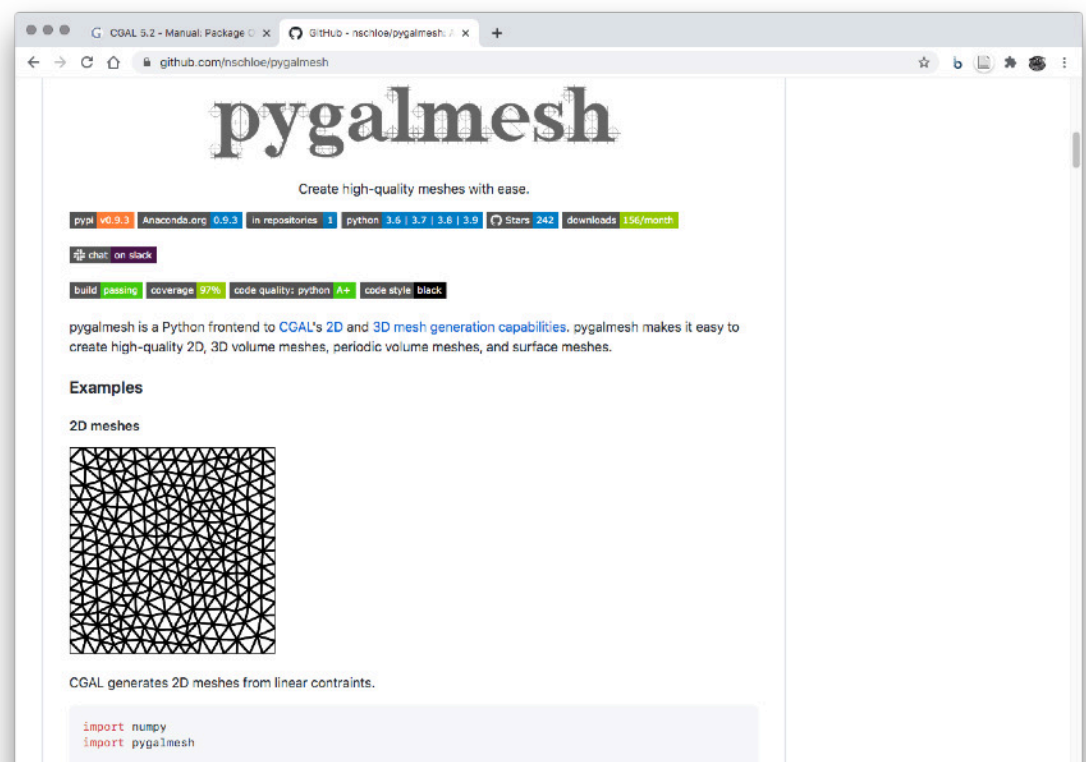

`https://github.com/nschloe/pygalmesh`

FE mesh from manual labelling

- Plies (0°/+60°/-60°) + Z-bundles + porosity
- Insertion of interface elements

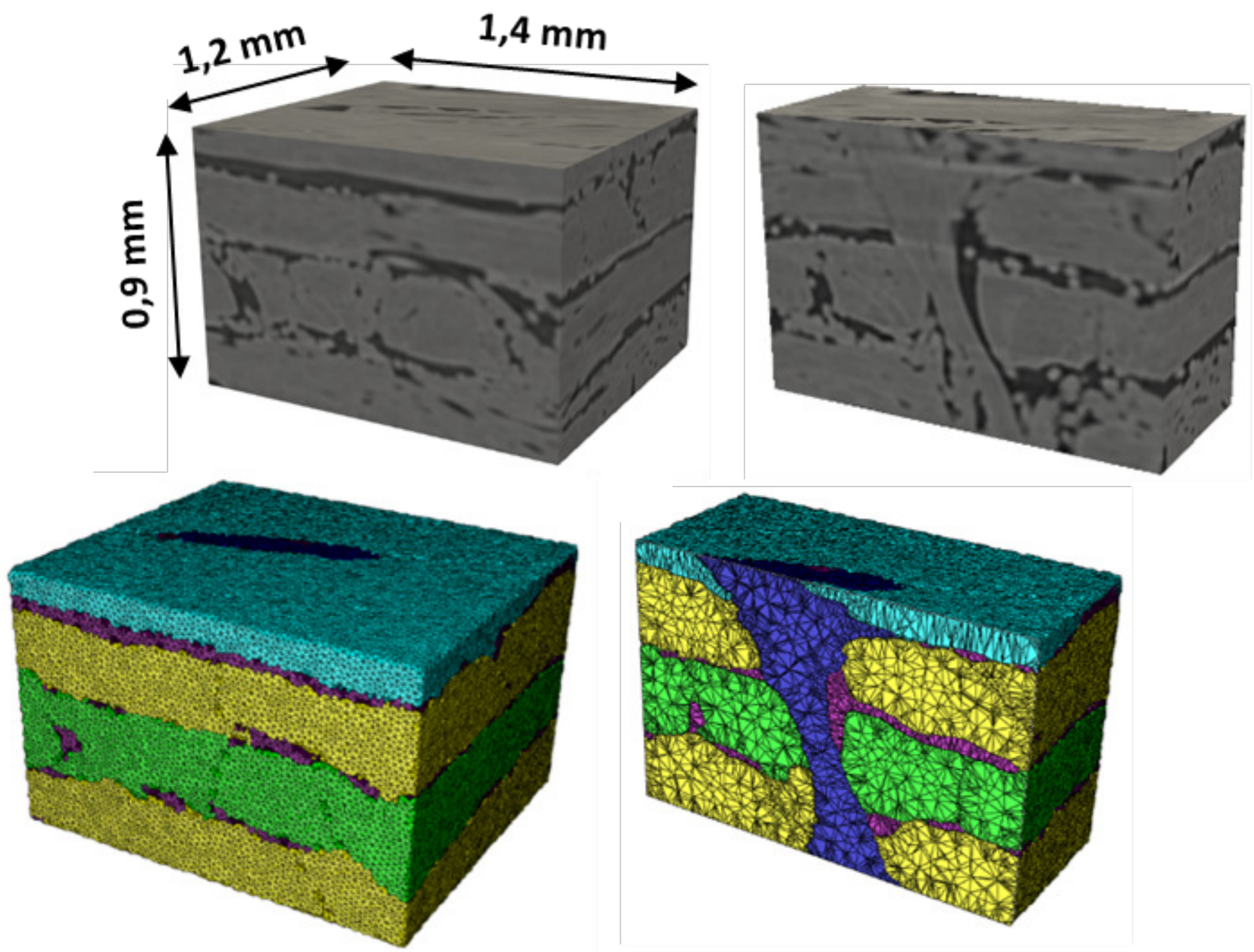

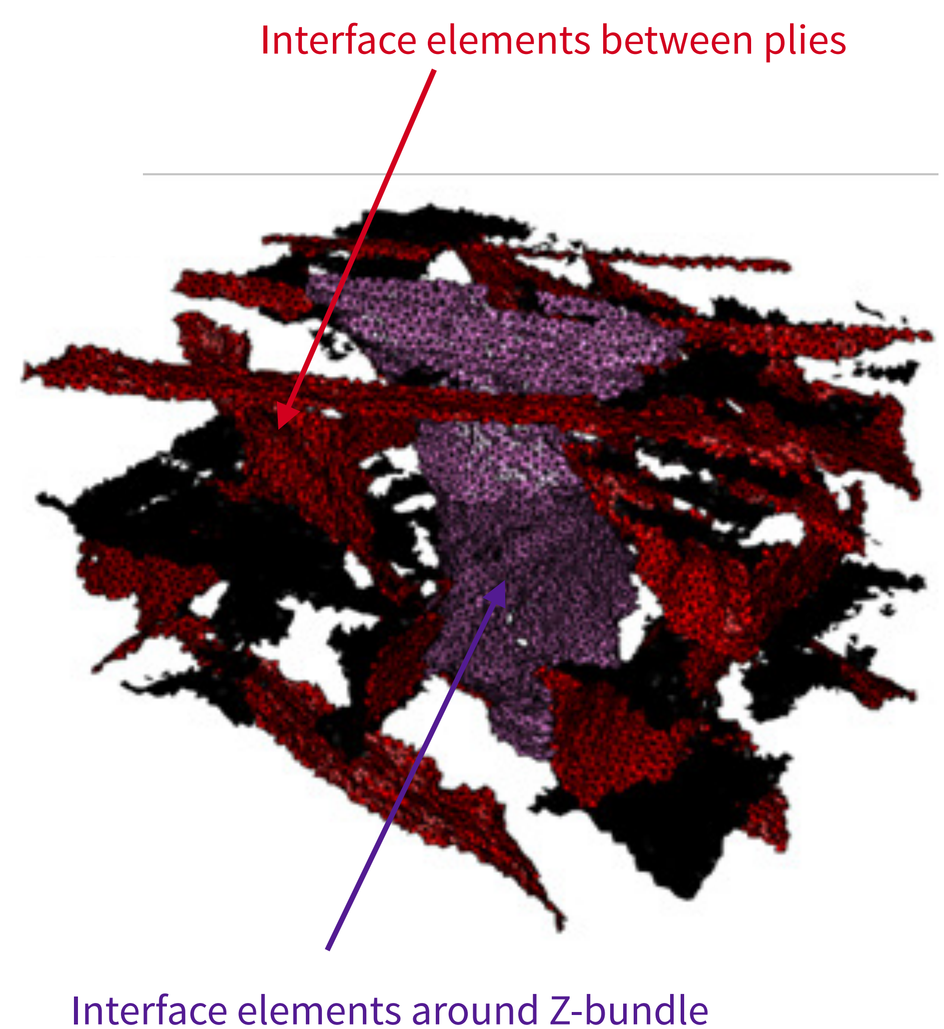

Automatisation of the labelling process

- Create masks for each entity by thresholding the local direction

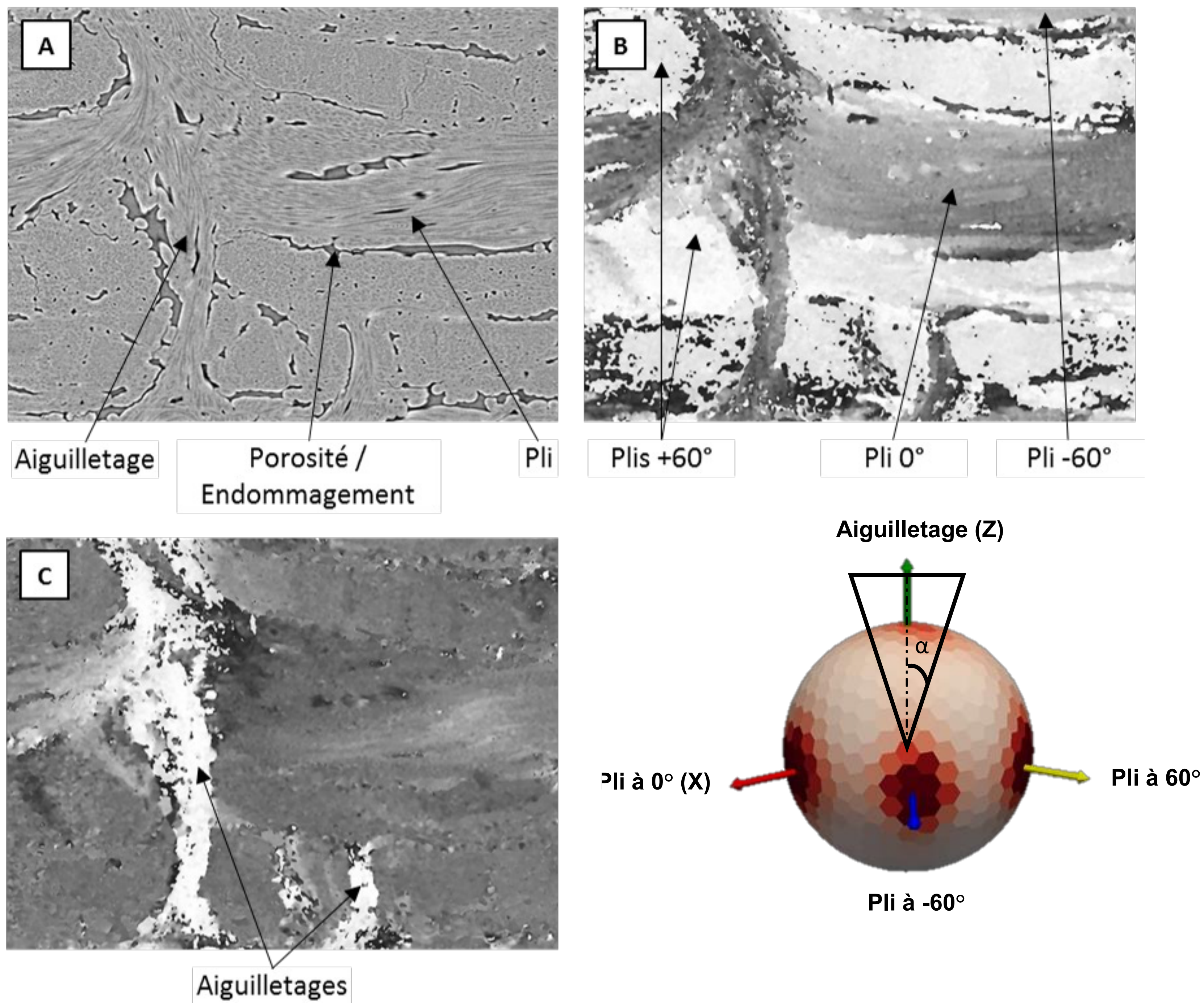

Local direction from structure tensor

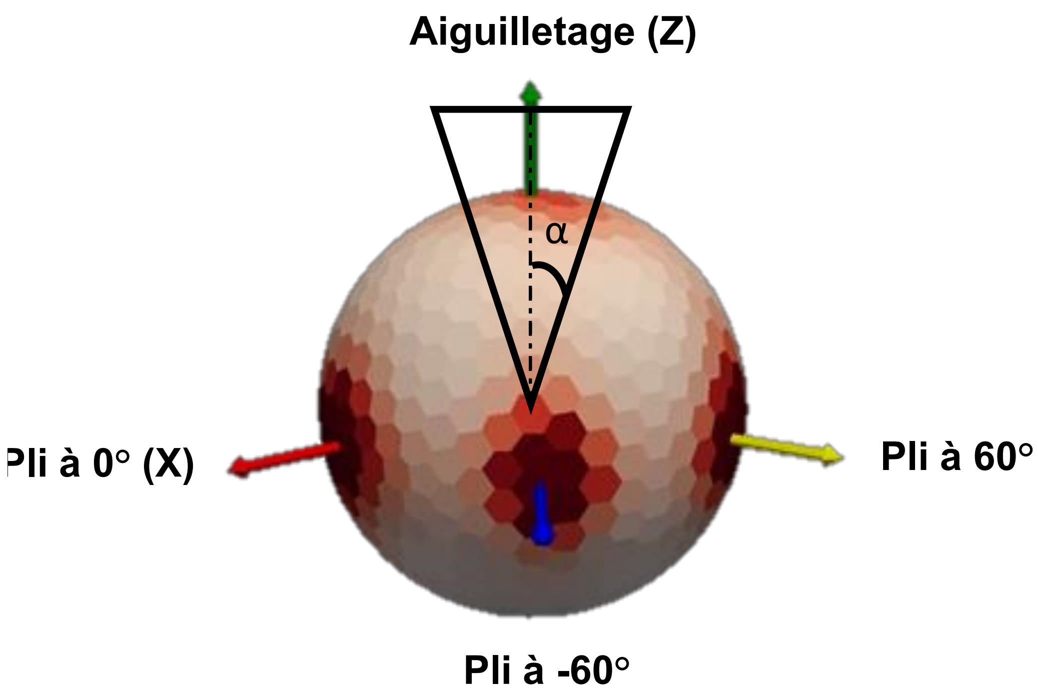

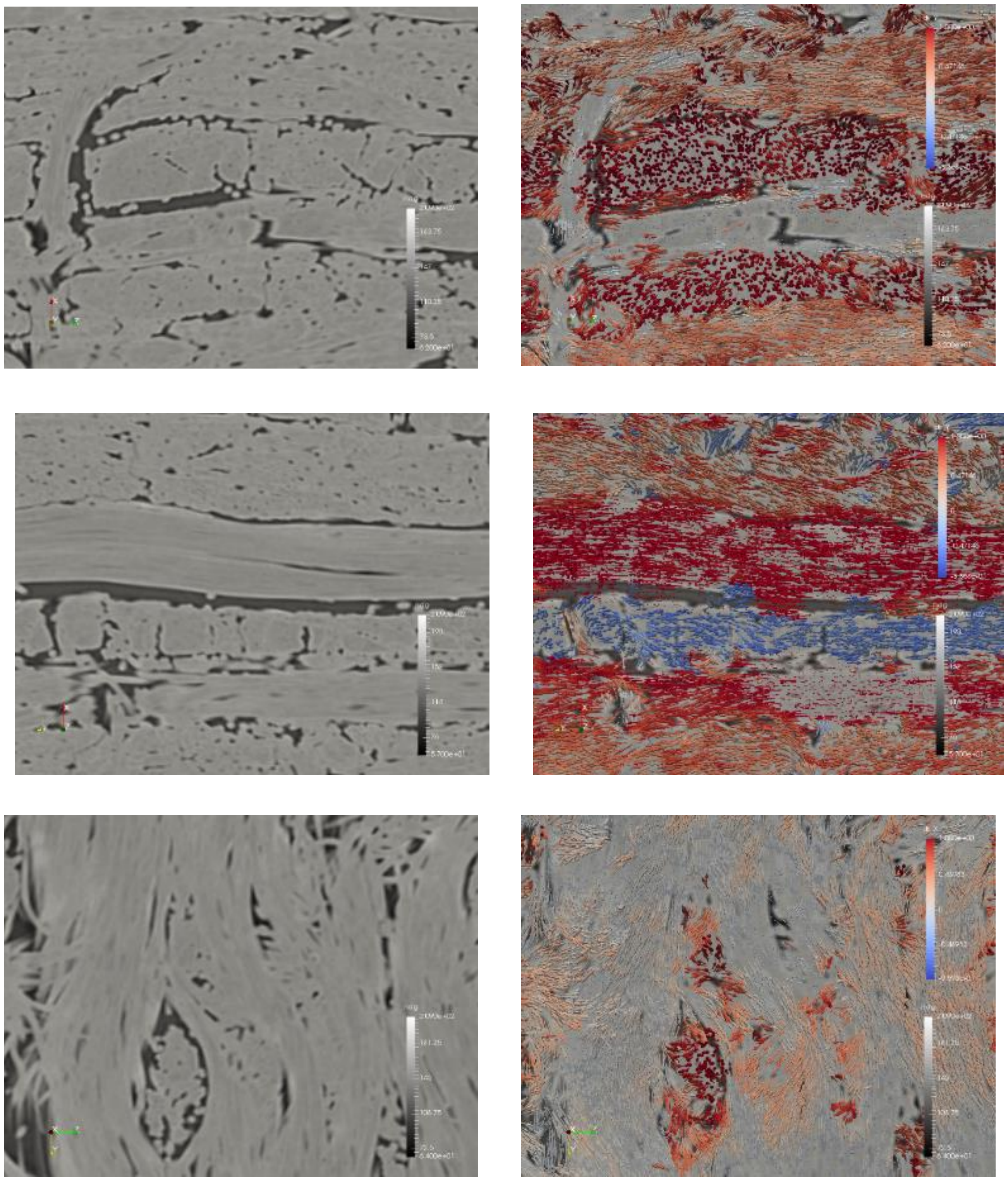

Automatisation of the labelling process

- Masks for ply bundles (one for each direction)

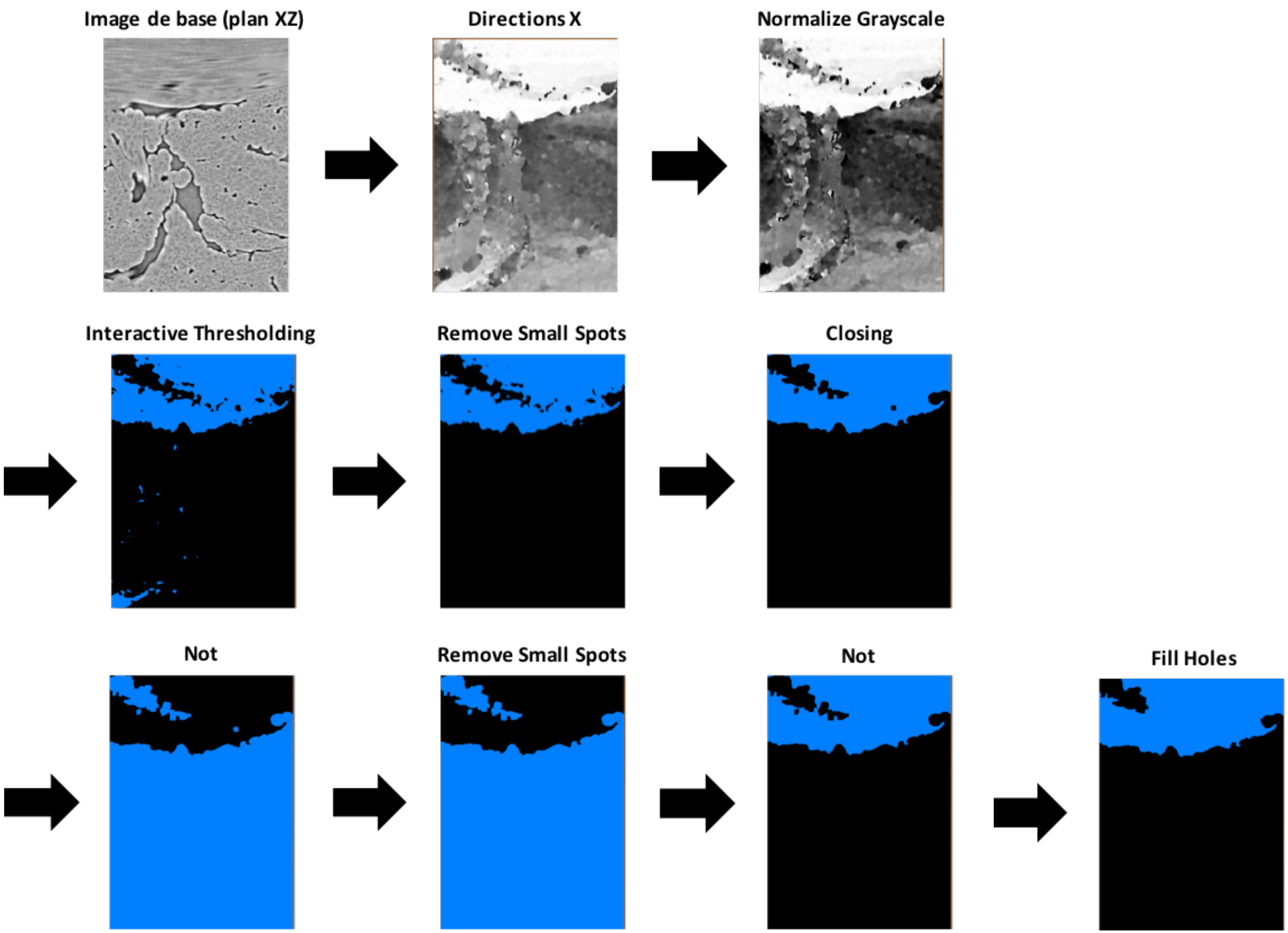

Automatisation of the labelling process

- Fusion of all the masks + cleaning

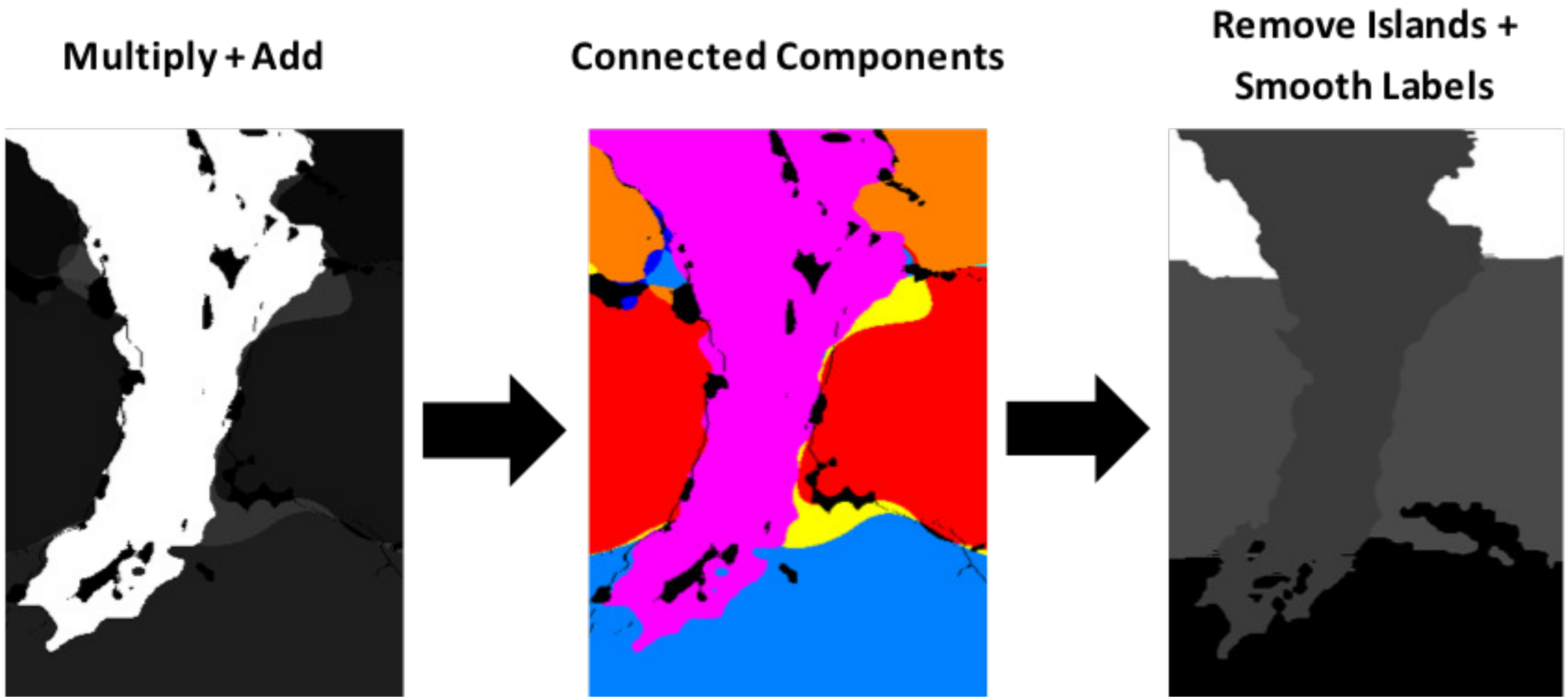

Automatisation of the labelling process

- Comparison with manual labelling

μCT　　Manual labelling　　Automated labelling

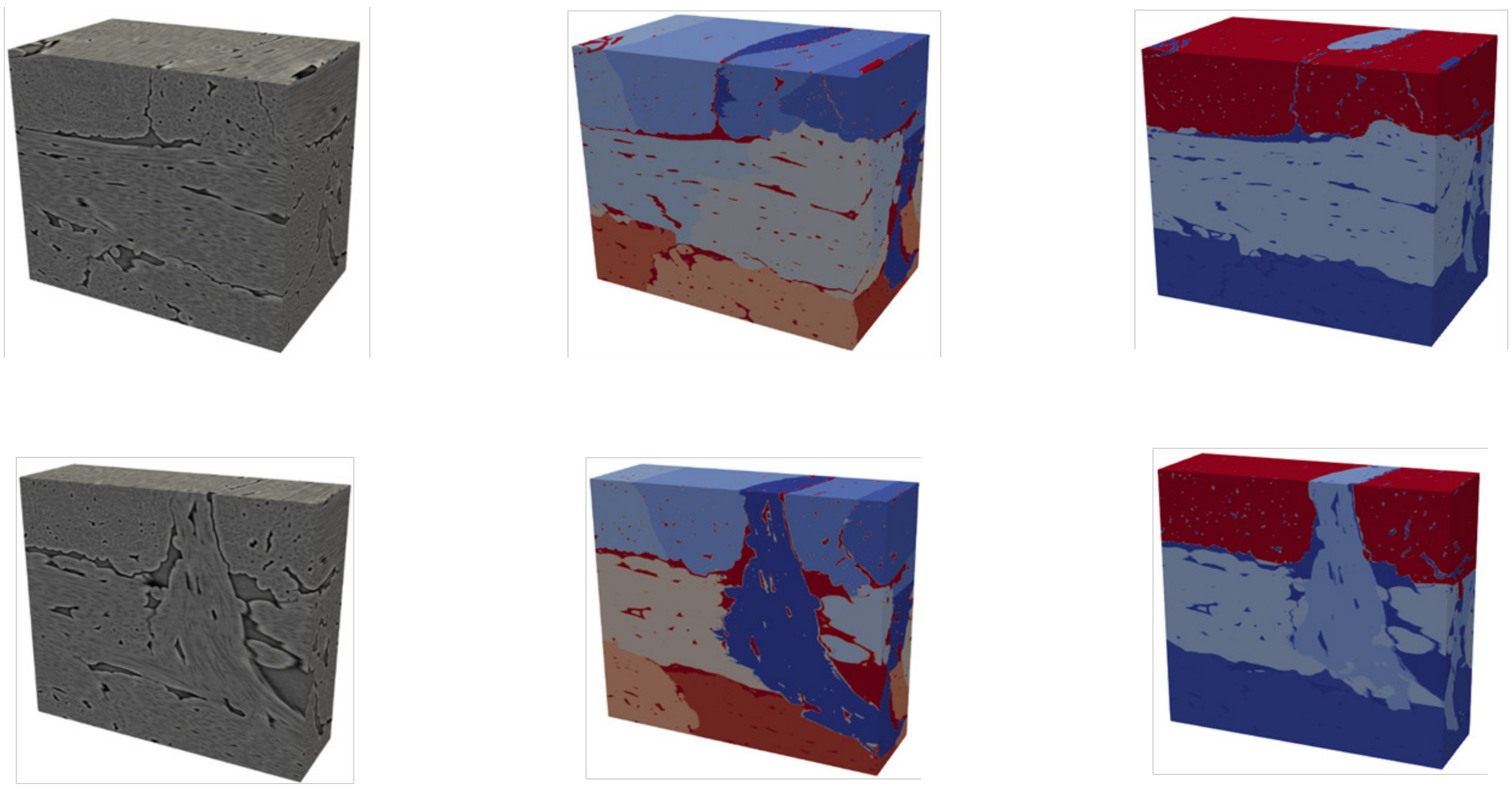

Automatisation of the labelling process

- Comparison with manual labelling

Manual labelling

Automated labelling

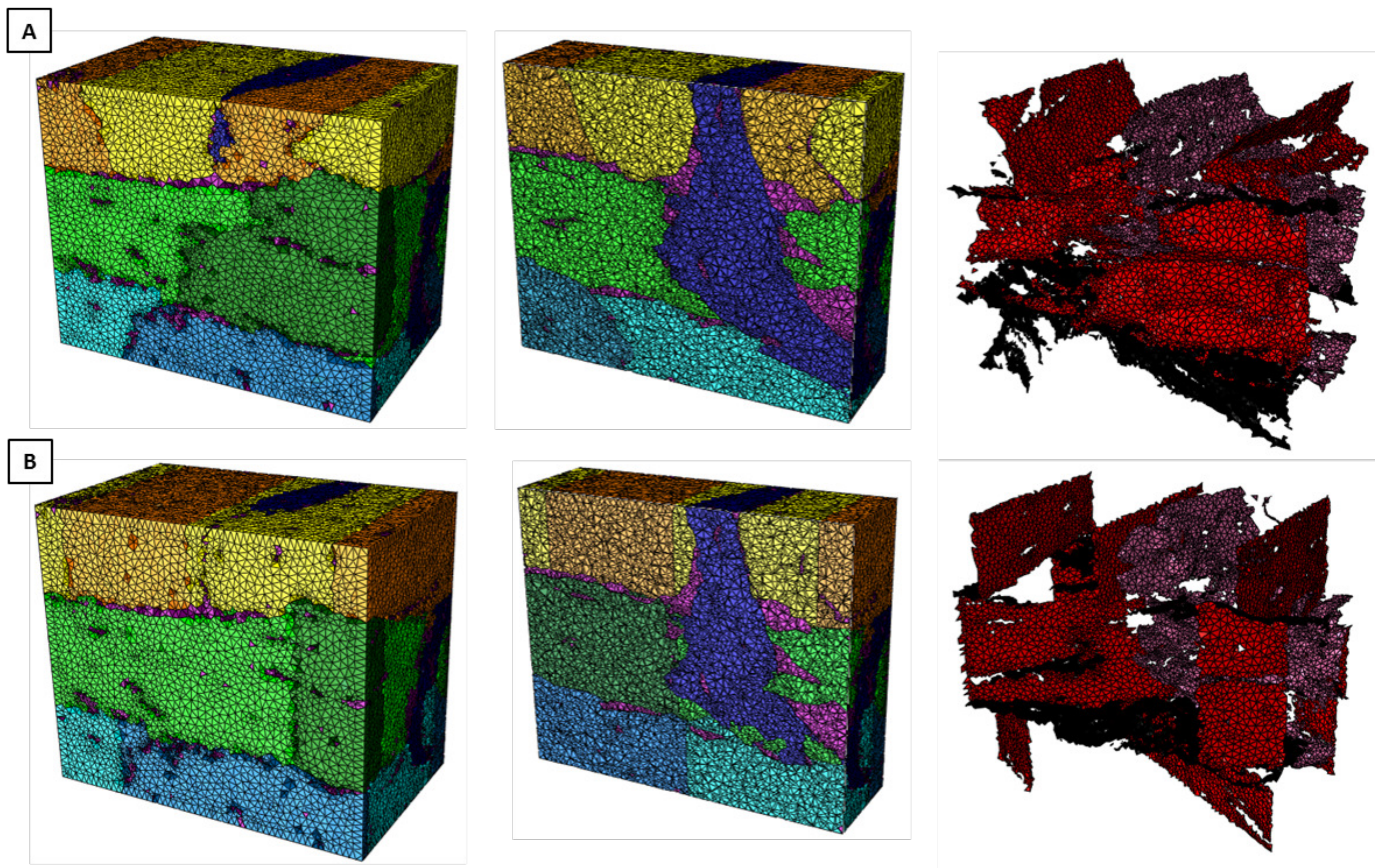

FE models from automated labelling

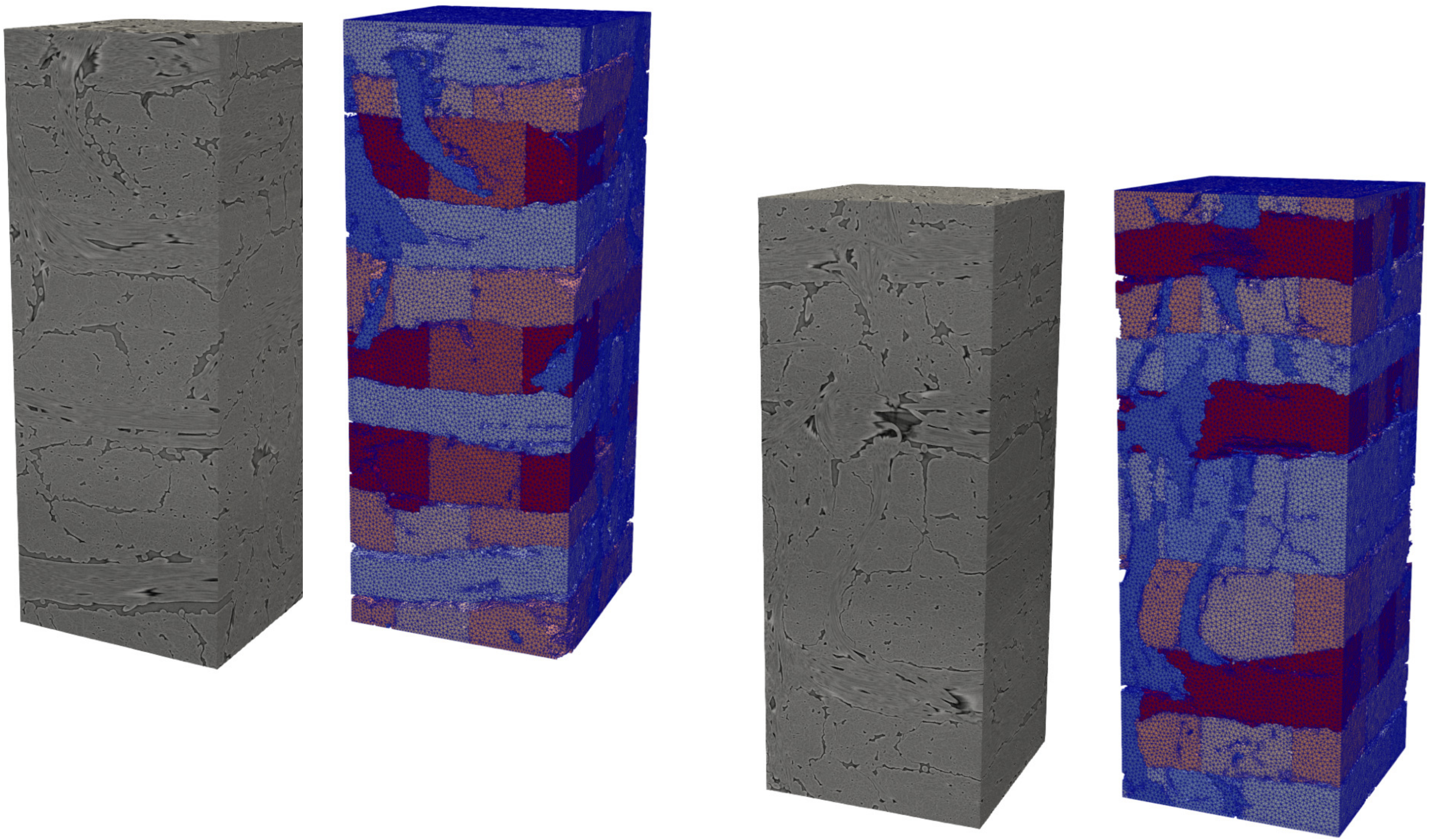

Prediction of the thermal expansion

- 5 large FE models extracted from different zones of the material
- Unilateral interface model with friction
- Predictions within the experimental variability (except at 500 °C because of unreliable data for matrix CTE)

XY-direction

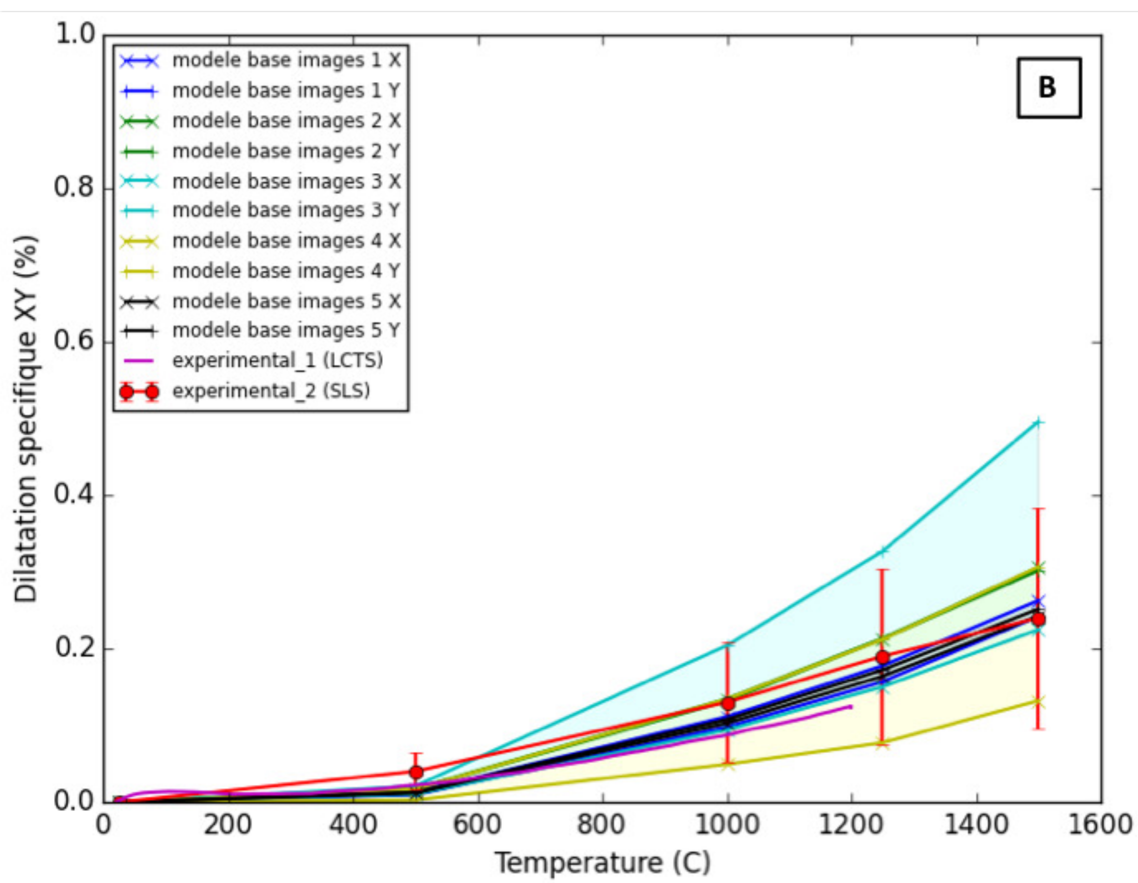

Z-direction

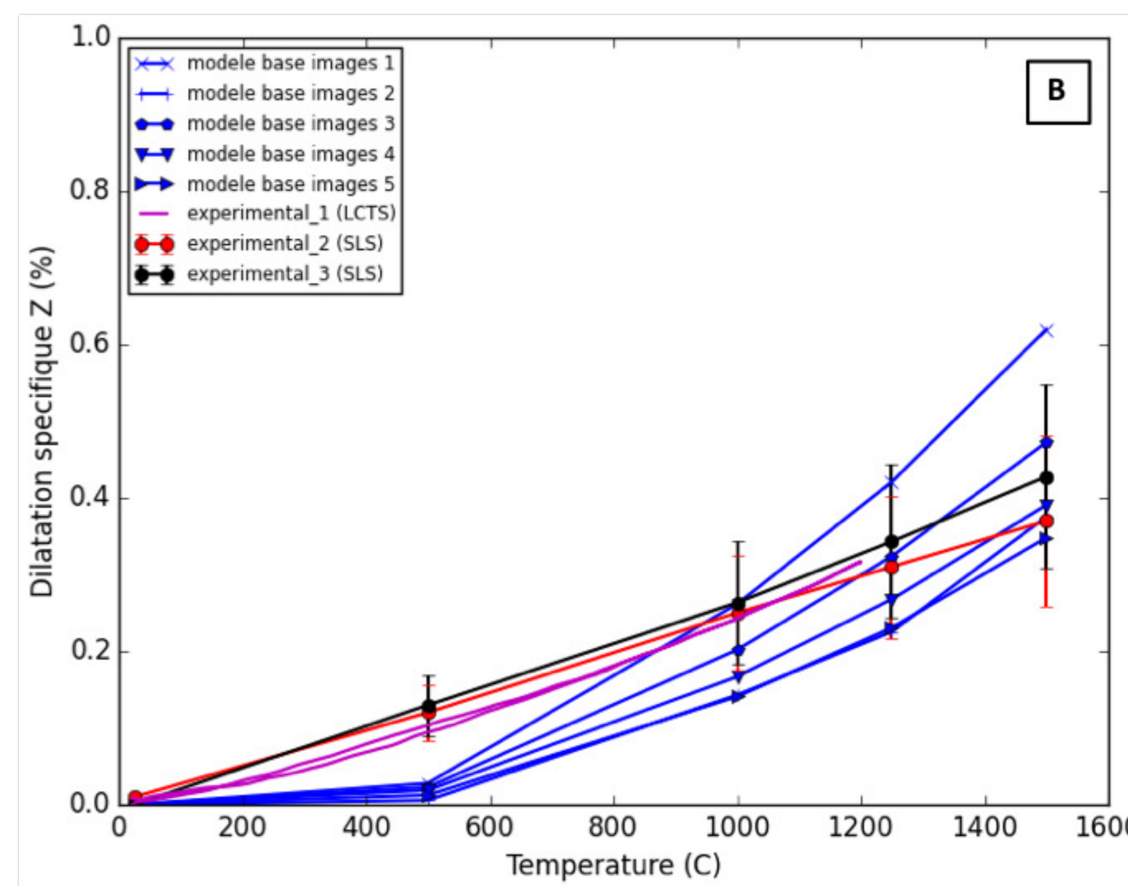

High-fidelity FE mesoscale models of woven CMC

Ph.D. of Vincent MAZARS (2018) & Jean BÉNÉZECH (2019)

High-fidelity FE mesoscale models of woven CMC

- Yarns + matrix
- Each yarn must be labelled individually
- Correct topology of the weaving pattern

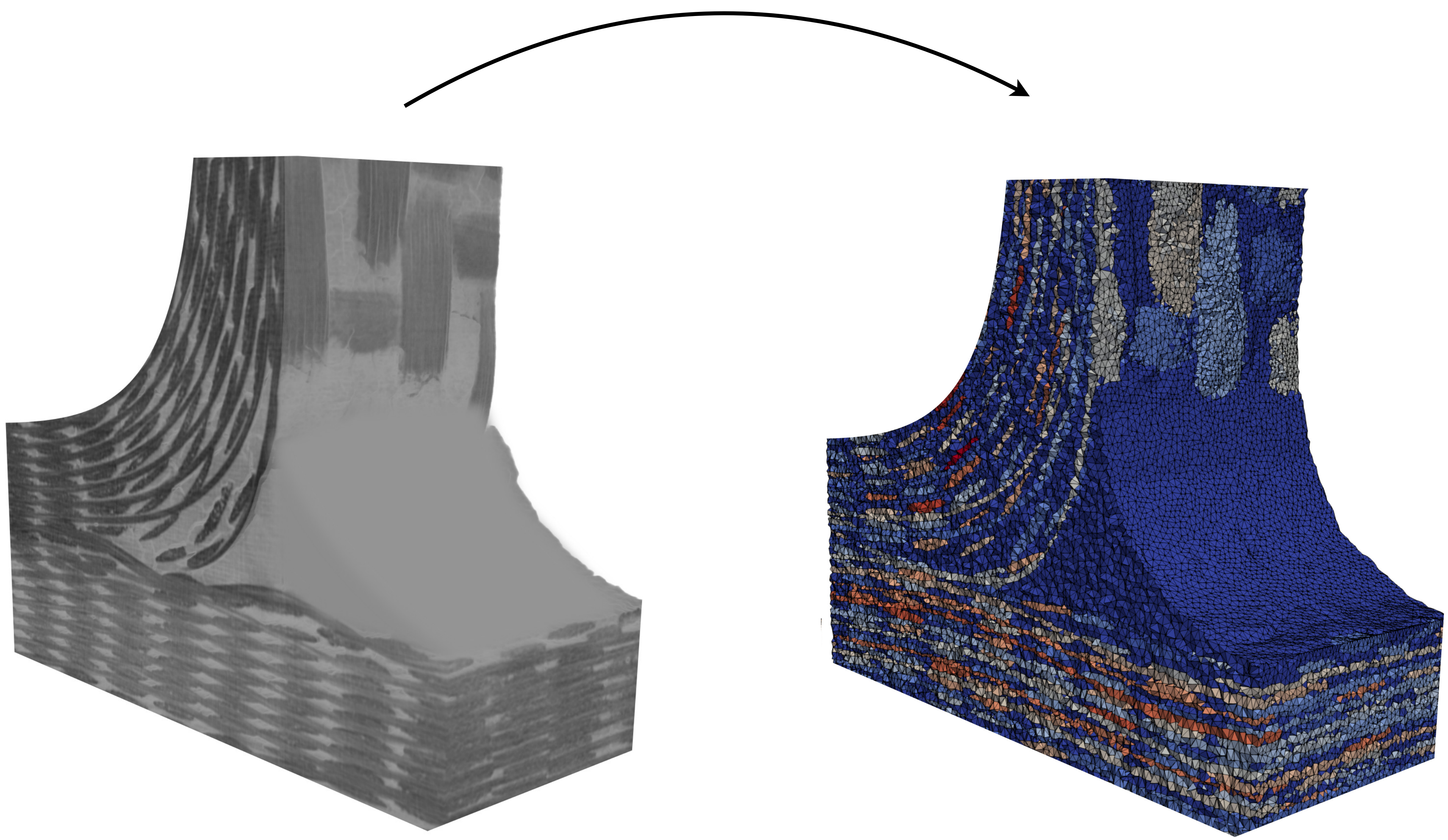

From idealised models…

- Geometric approach

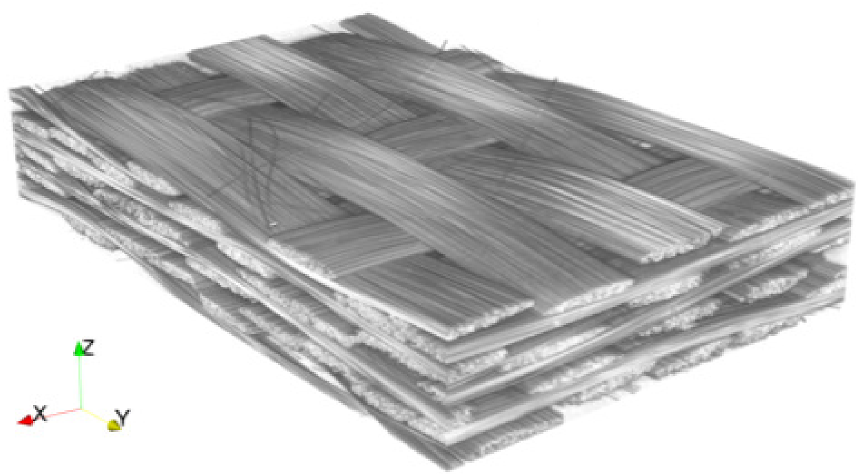

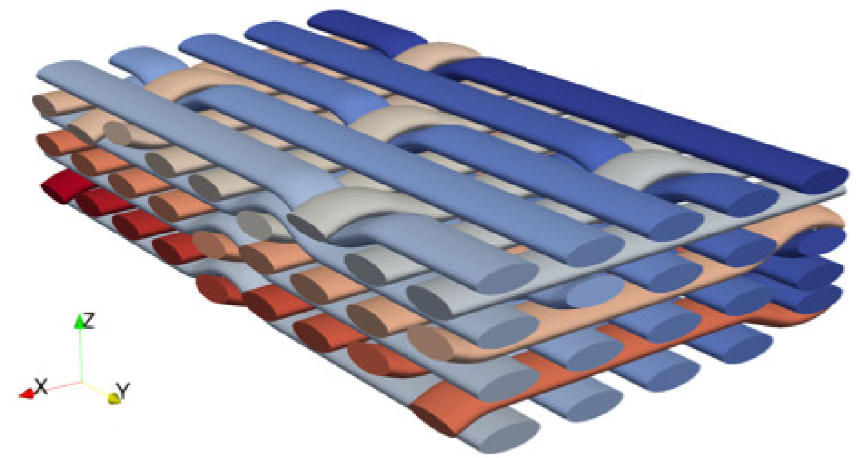

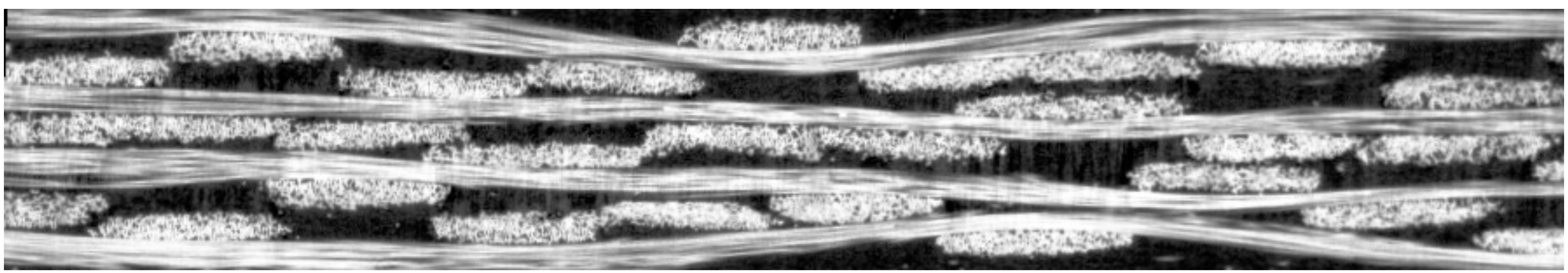

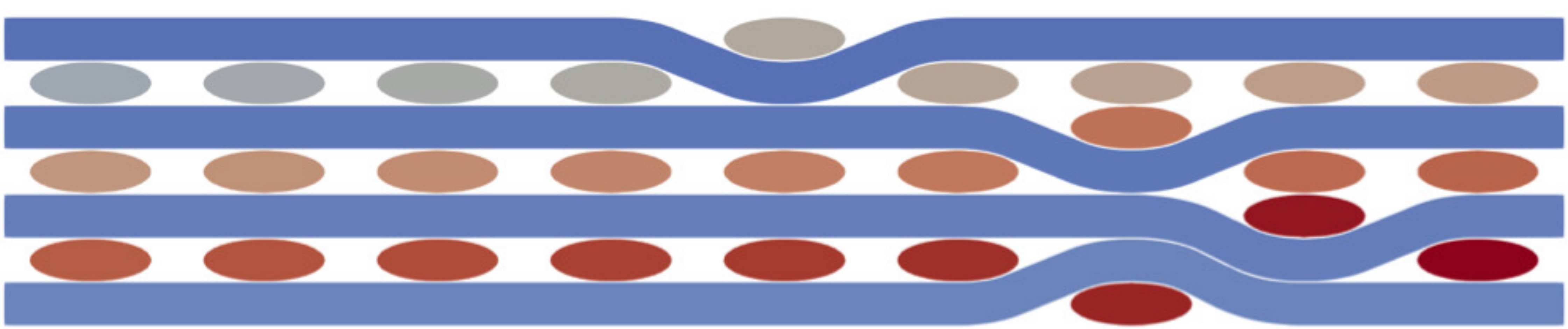

G.Couégnat, Approche multiéchelle du comportement mécanique des matériaux composites à renfort tissé, Thèse de doctorat, Université Bordeaux 1 (2008).

From idealised models…

- “Mechanistic” approach

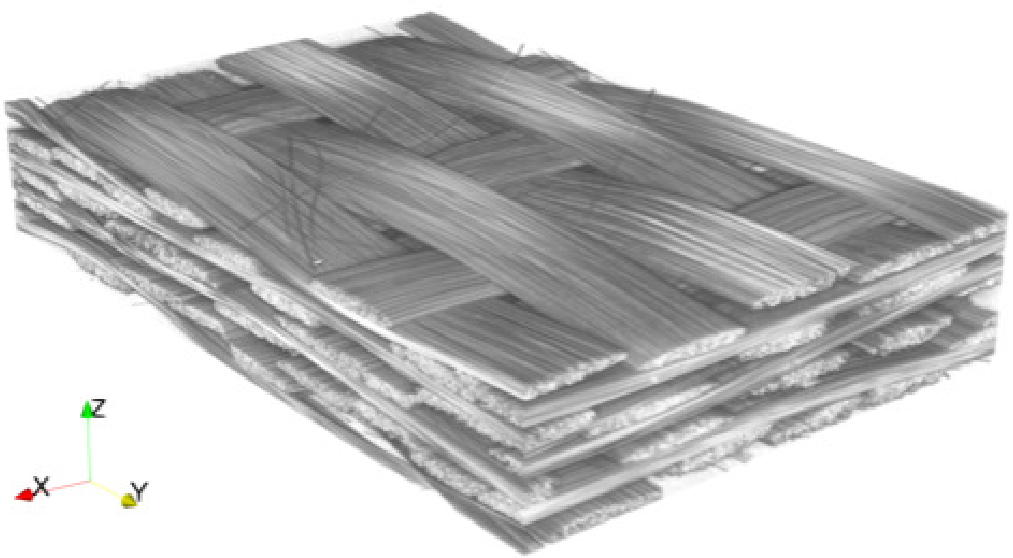

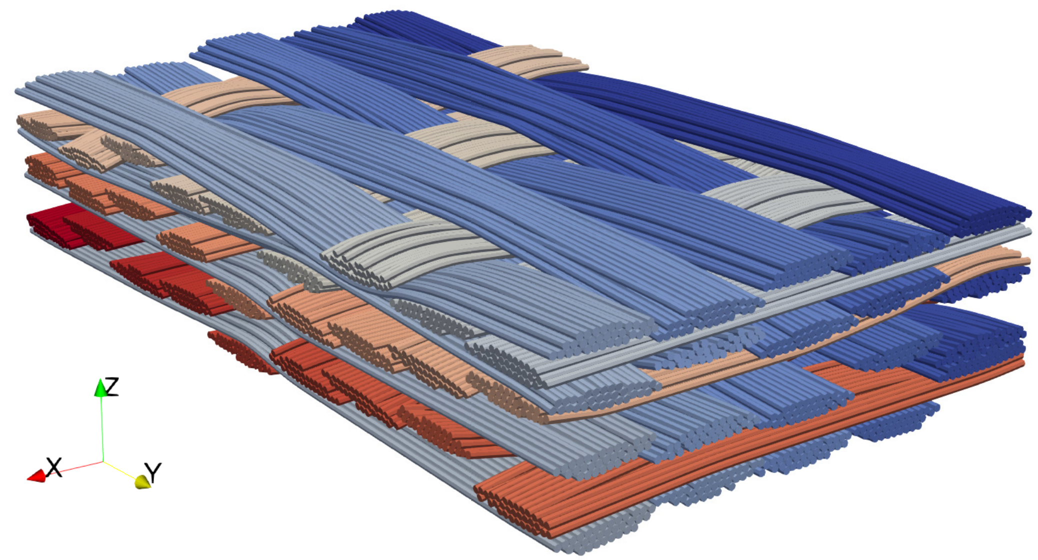

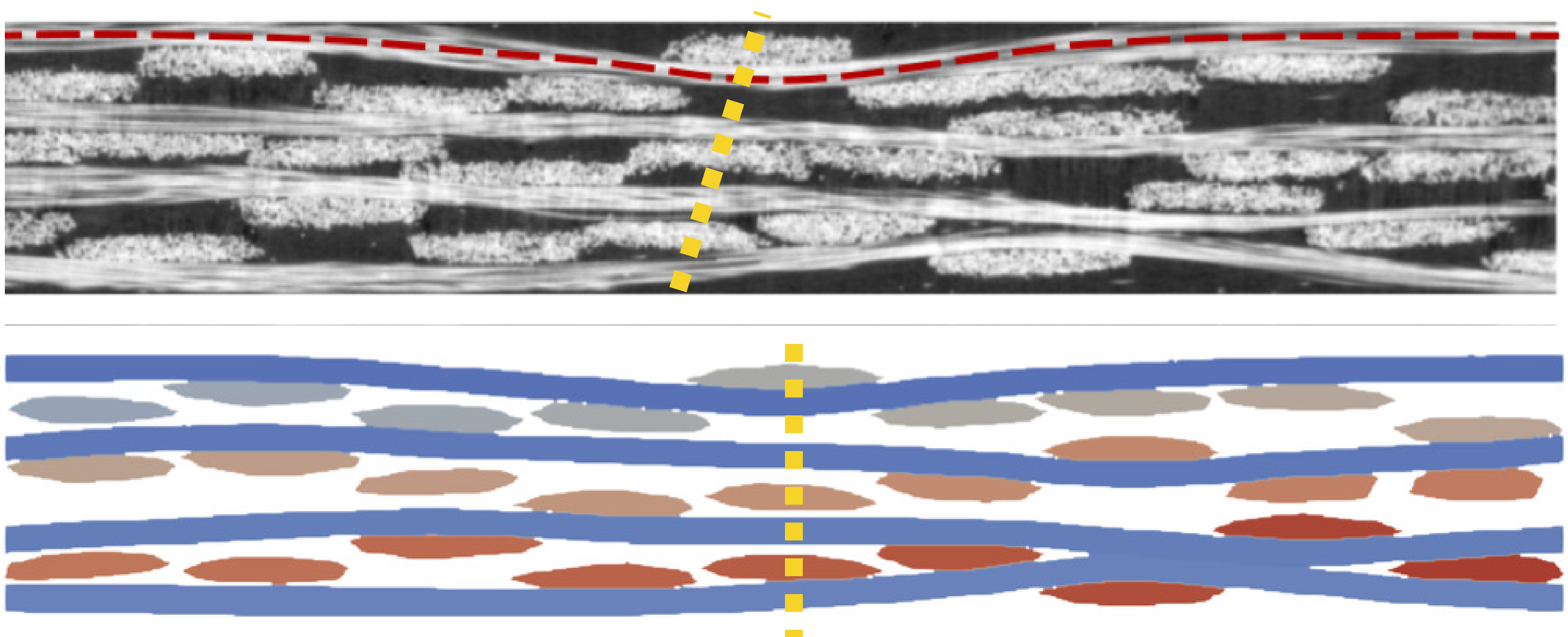

G. Couégnat & al., Towards realistic geometric modeling of woven fabrics, in Proceedings of ICCM19, Montréal (2013)

… to image-based approaches

- Structure tensor
- Easy to separate weft from warp, but…

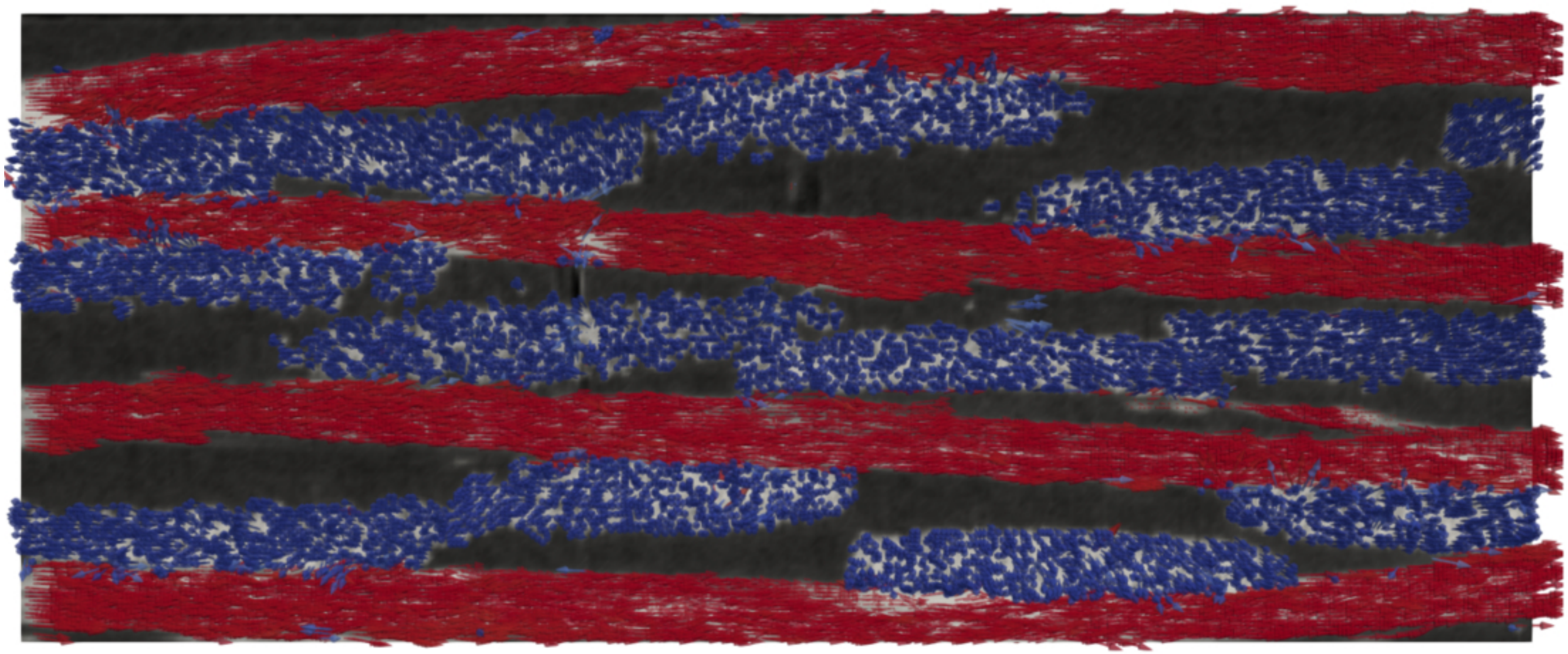

Limits of image-based approaches

- … hard to separate yarns for one another without prior information

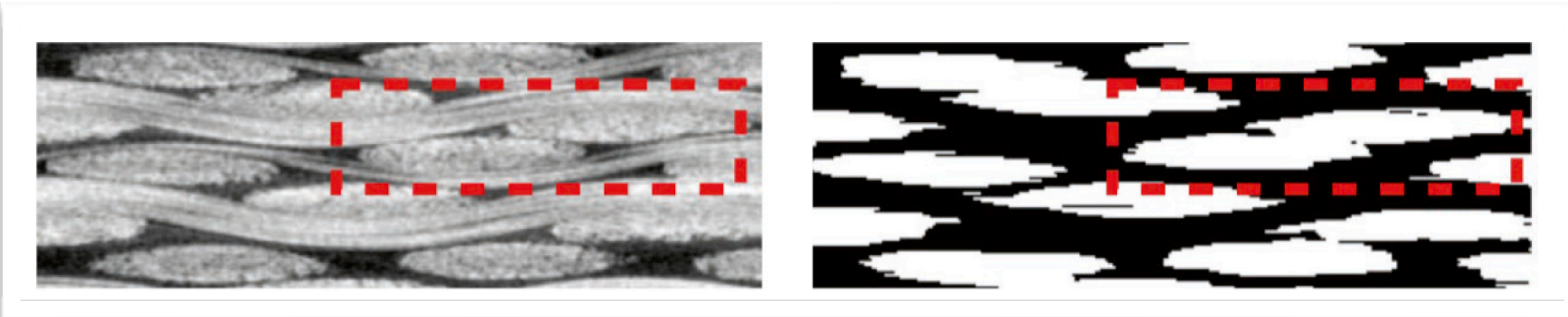

W. Huang, P. Causse, V. Brailovski, H. Hu, and F. Trochu,"Reconstruction of mesostructural material twin models of engineering textiles based on Micro-CT Aided Geometric Modeling," Composites Part A: Applied Science and Manufacturing, vol. 124, p. 105481, Sep 2019.

A priori topologique

A priori topologique

- Notion of yarns is indeed subjective

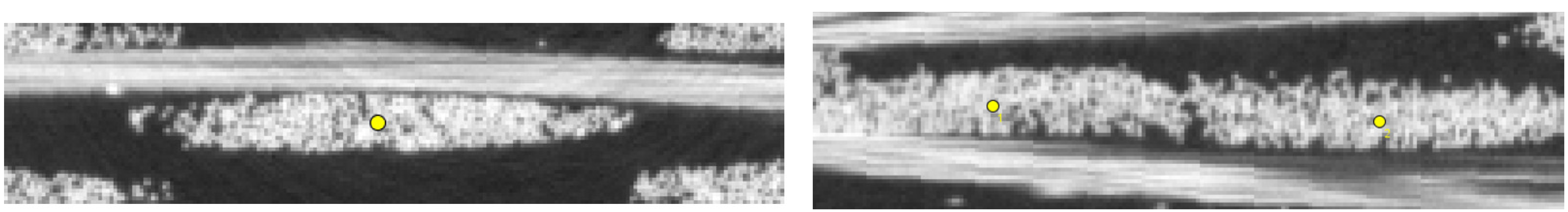

Limits of image-based approach

- Yarns need to be reconstructed *a posteriori* to retrieve continuity and correct topology
- Prescribed weaving pattern is not ensured…

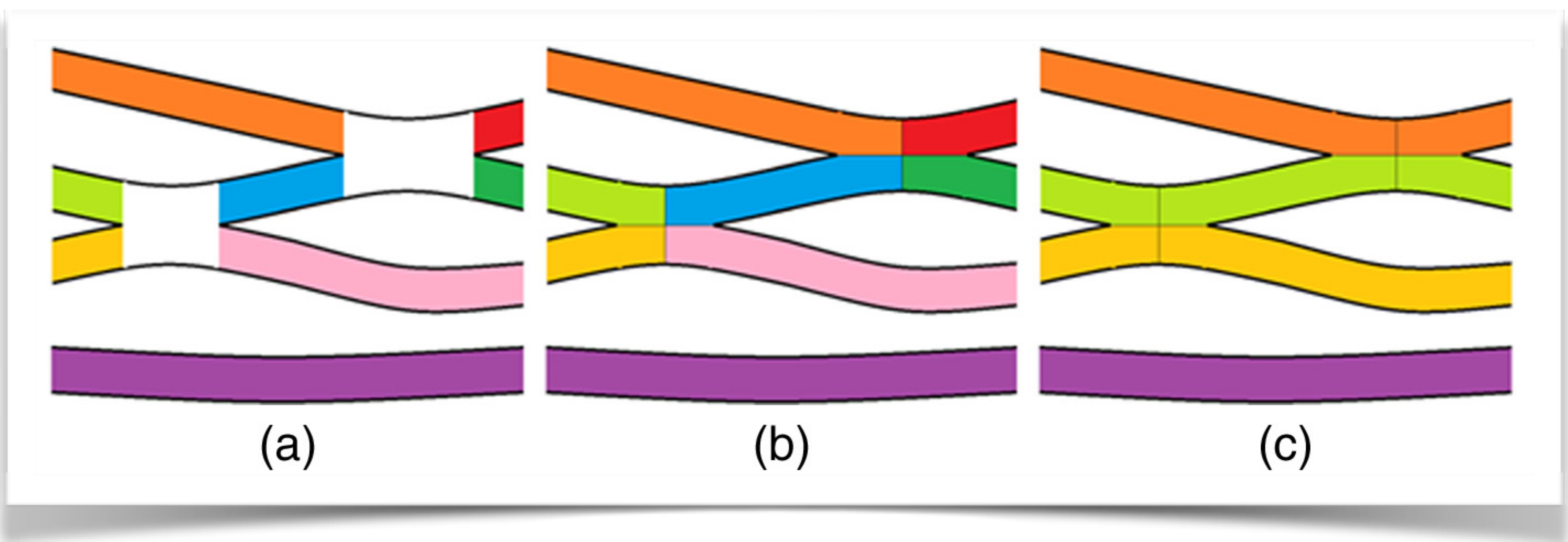

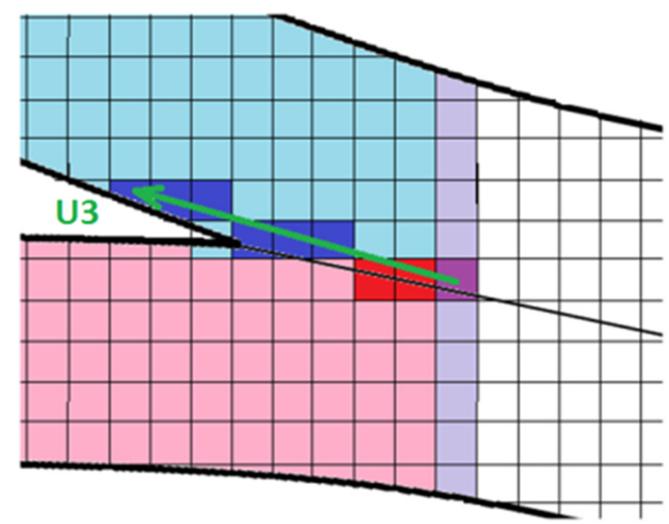

C. Chapoullié, J.-P. Da Costa, M. Cataldi, G. L. Vignoles, and C. Germain, “Orientation-guided two-scale approach for the segmentation and quantitative description of woven bundles of fibers from three-dimensional tomographic images,” Journal of Electronic Imaging, vol. 24, p. 061113, Nov 2015

Limits of image-based approach

- Practically, incorrect topology and very user-dependent

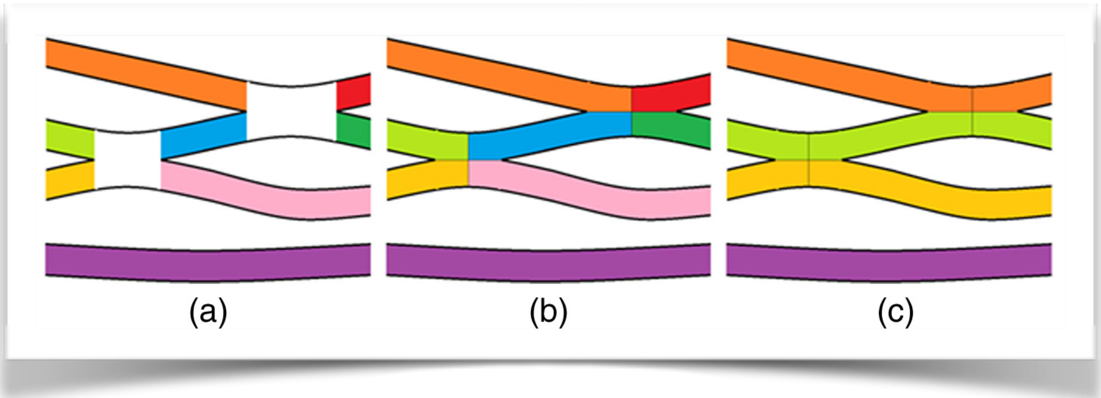

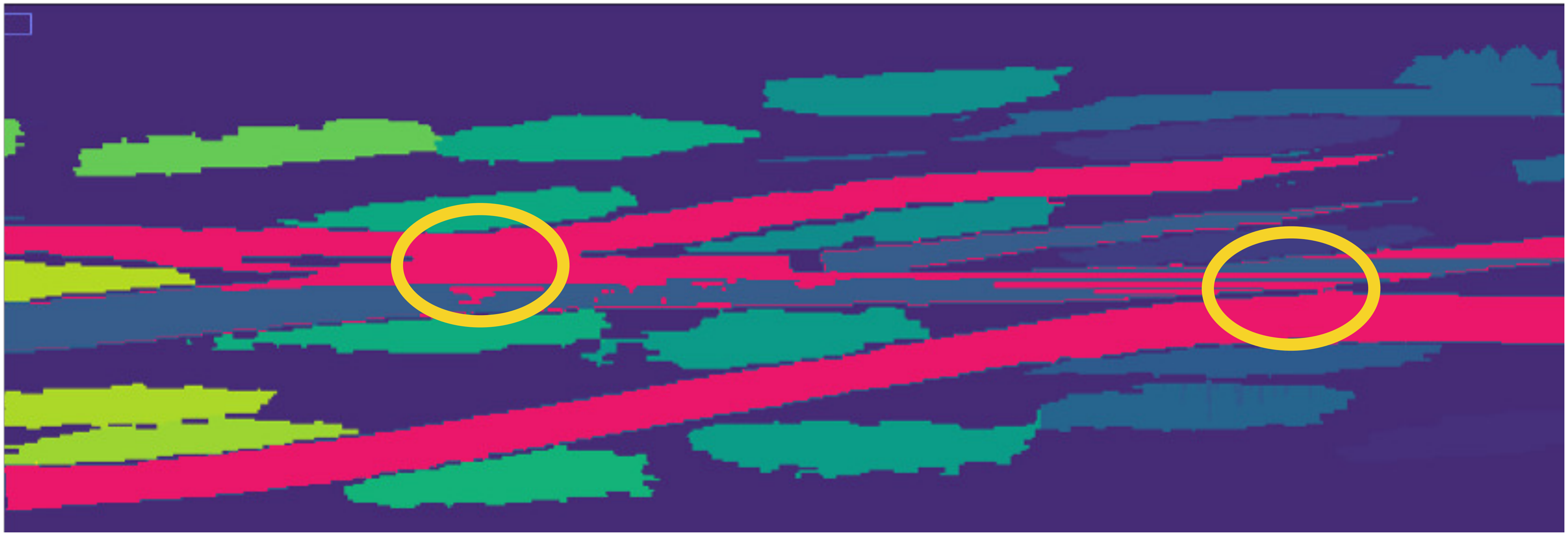

Variational segmentation approach

- Combine image-based approach with a priori geometric model

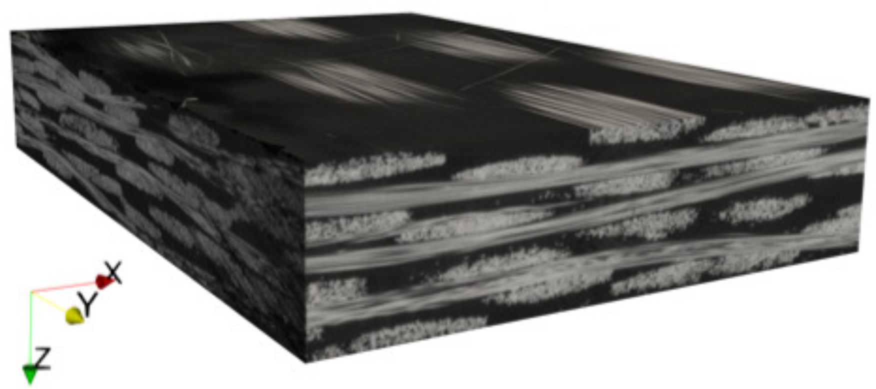

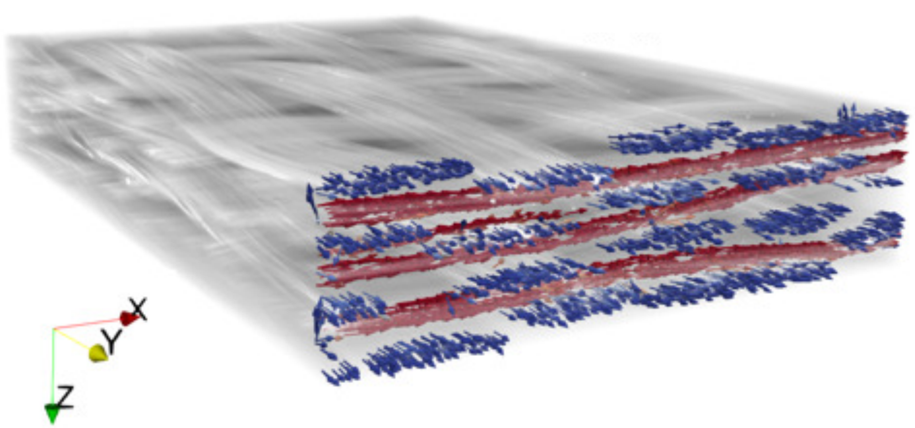

+

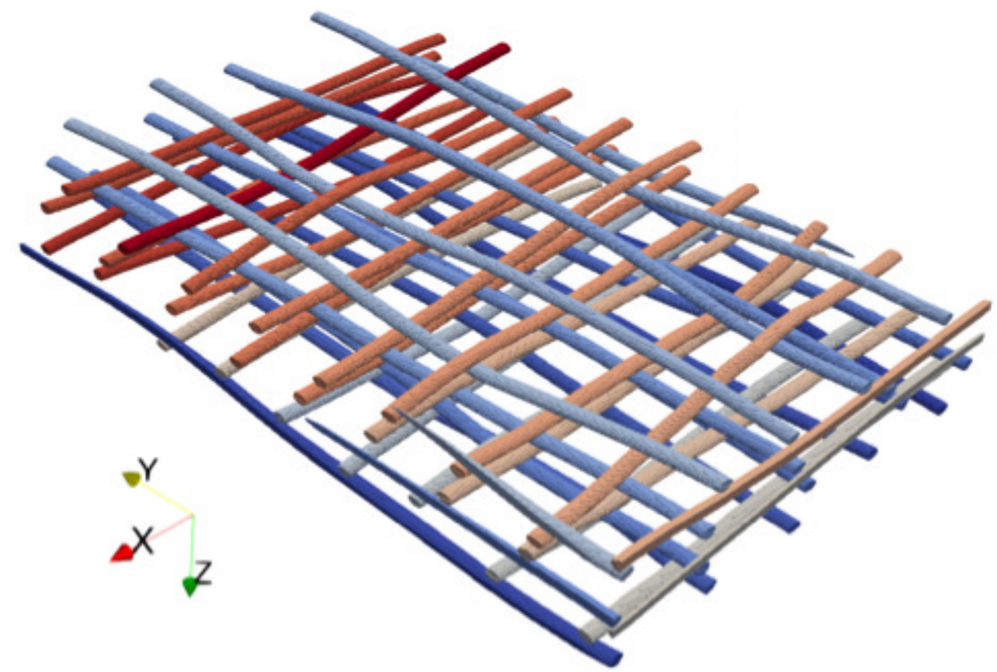

J. Bénézech, G. Couégnat, Variational segmentation of textile composite preforms from x-ray computed tomography, Composite Structures 230 (2019) 111496. doi:10.1016/j.compstruct.2019.111496.

Variational segmentation approach

- Underlying geometric model
- Each yarn is described by its centreline and some cross-sections

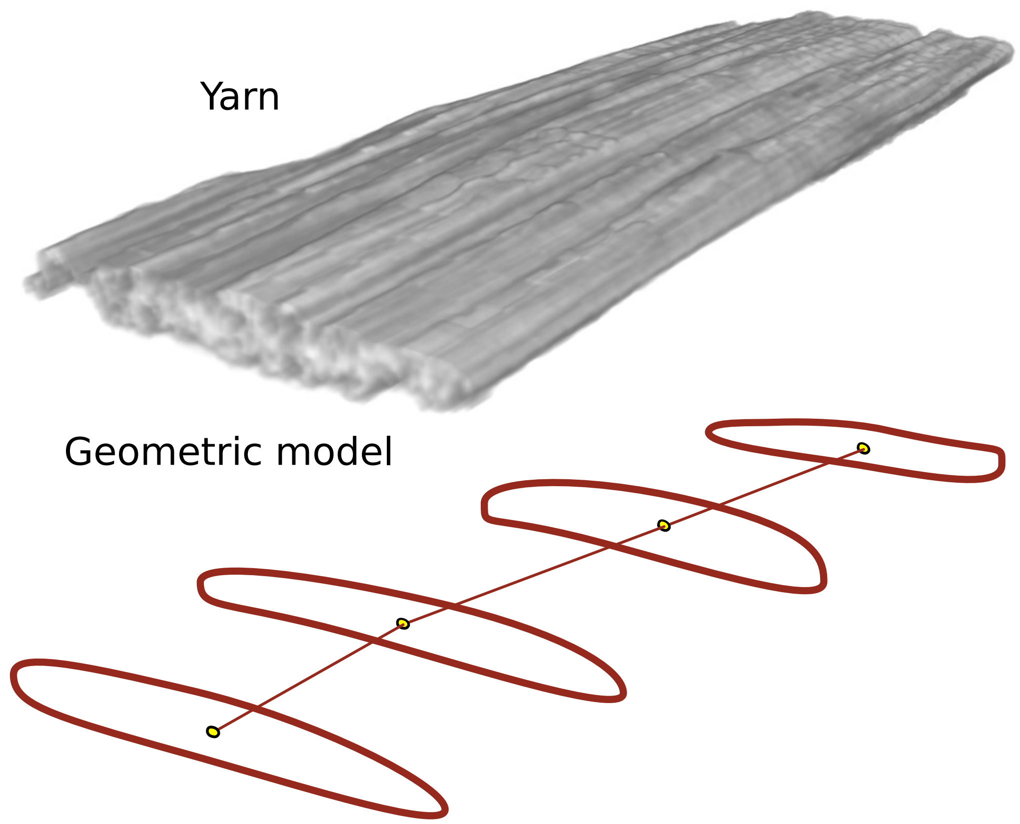

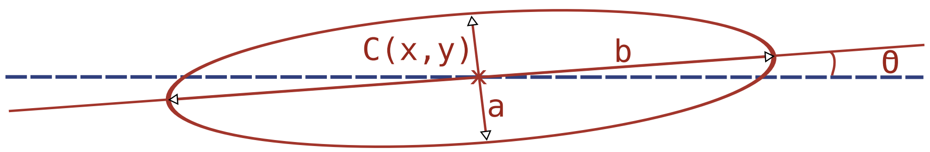

Elliptical representation

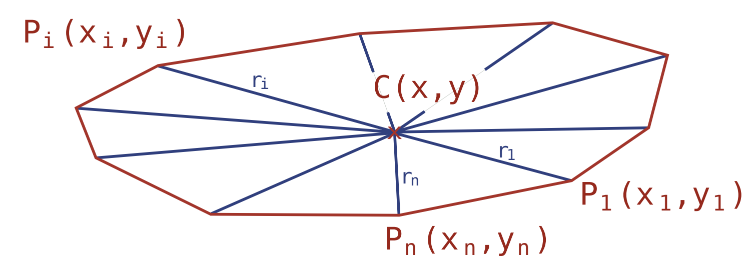

Polygonal representation

J. Bénézech, G. Couégnat, Variational segmentation of textile composite preforms from x-ray computed tomography, Composite Structures 230 (2019) 111496. doi:10.1016/j.compstruct.2019.111496.

Variational segmentation approach

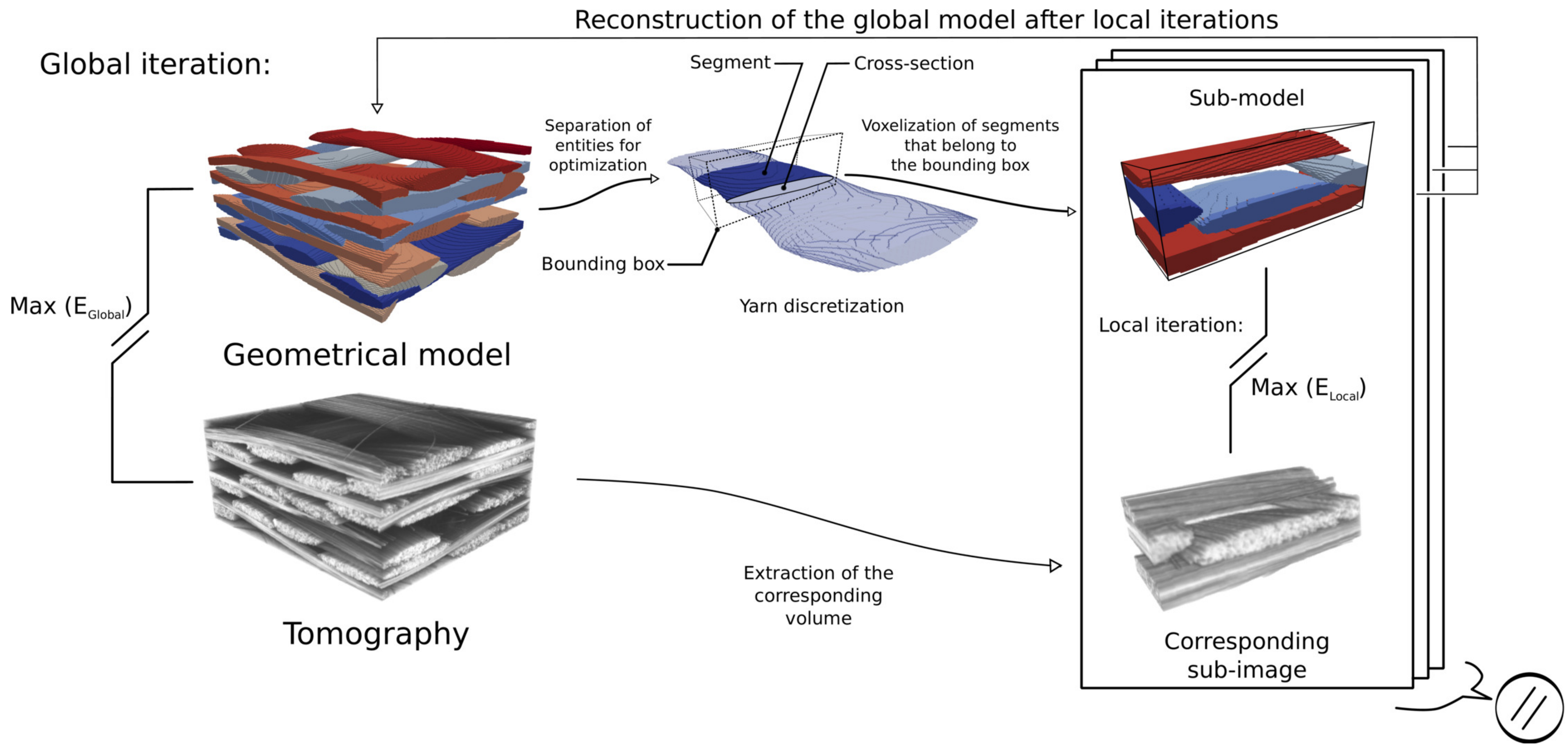

$$\max_{p_i} E = \alpha E_g + \beta E_d - \gamma(E_p + E_i)$$

Geometric parameters

Grayscale similarity

Local direction similarity

Regularisation term

Variational segmentation approach

- Convergence of the optimisation heuristic

$$E = \alpha E_g + \beta E_d - \gamma(E_p + E_i)$$

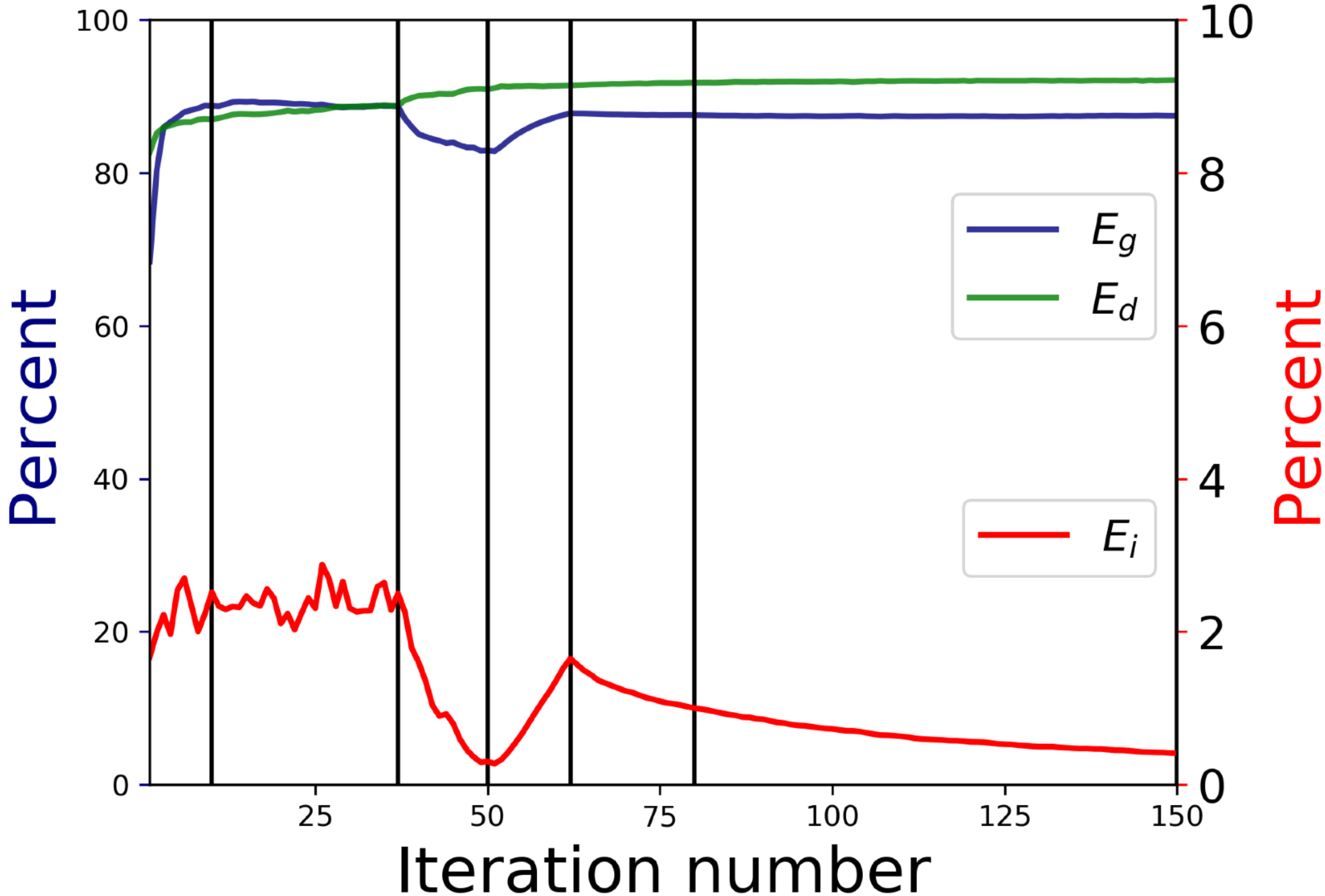

Comparison with manual segmentation

µCT

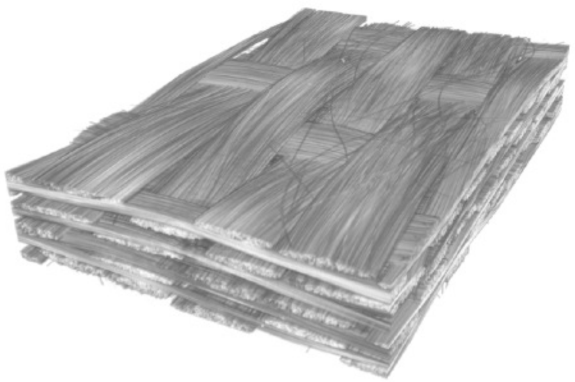

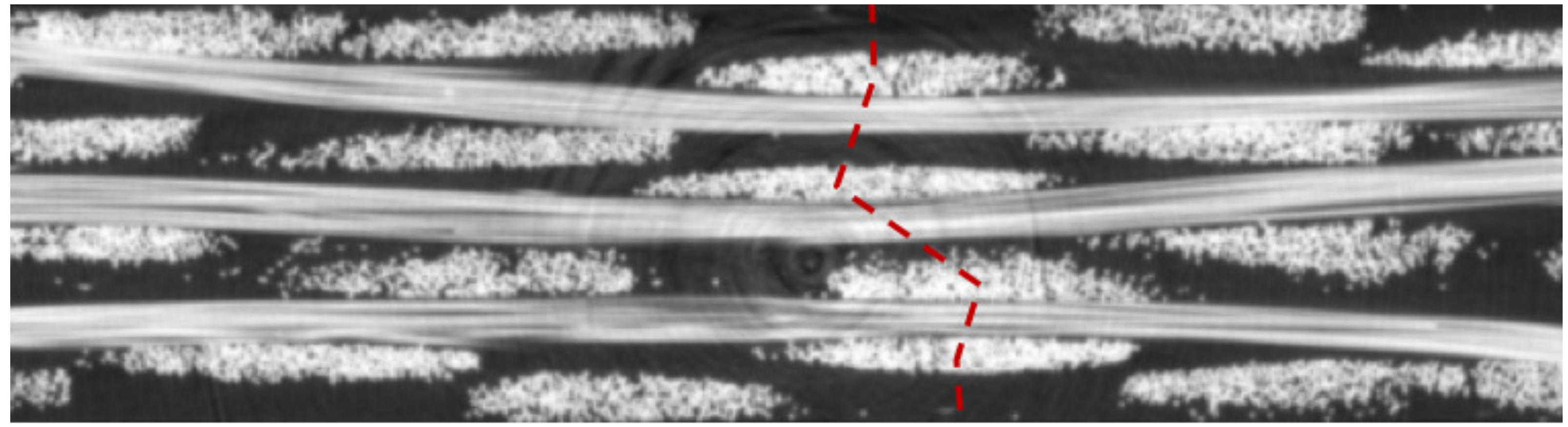

variational segmentation

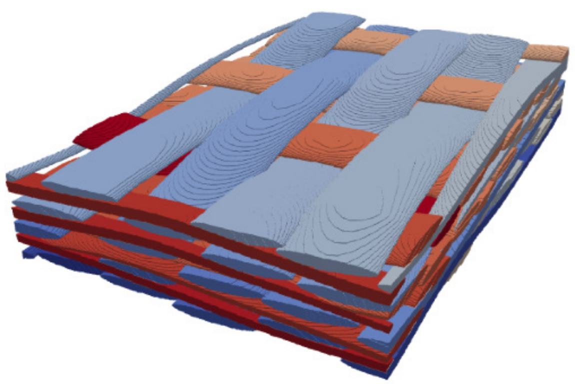

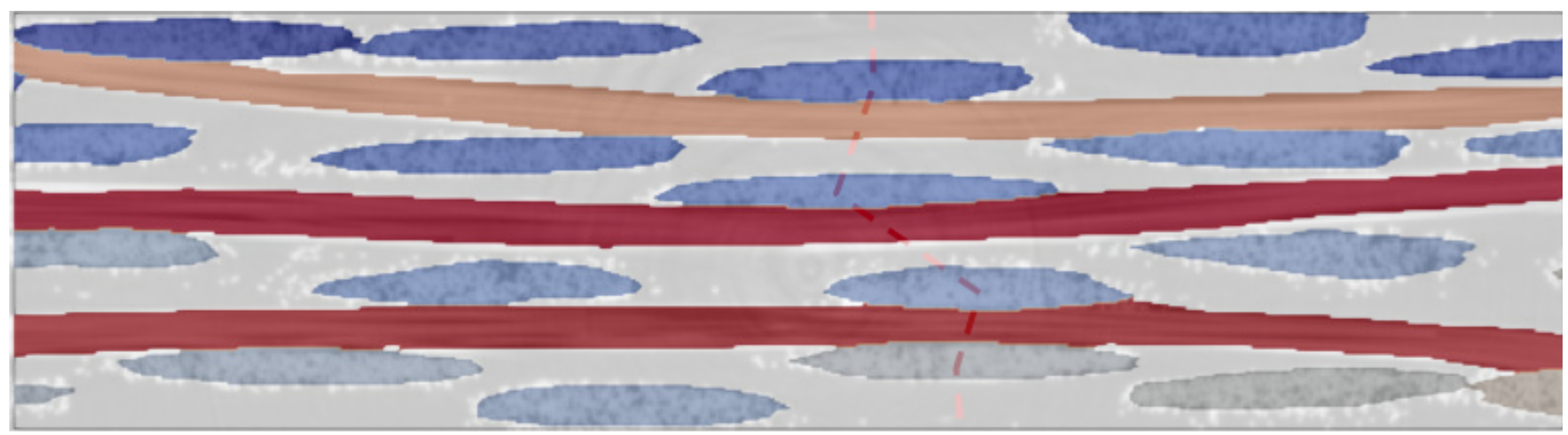

manual segmentation

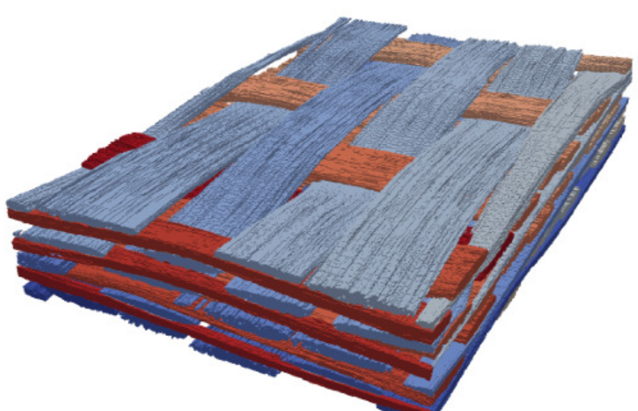

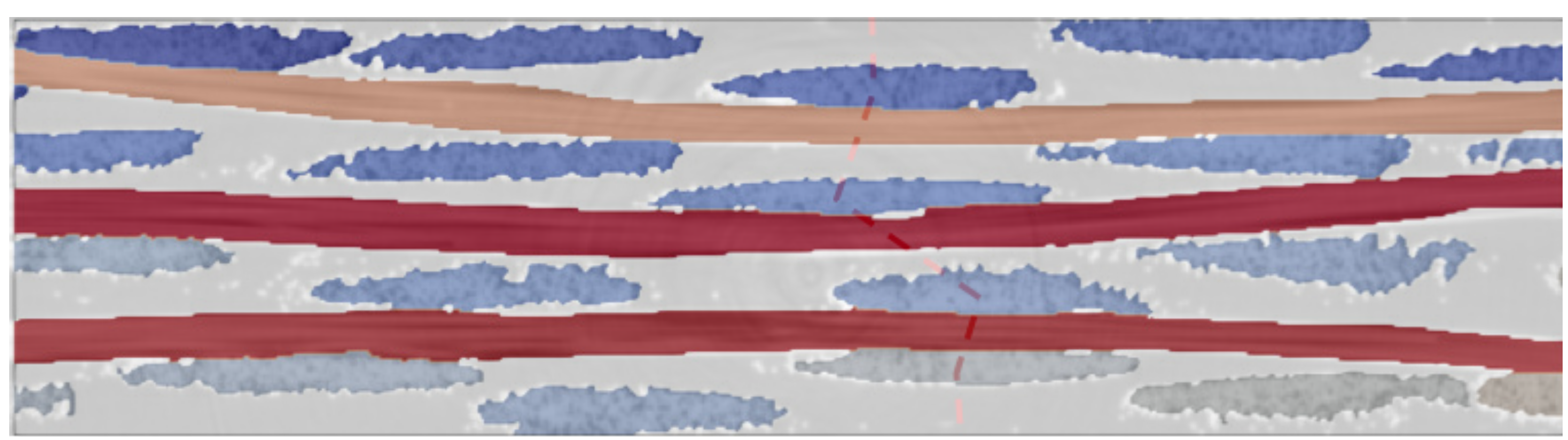

Variational segmentation approach

- Image-based model with guaranteed topology

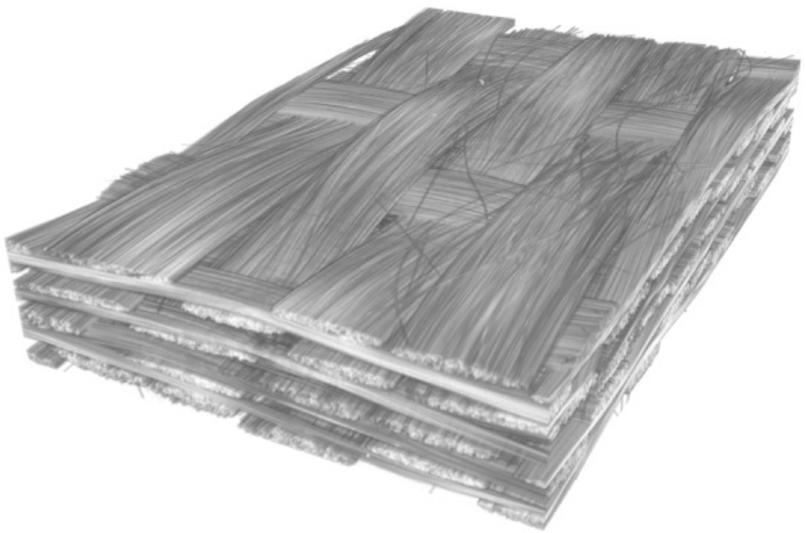
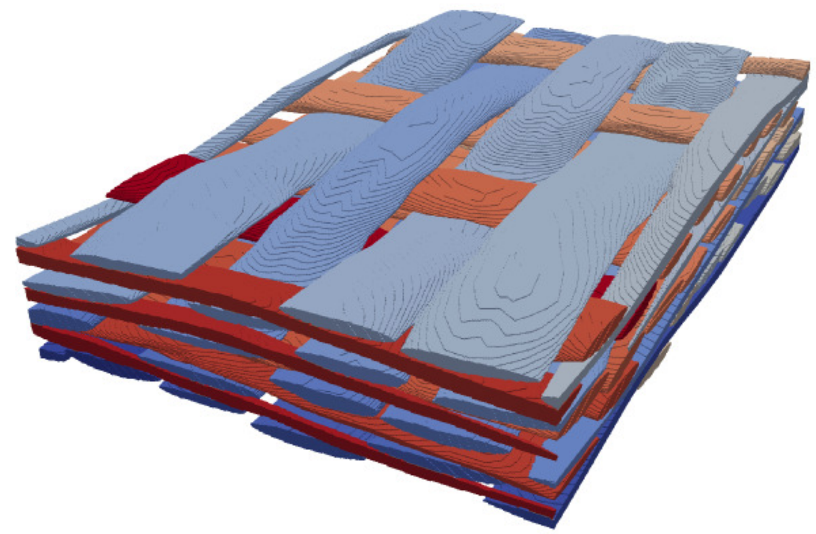
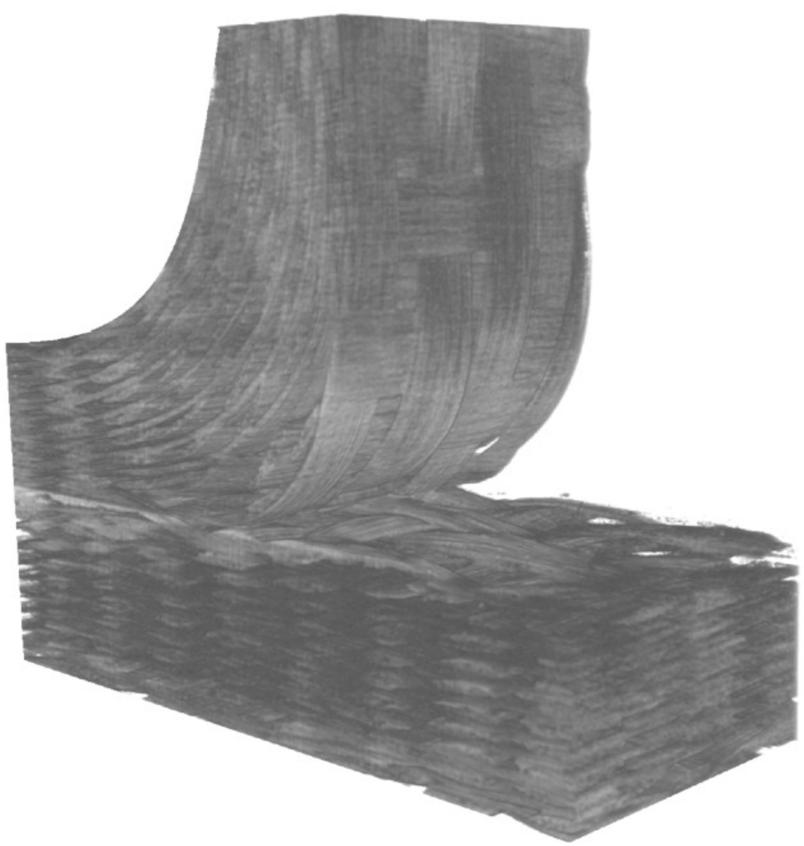
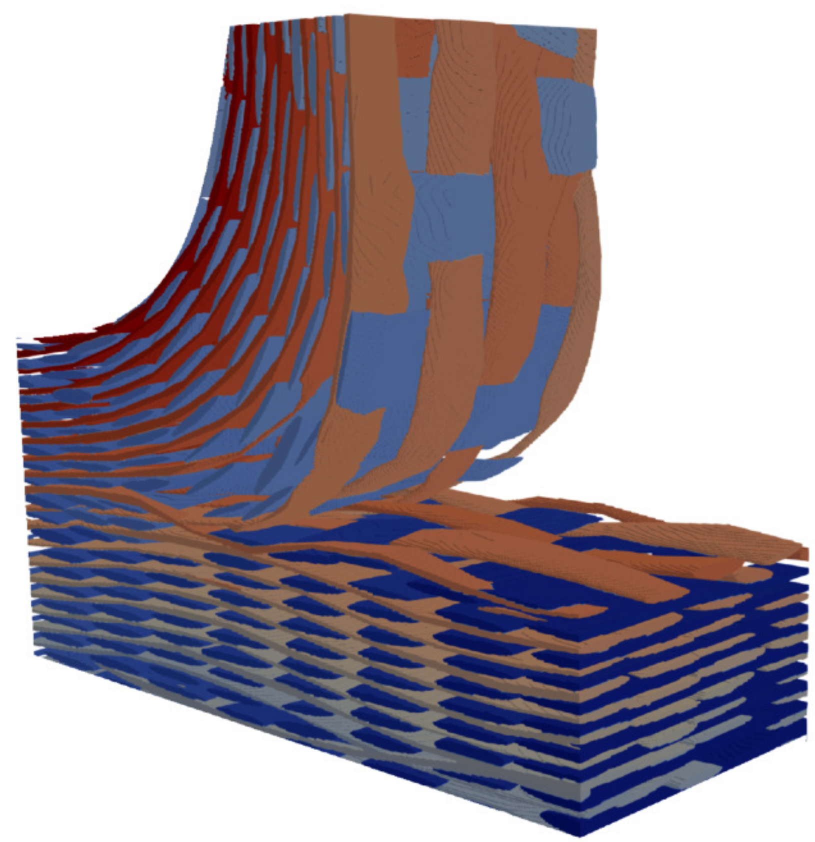

Mesh generation

- Convert geometrical model to “virtual” 3D image
- Easy to correct residual interpenetration or to add matrix
- Quality conformal tetrahedral volume mesh

(c)

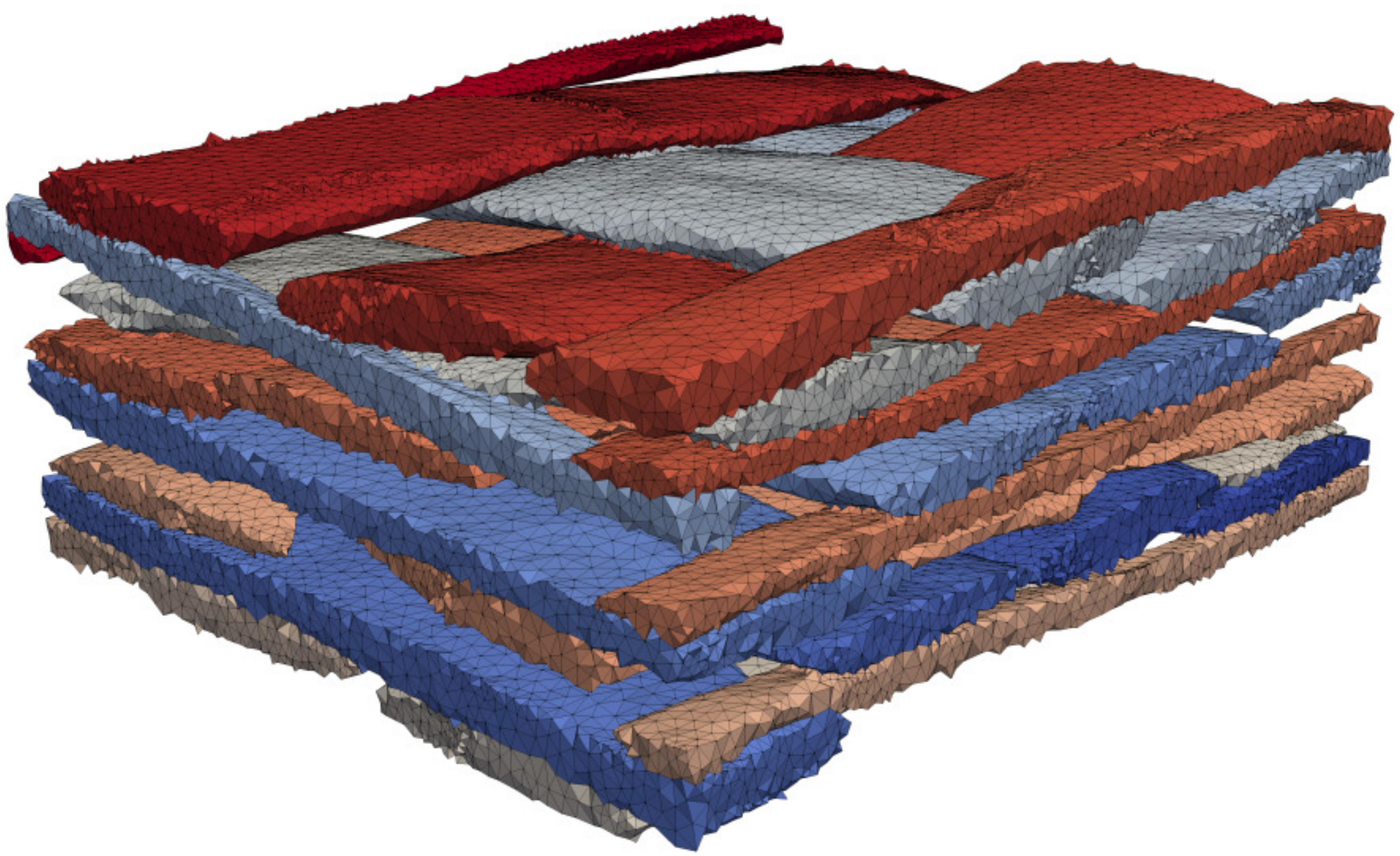

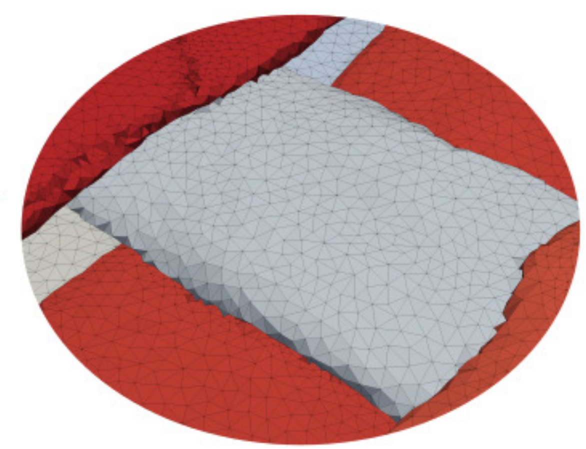

CMC digital twins

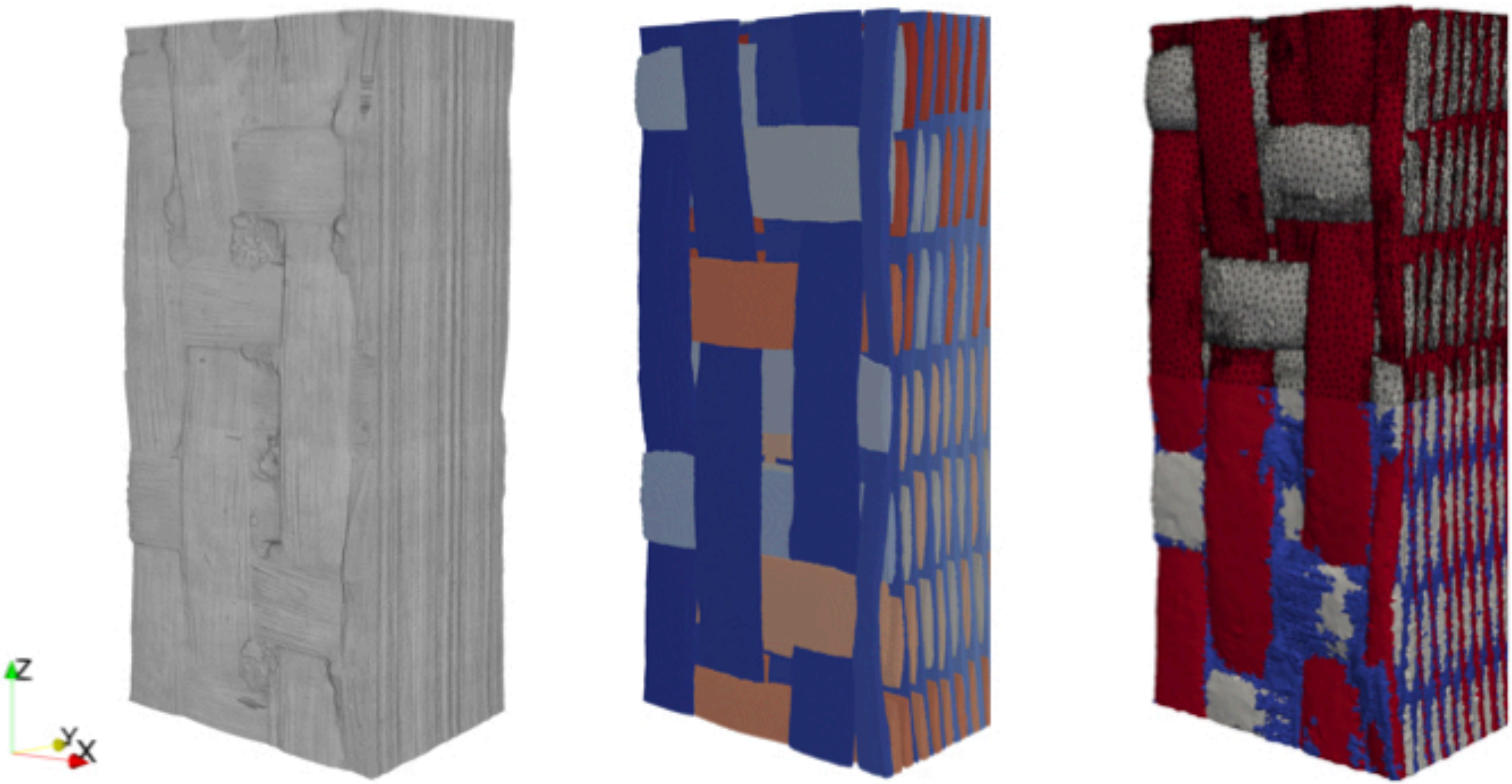

CMC digital twins

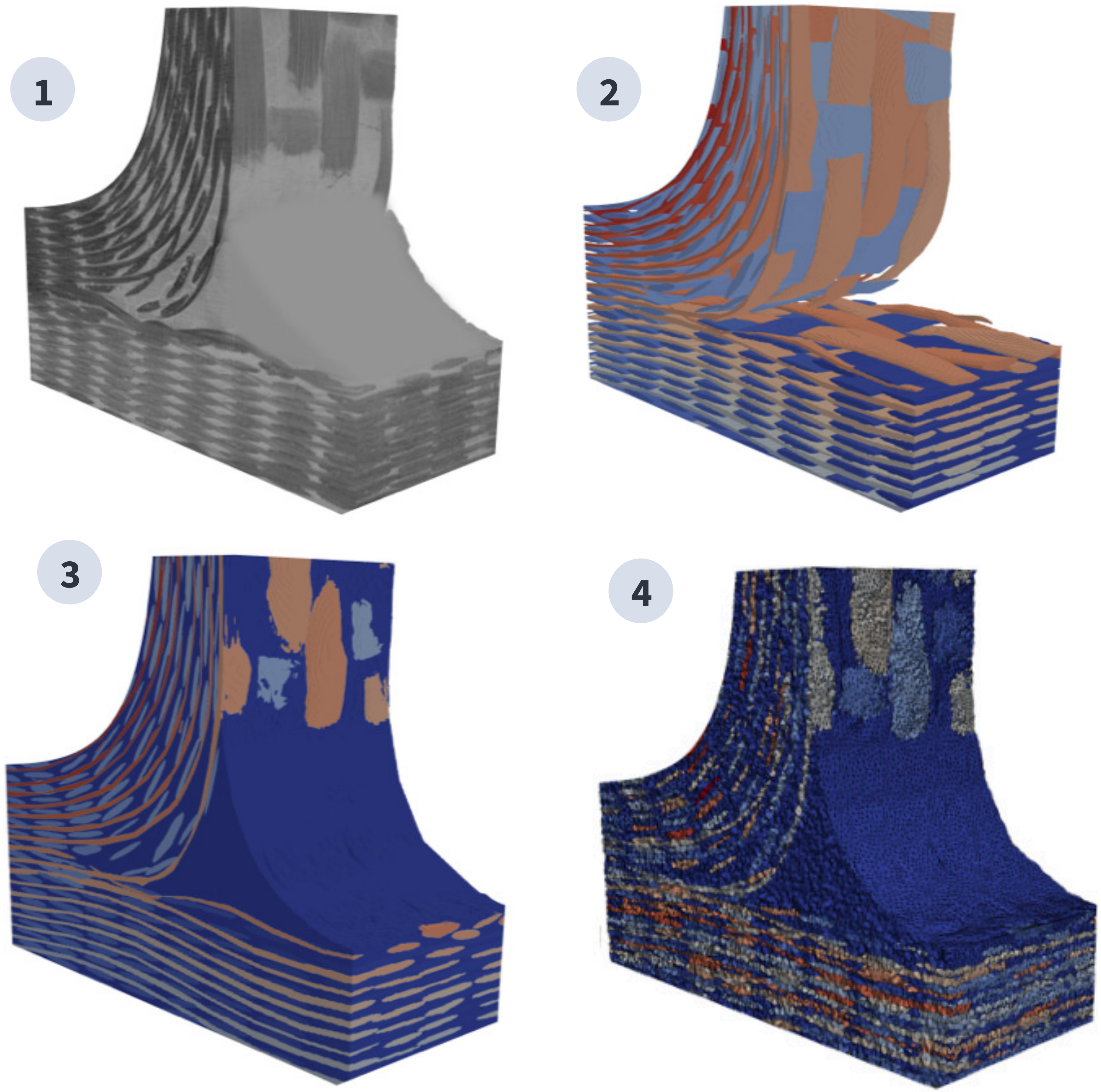

Damage simulation in L-shape woven junctions

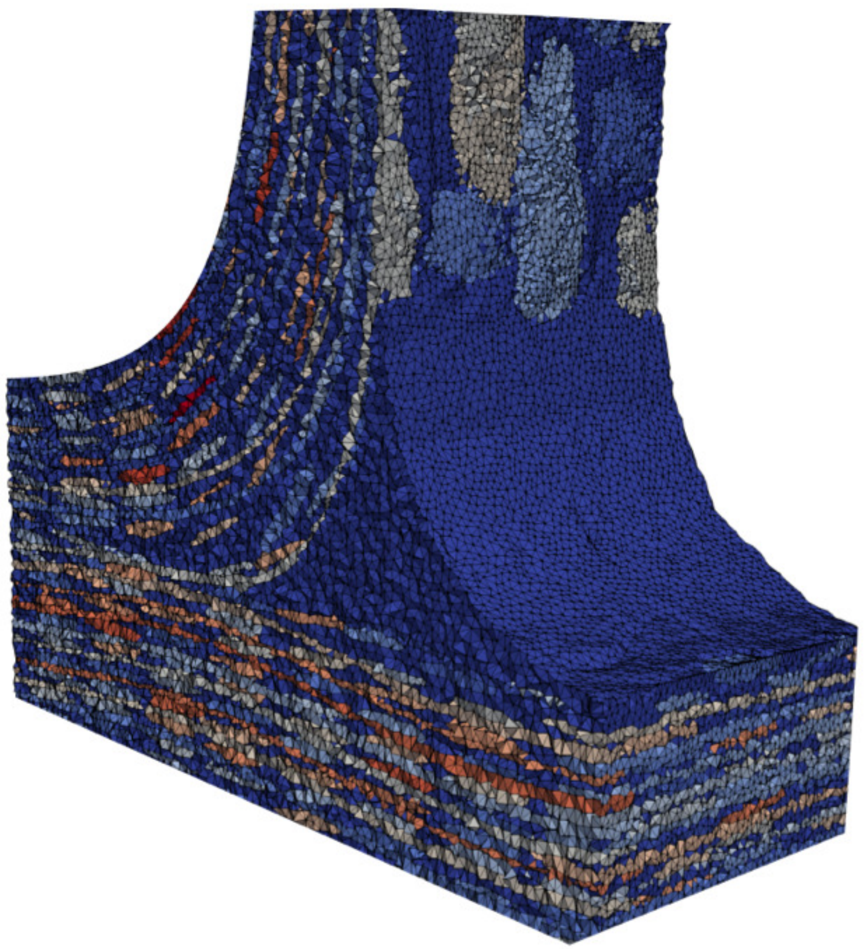

warp

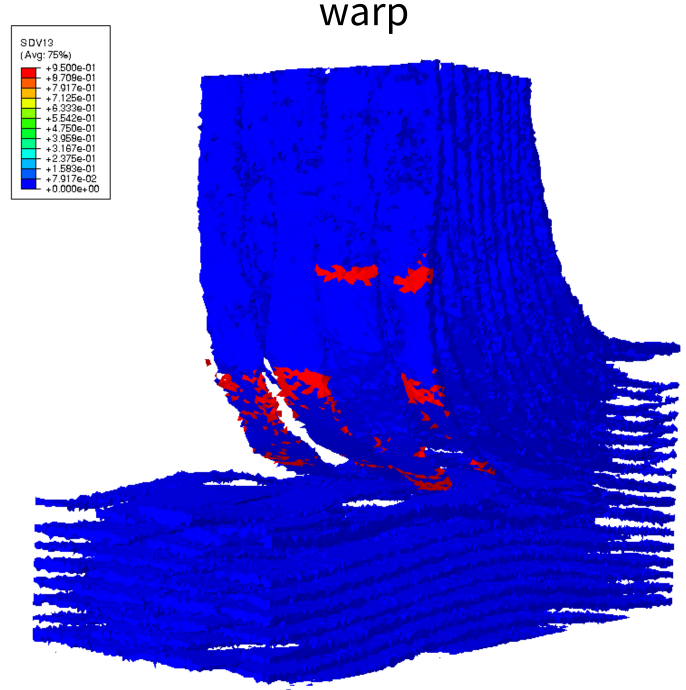

matrix

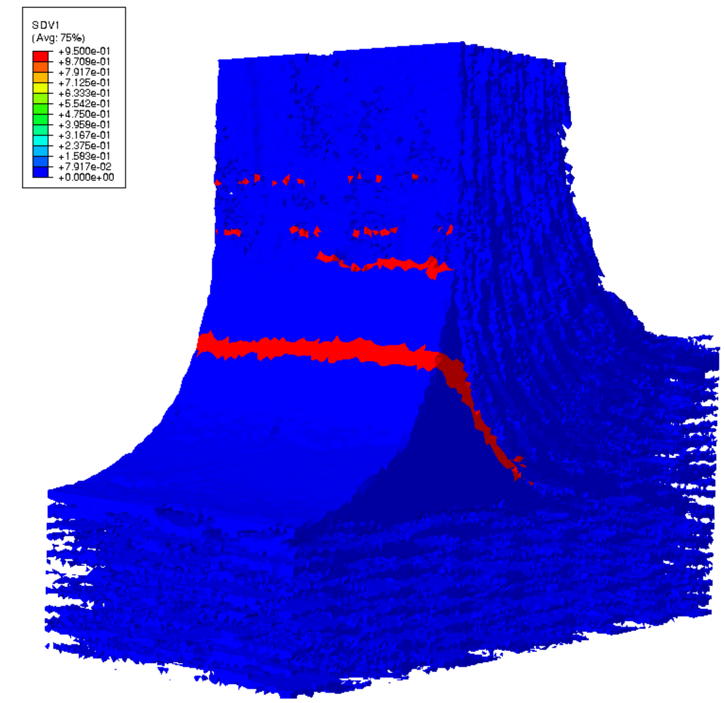

weft

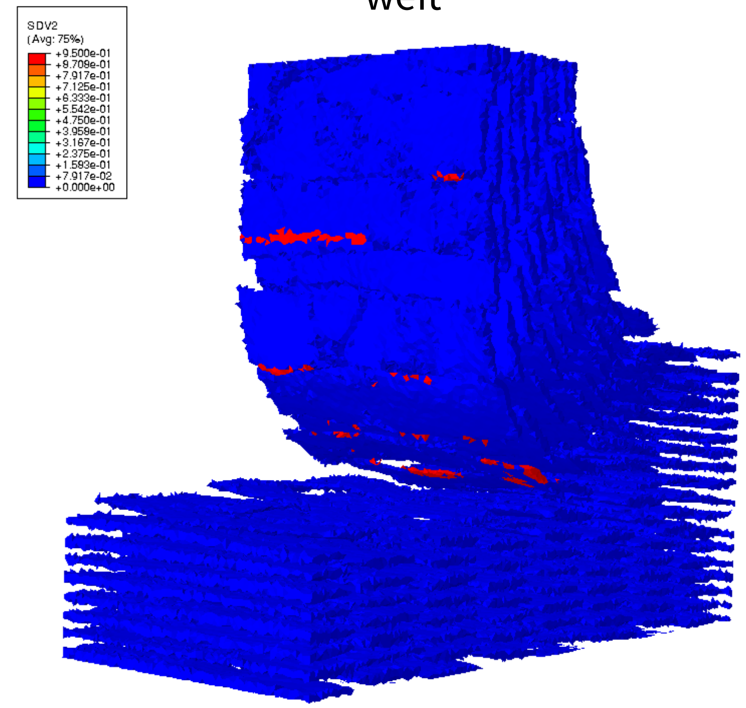

Damage simulation in L-shape woven junctions

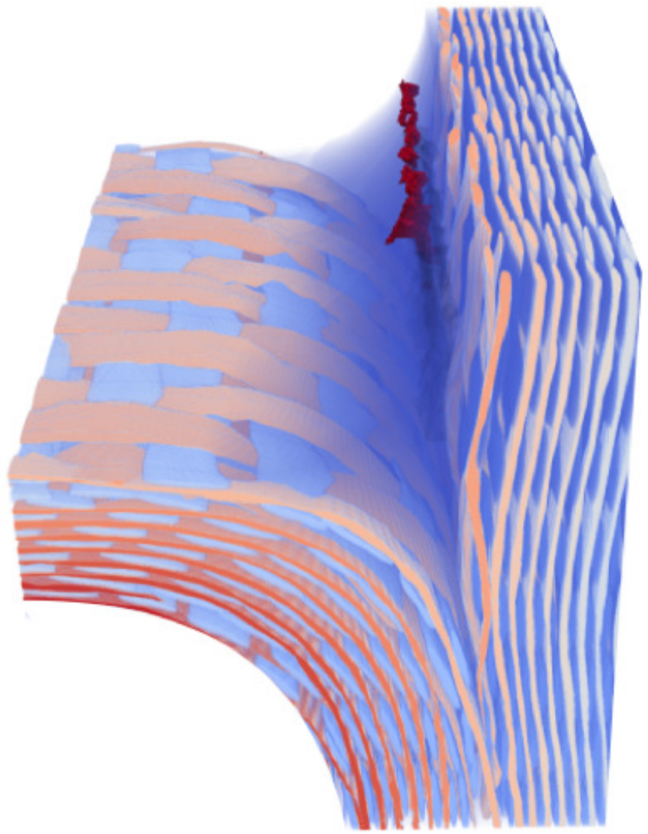

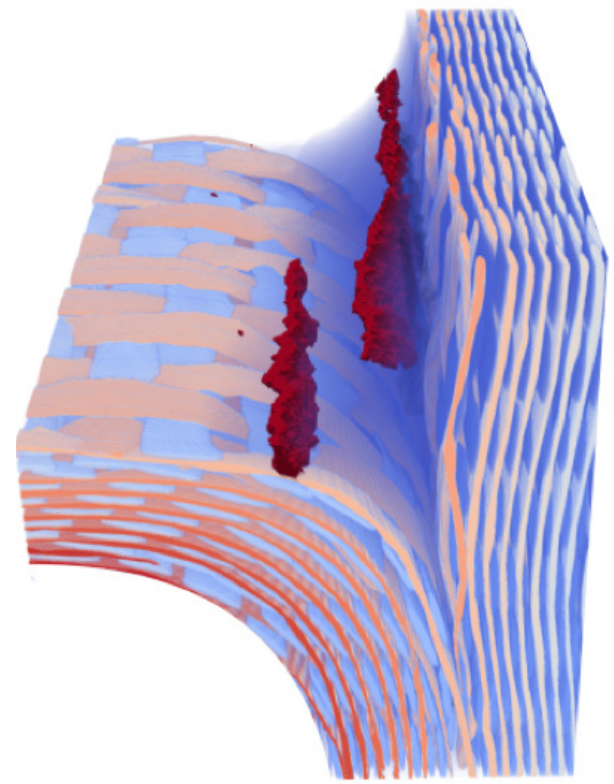

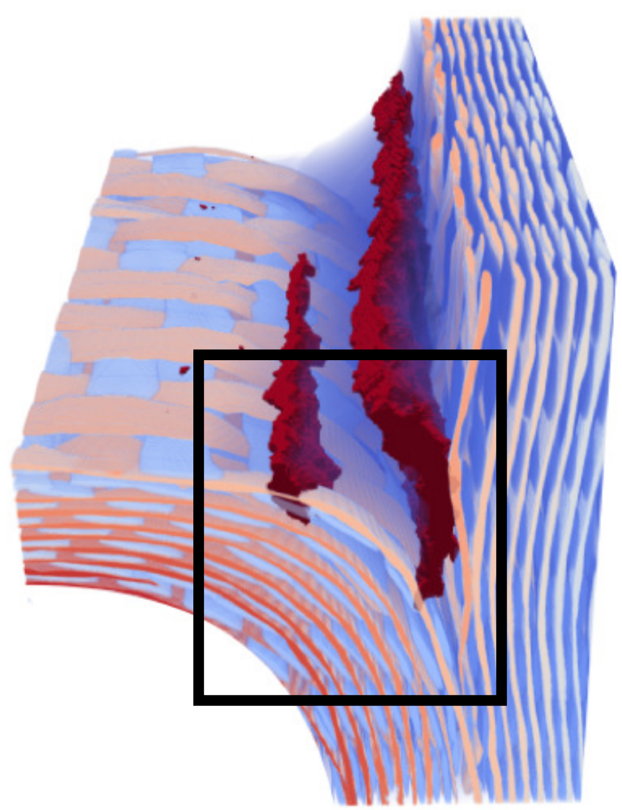

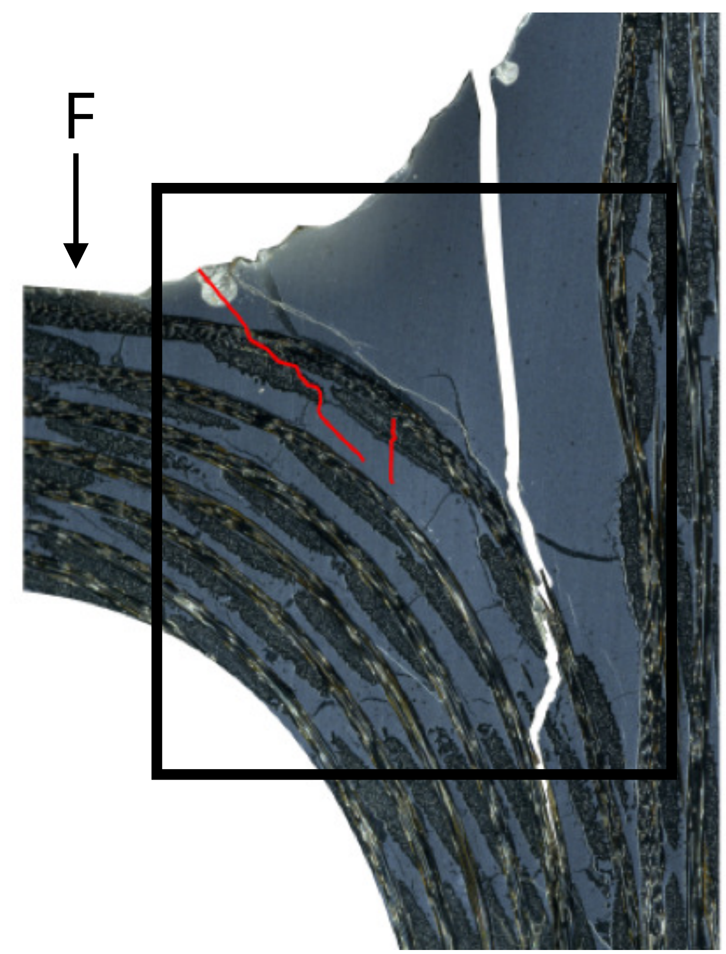

Comparison with *in situ* tests

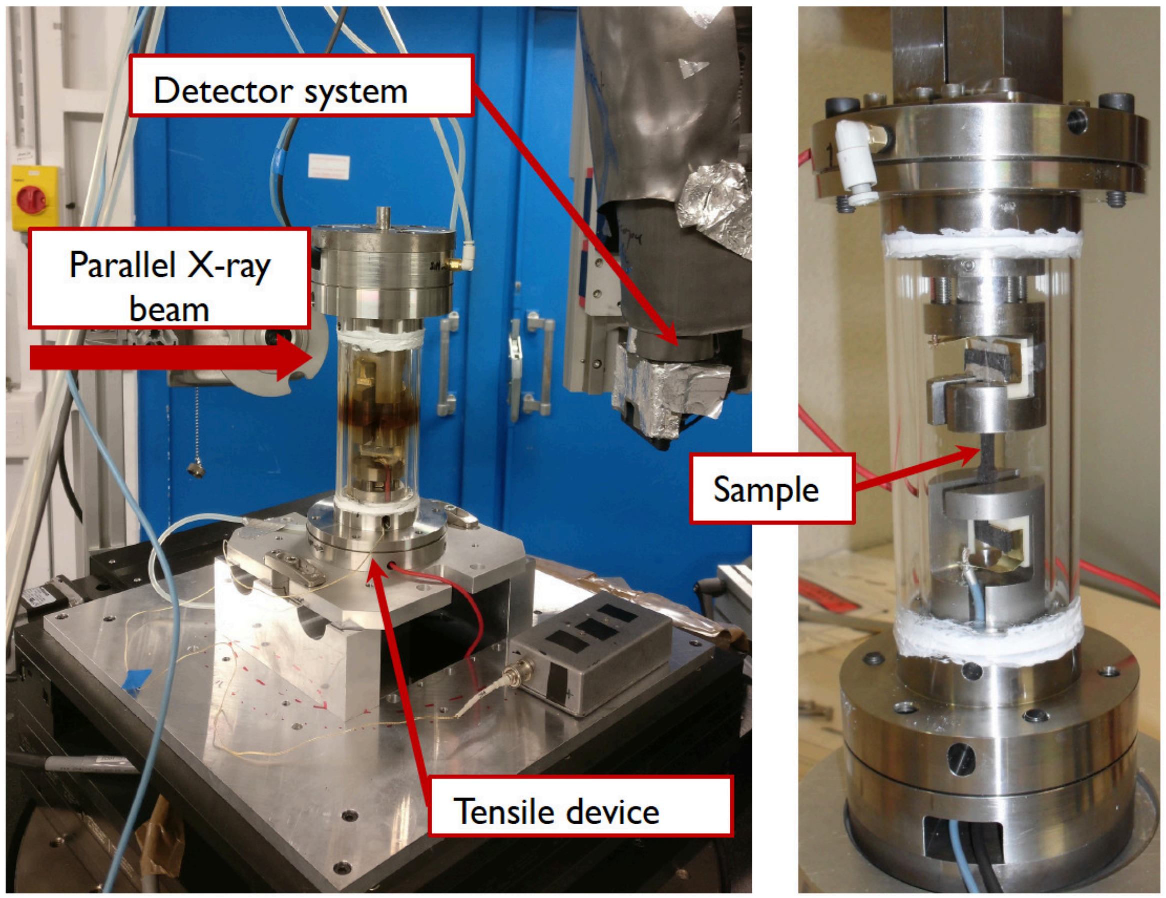

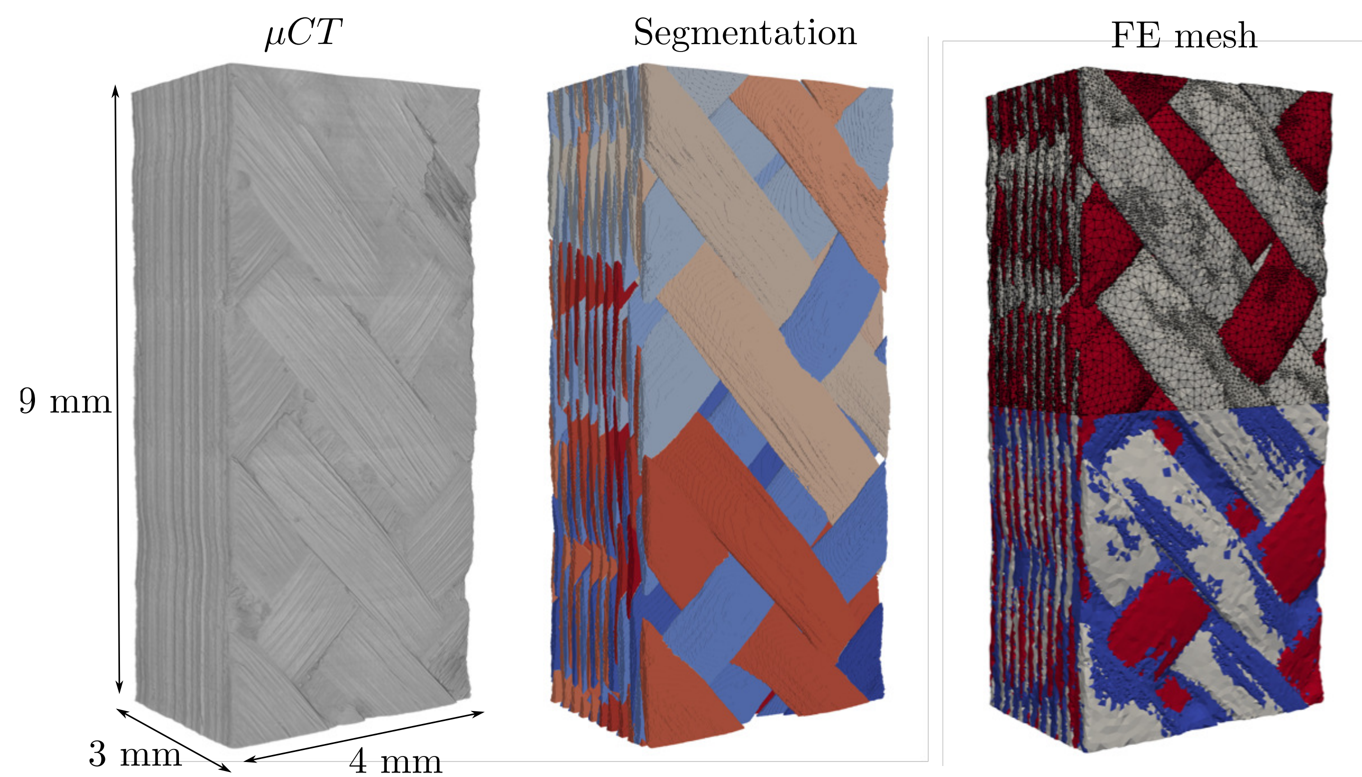

V. Mazars, O. Caty, G. Couégnat, A. Bouterf, S. Roux, S. Denneulin, J. Pailhès, G. L. Vignoles, Damage investigation and modeling of 3d woven ceramic matrix composites from x-ray tomography in-situ tensile tests, Acta Materialia 140 (2017) 130–139. doi:10.1016/j.actamat.2017.08.034.
V. Mazars, G. Couégnat, O. Caty, S. Denneulin, G. Vignoles, Multi-scale damage modeling of 3D ceramic matrix composites from in-situ X-ray tensile tests, in: ECCM18, Athens, Greece, 2018, pp. 24 – 28.

Comparison with *in situ* tests

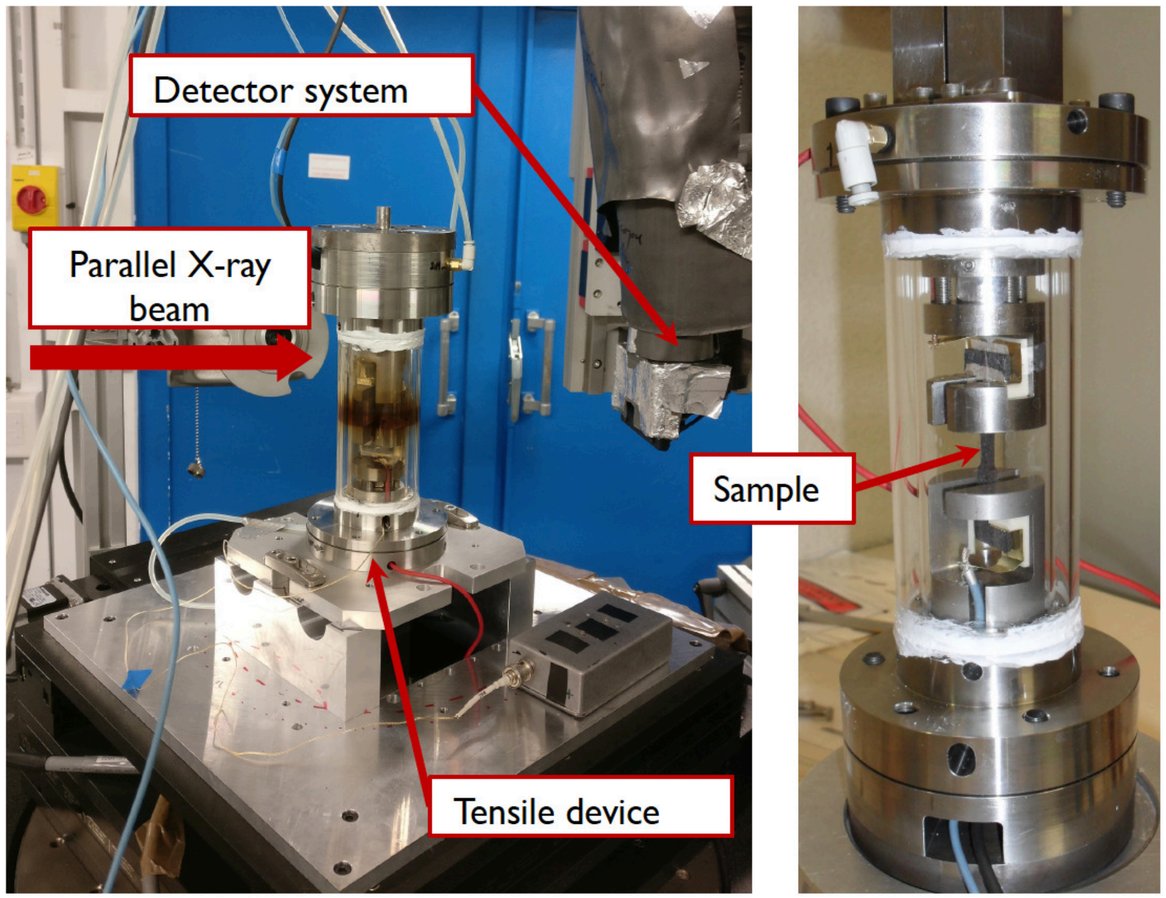

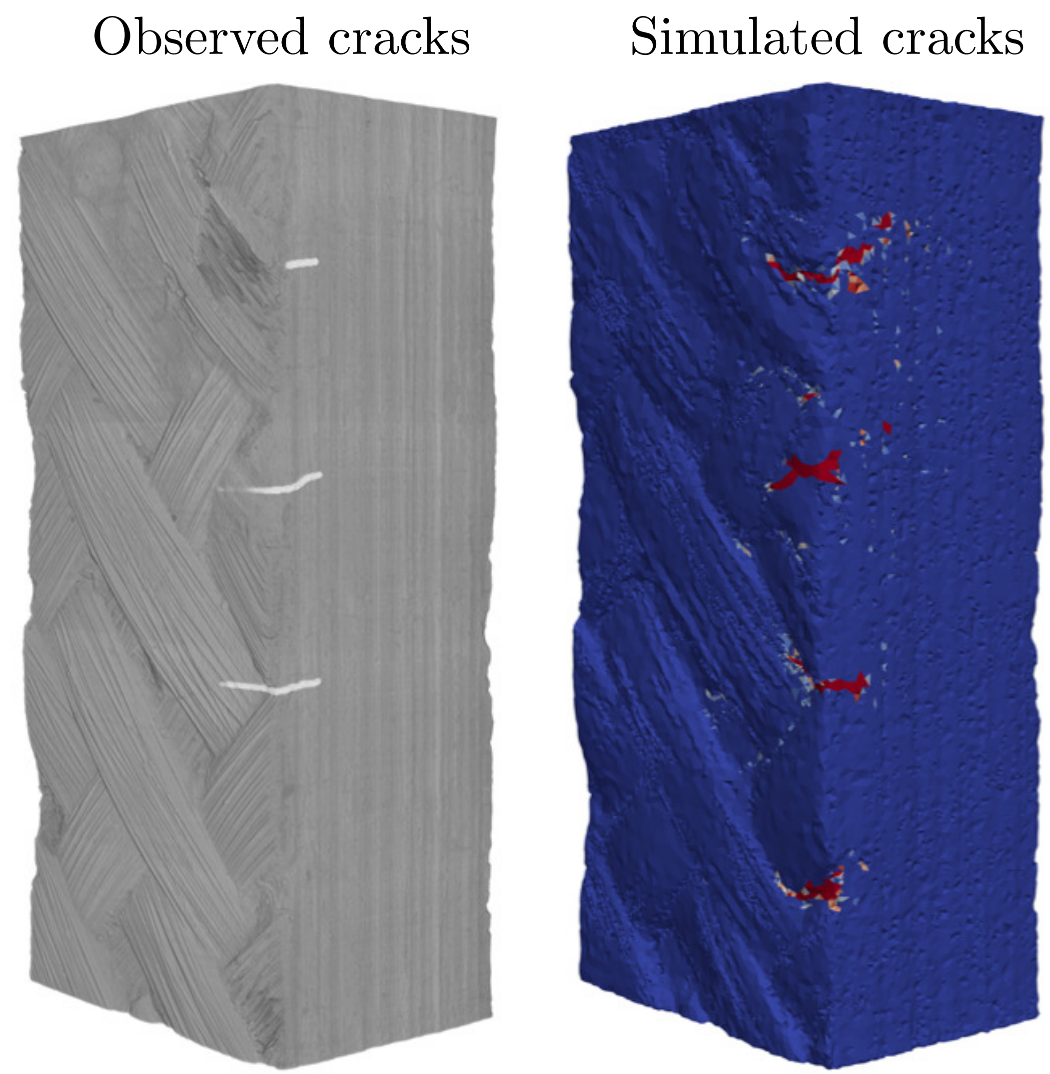

V. Mazars, O. Caty, G. Couégnat, A. Bouterf, S. Roux, S. Denneulin, J. Pailhès, G. L. Vignoles, Damage investigation and modeling of 3d woven ceramic matrix composites from x-ray tomography in-situ tensile tests, Acta Materialia 140 (2017) 130–139. doi:10.1016/j.actamat.2017.08.034.
V. Mazars, G. Couégnat, O. Caty, S. Denneulin, G. Vignoles, Multi-scale damage modeling of 3D ceramic matrix composites from in-situ X-ray tensile tests, in: ECCM18, Athens, Greece, 2018, pp. 24 – 28.

Conclusion

Conclusion

- Need for high-fidelity models of complex textile preforms
- Extensive use of structure tensor to detect local fibre direction
- Models with incremental complexity/level of description
- Generation of conforming tetrahedral meshes
- CMC digital twins for multiscale damage simulations

Questions?

Guillaume COUÉGNAT
couegnat@lcts.u-bordeaux.fr

Appendices

Variational segmentation approach

$$E = \alpha E_g + \beta E_d - \gamma (E_p + E_i)$$

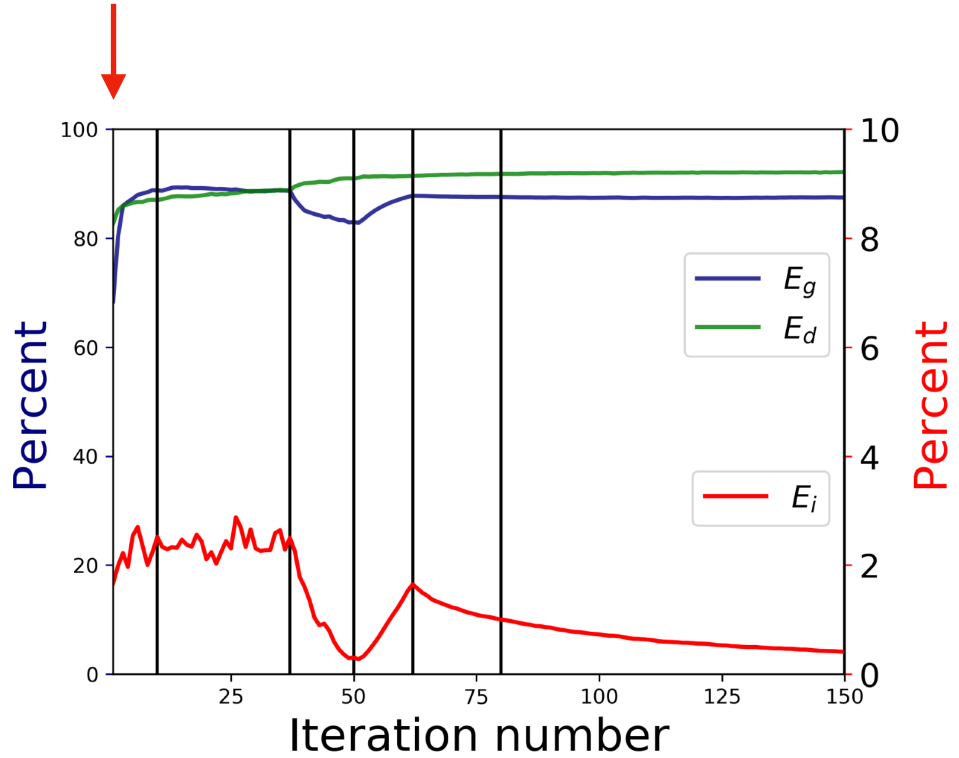

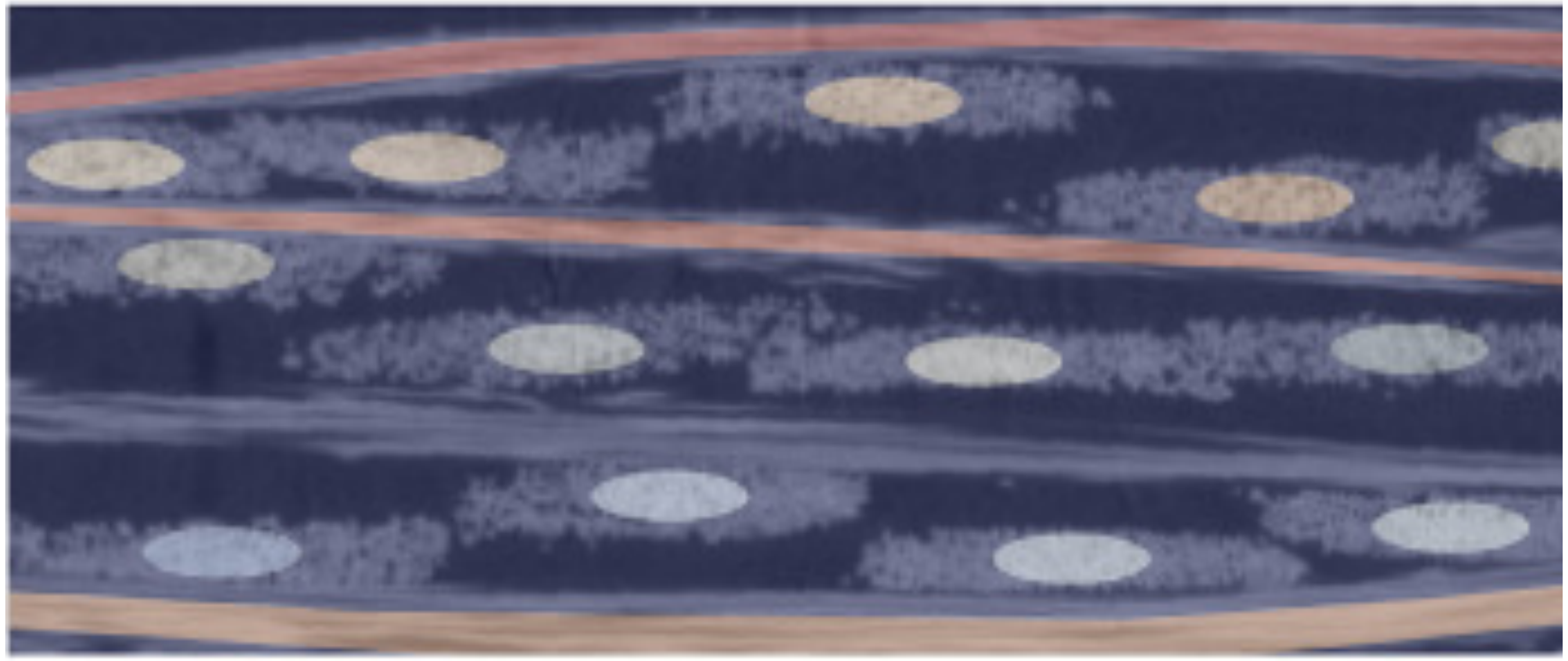

Initial geometric model with elliptic sections

$$\alpha \gg \beta \gg \gamma$$

Variational segmentation approach

$$E = \alpha E_g + \beta E_d - \gamma (E_p + E_i)$$

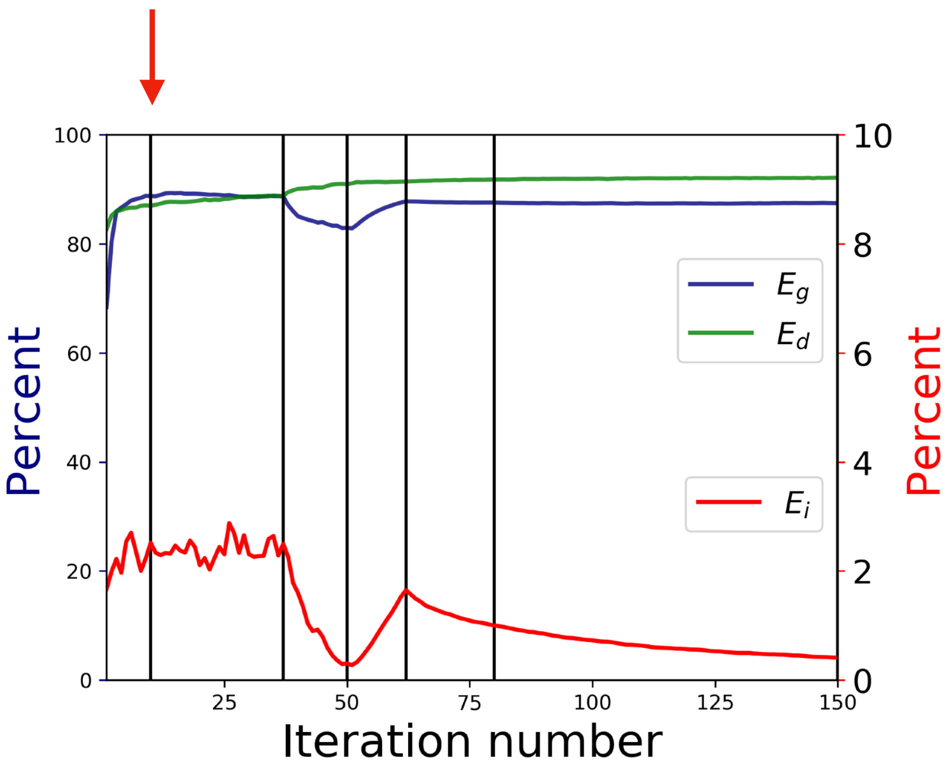

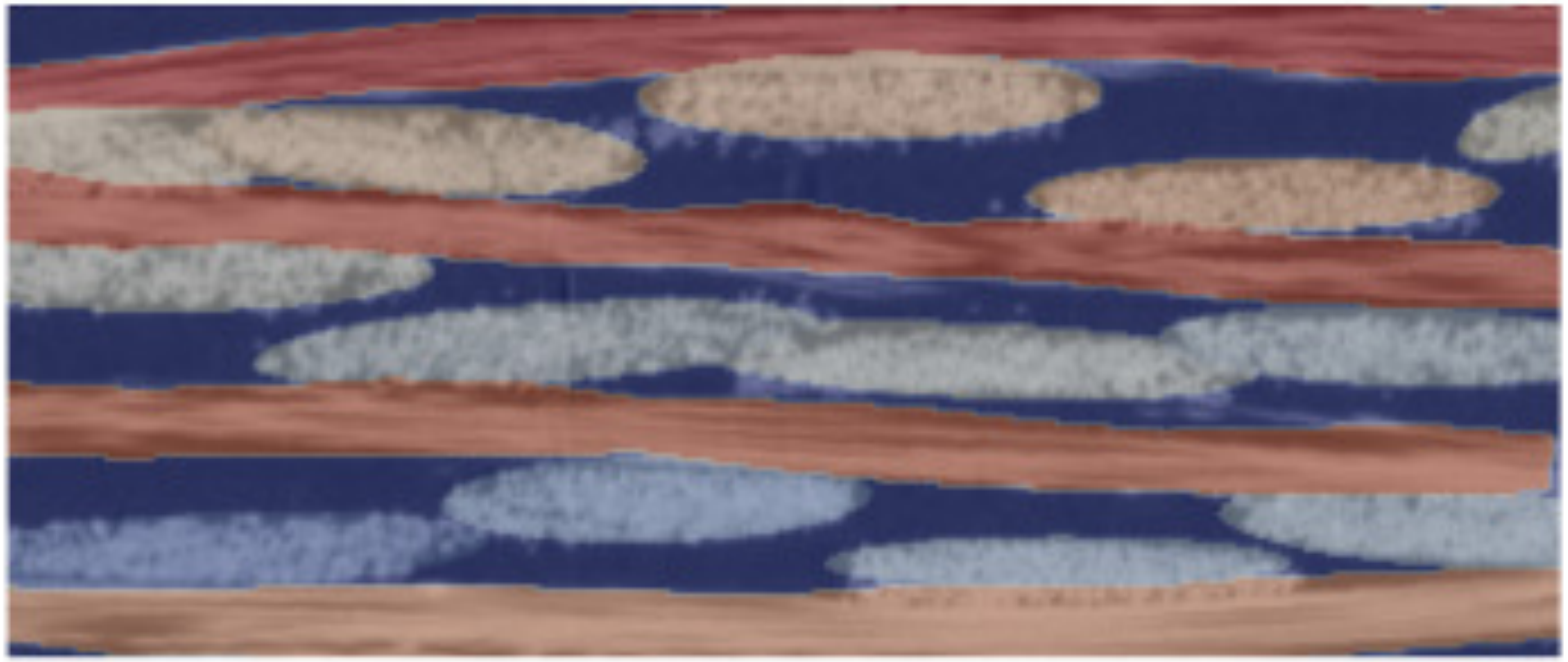

$$\alpha \approx \beta \gg \gamma$$

Variational segmentation approach

$$E = \alpha E_g + \beta E_d - \gamma(E_p + E_i)$$

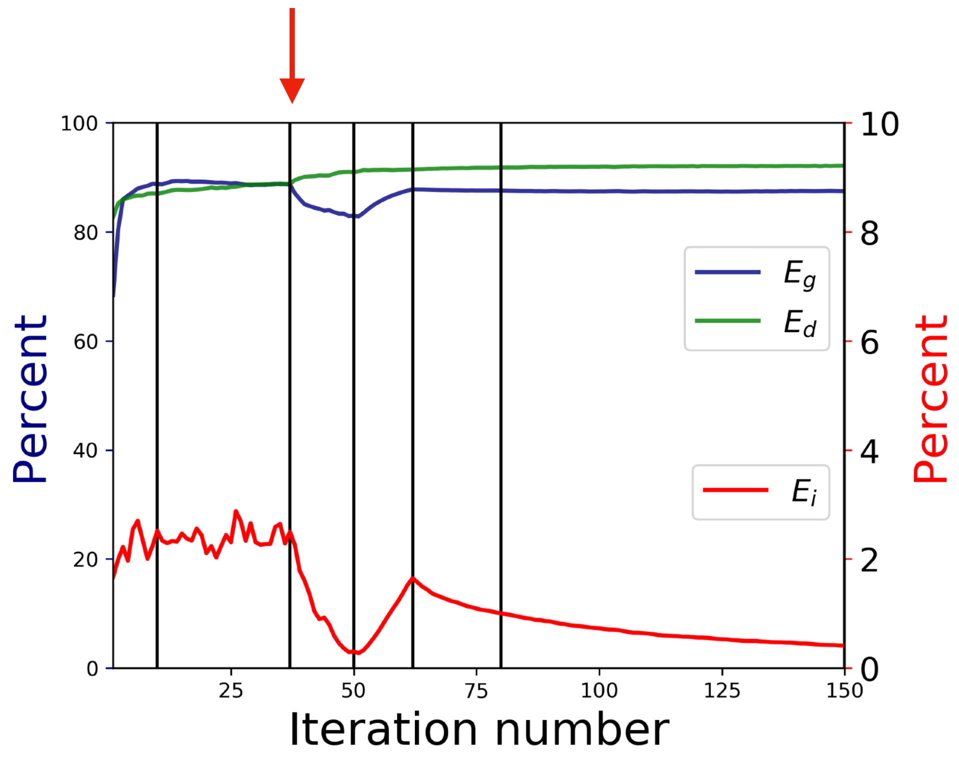

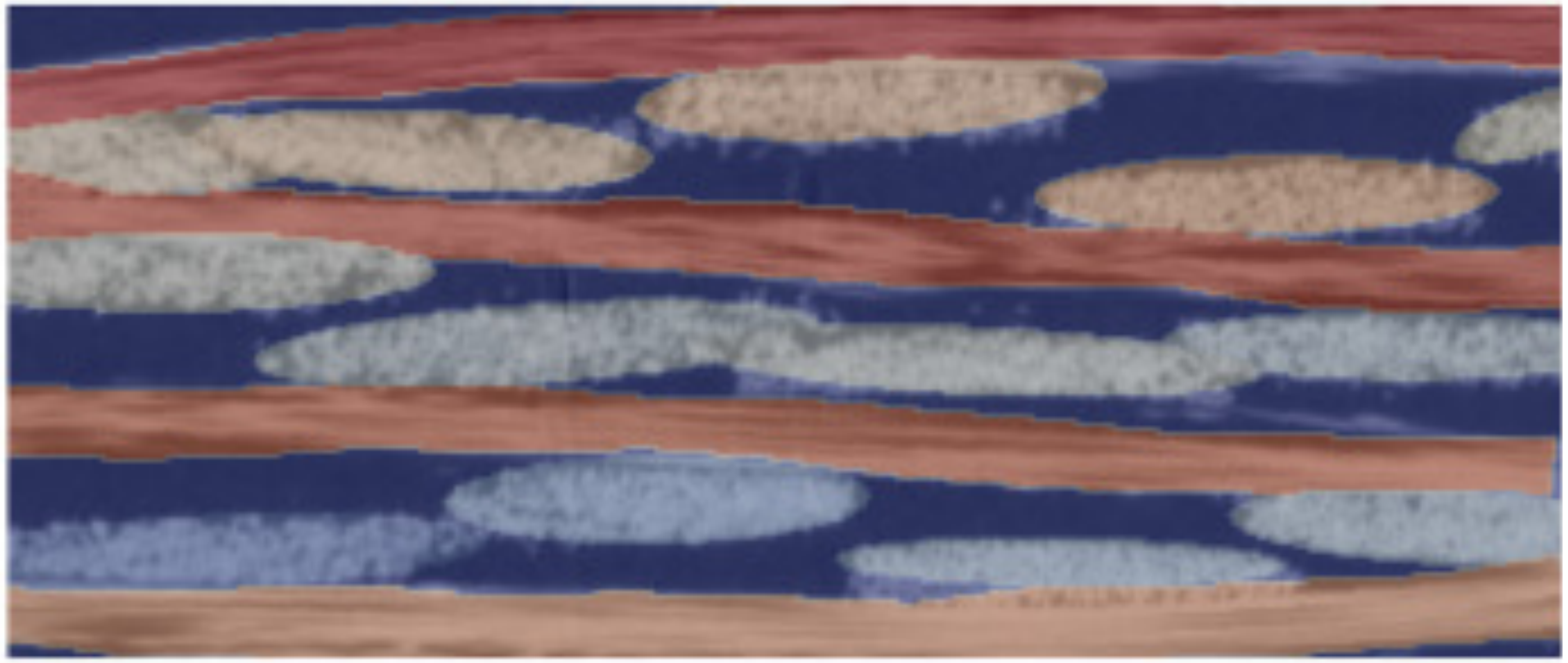

$$\alpha \approx \beta \approx \gamma$$

Variational segmentation approach

$$E = \alpha E_g + \beta E_d - \gamma (E_p + E_i)$$

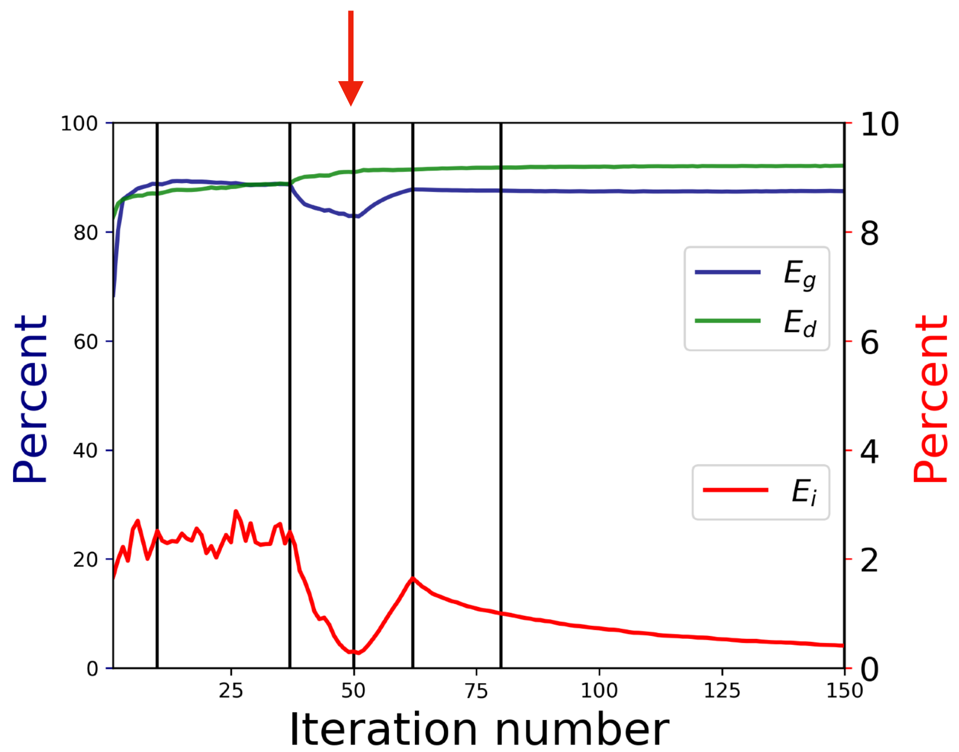

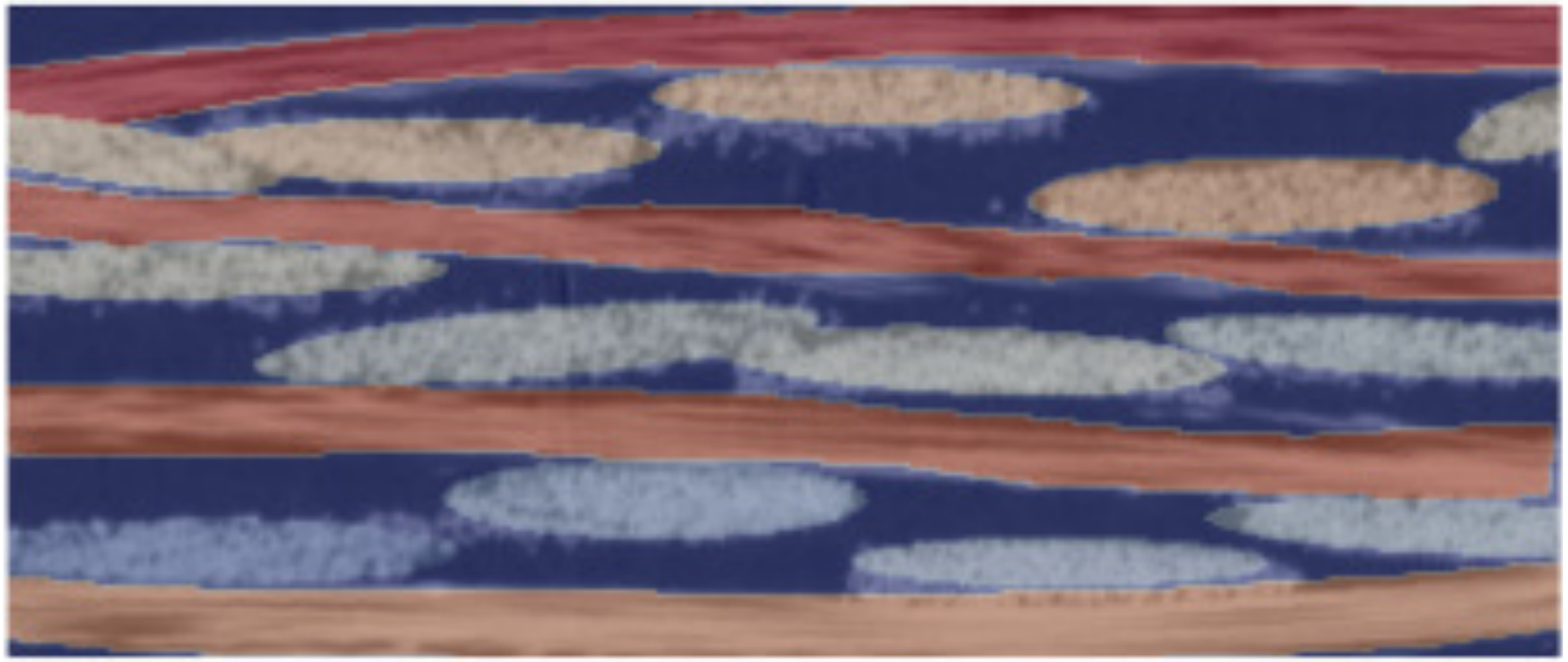

Best elliptic model with minimal interpenetration

$$\alpha \approx \beta \approx \gamma$$

Variational segmentation approach

$$E = \alpha E_g + \beta E_d - \gamma(E_p + E_i)$$

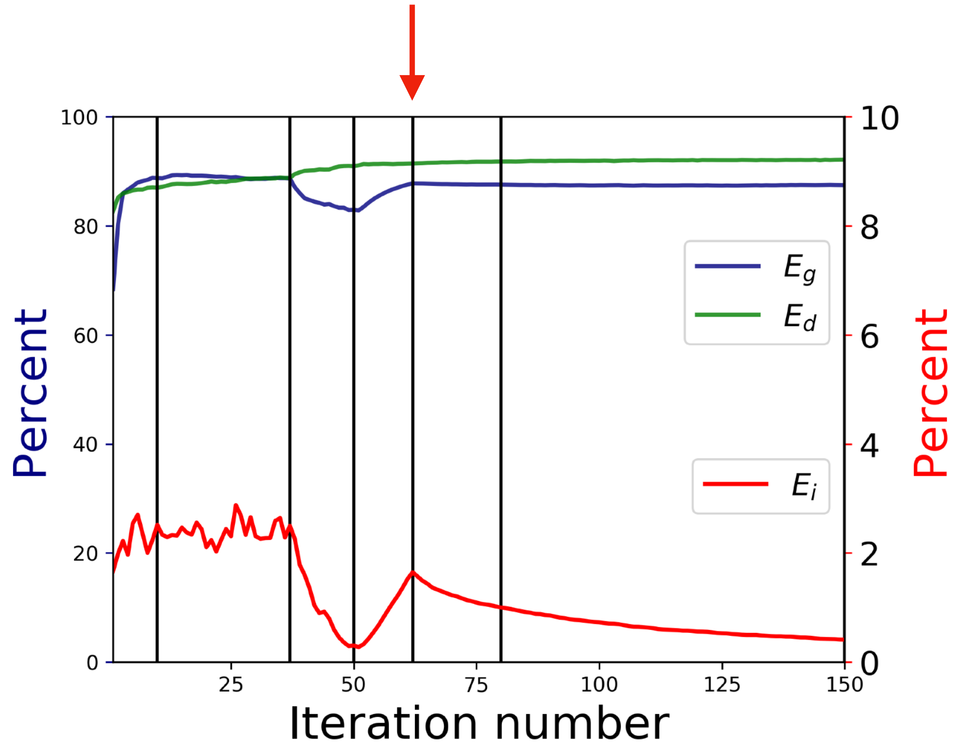

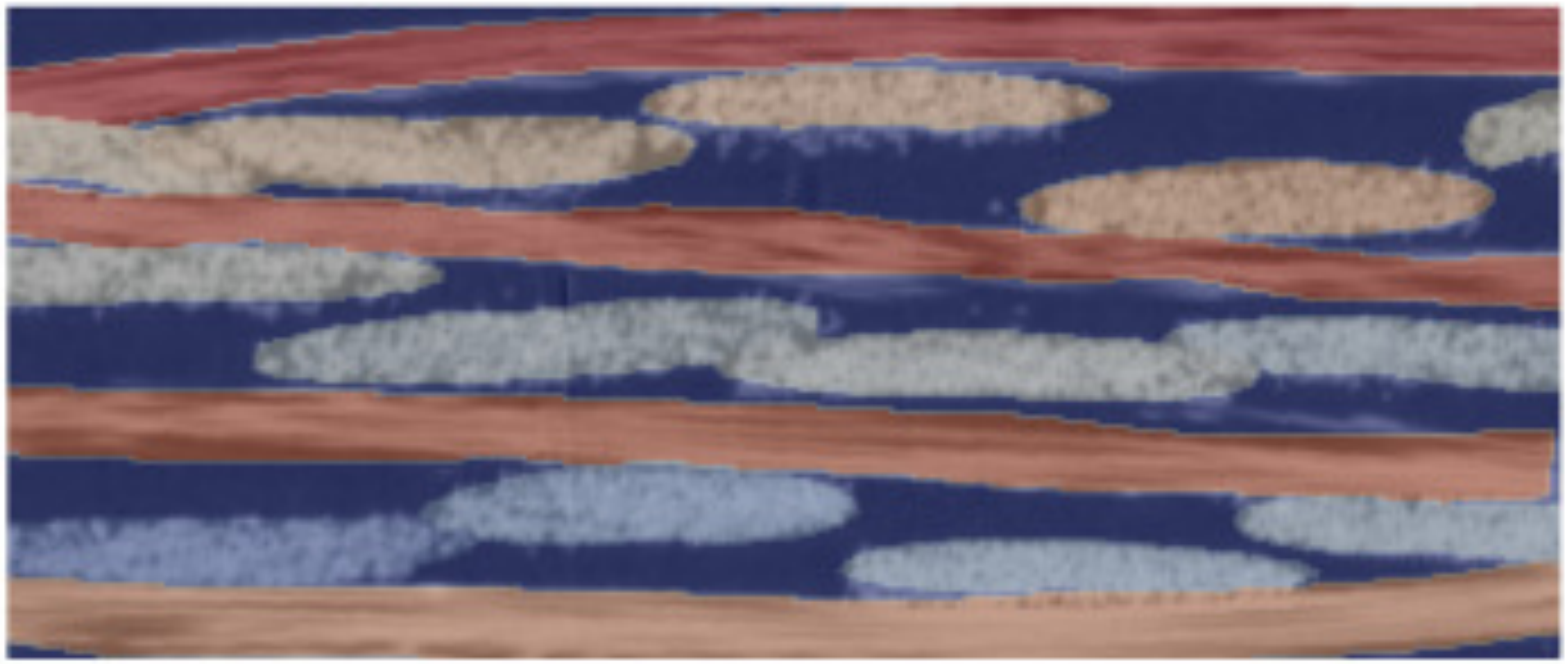

Switched to polygonal sections

$$\alpha \approx \beta \gg \gamma$$

Variational segmentation approach

$$E = \alpha E_g + \beta E_d - \gamma (E_p + E_i)$$

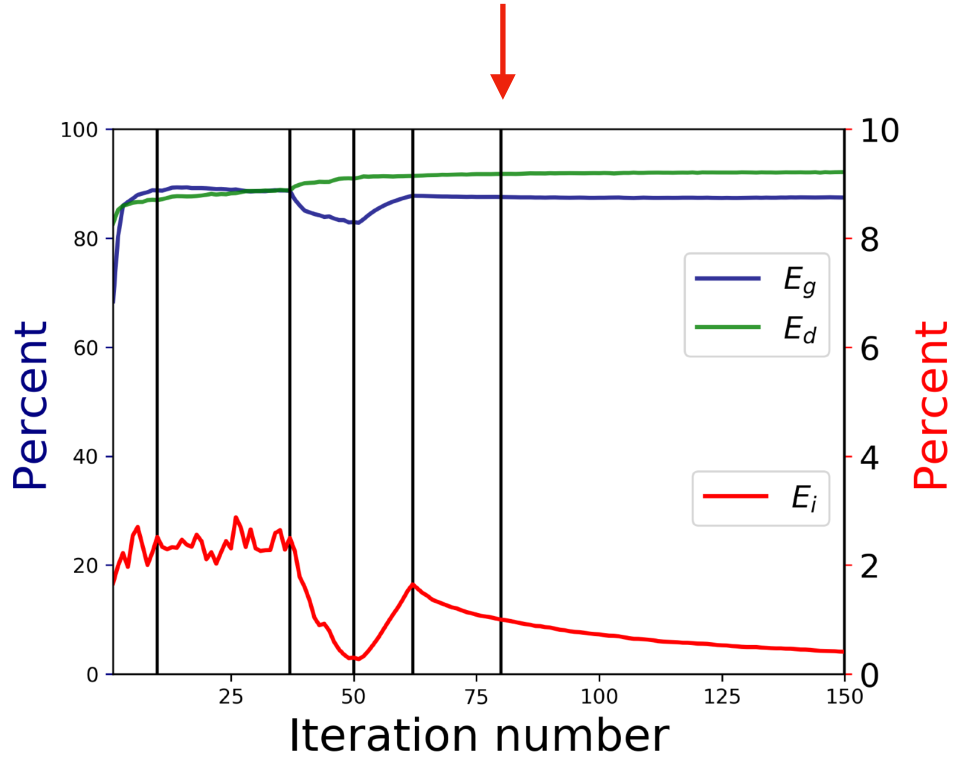

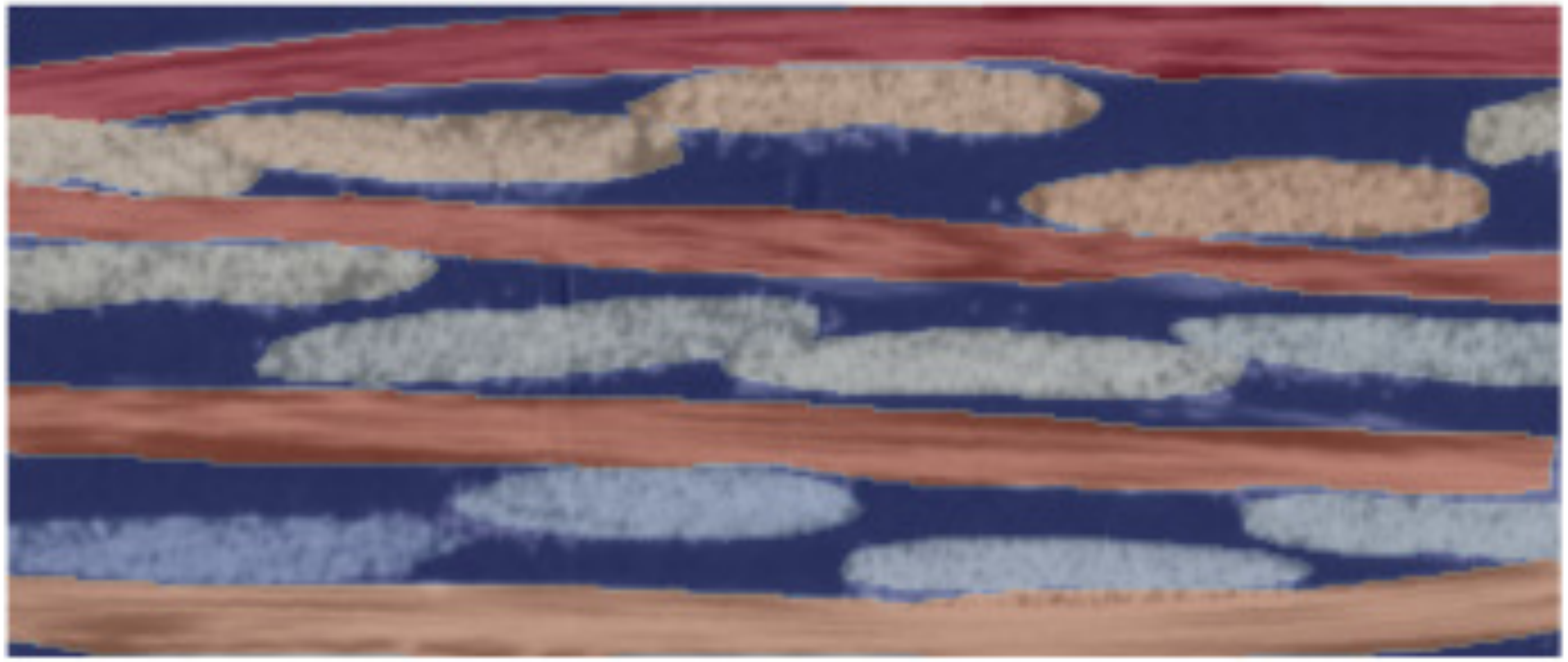

Best model with polygonal sections

$$\alpha \approx \beta \approx \gamma$$

Multiscale damage modelling framework

- Virtual tests at micro-scale

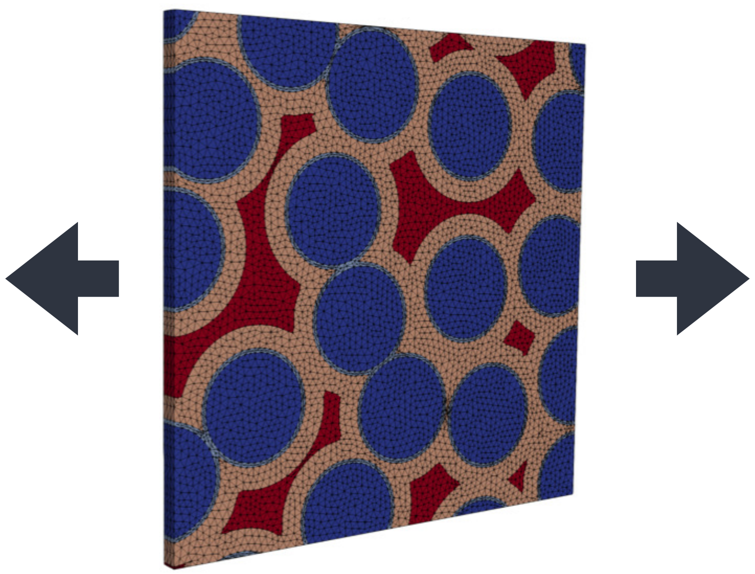

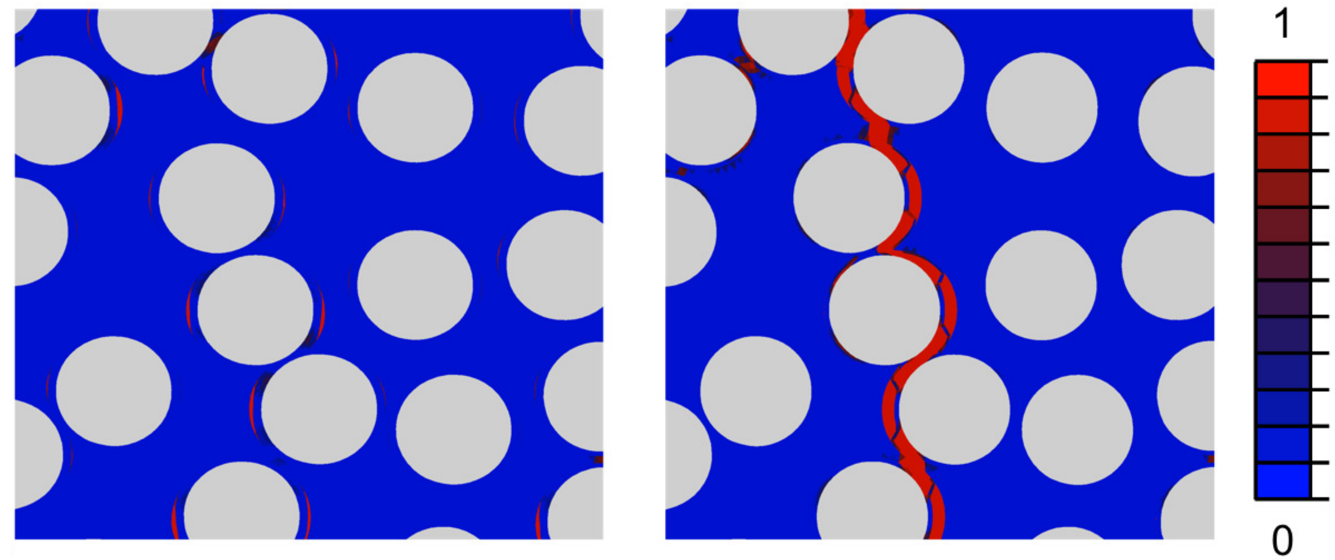

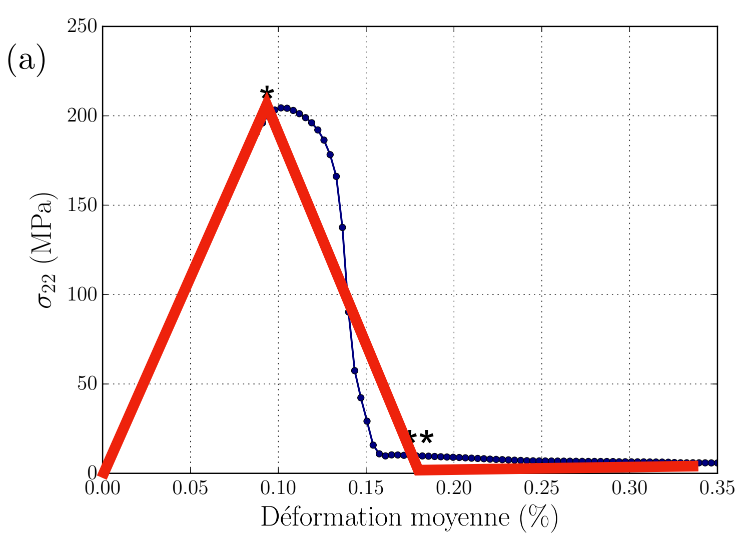

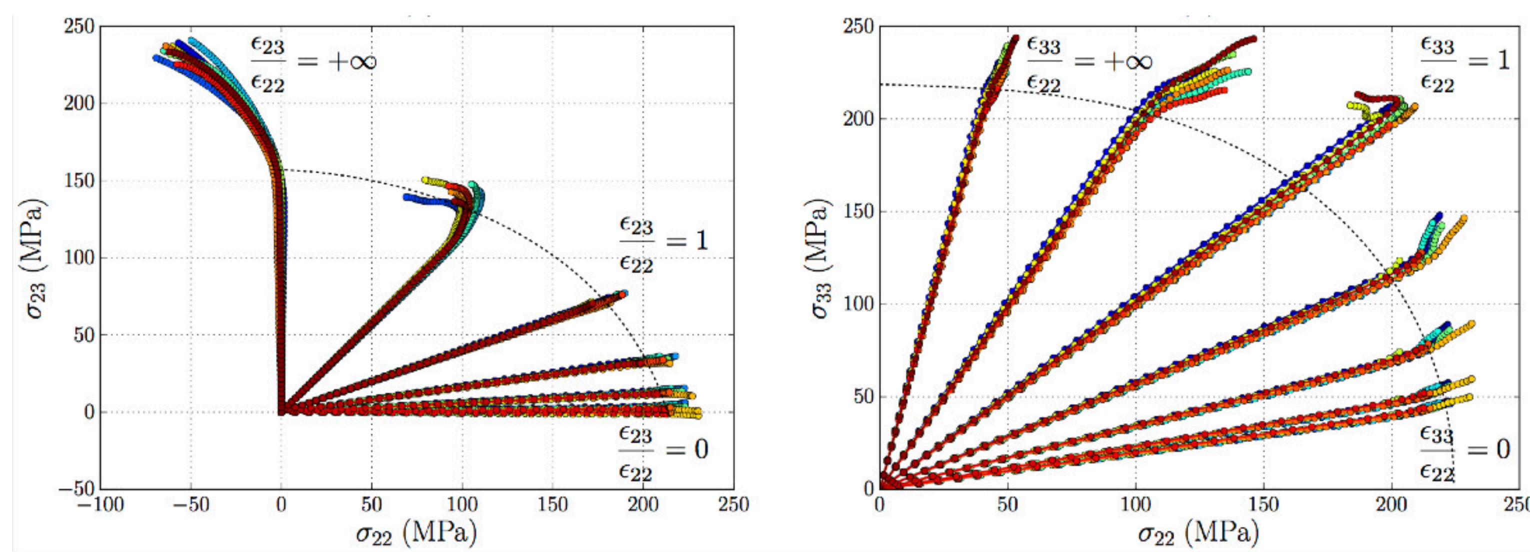

Multiscale damage modelling framework

- Stochastic micro-meso bridge

Virtual tests database

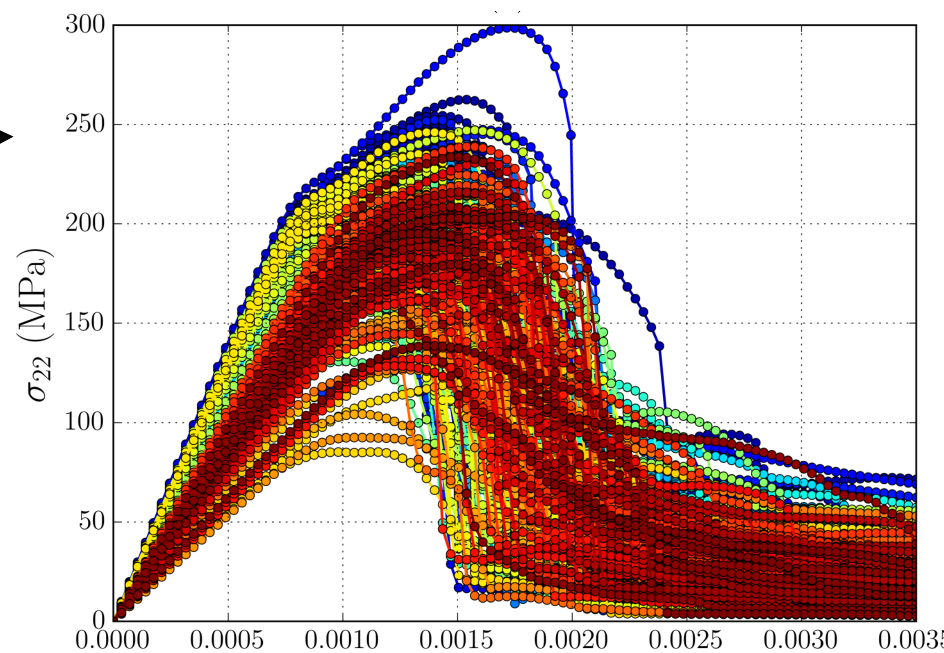

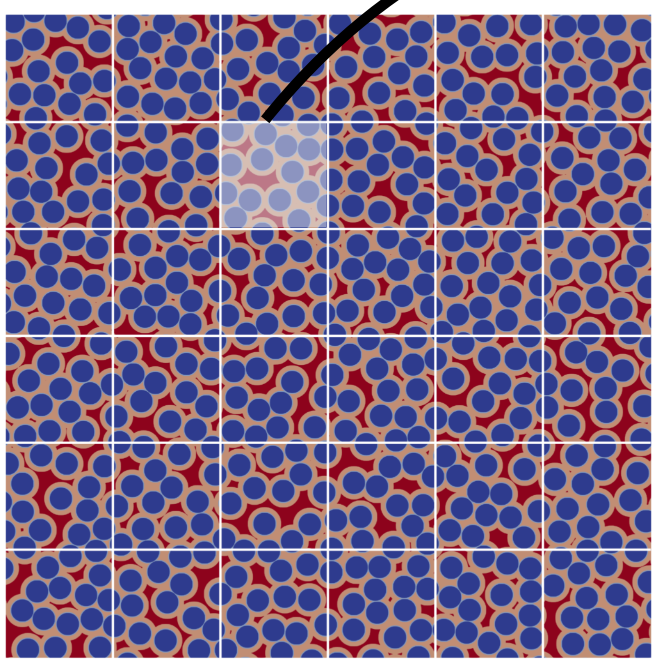

Microscale (fine mesh)

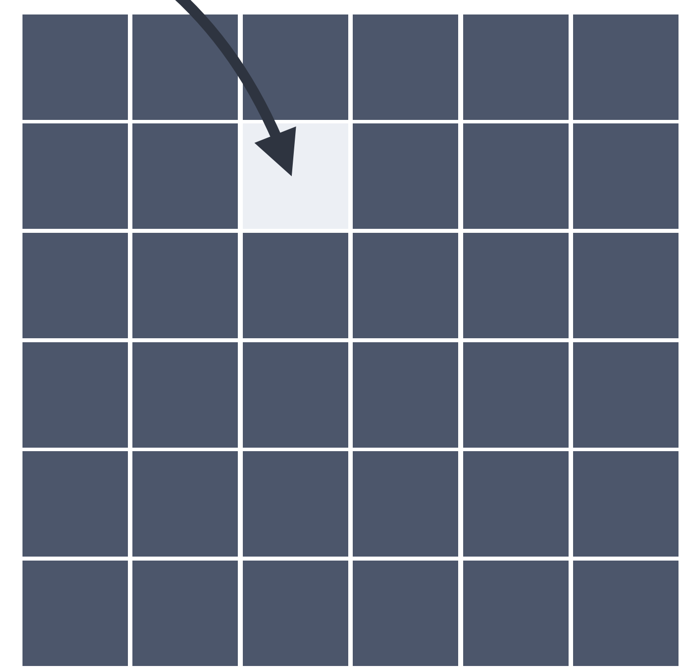

Mesoscale (coarse mesh)

Multiscale damage modelling framework